



Innovations in metamaterial and metasurface antenna design: The role of deep learning



Muhammad Kamran Shereen^{a,*}, Xiaoguang Liu^a, Xiaohu Wu^a, Salah Ud Din^a, Ayesha Naseem^b, Shehryar Niazi^b, Muhammad Irfan Khattak^c

^a School of Microelectronics, Southern University of Science and Technology, Shenzhen 518055, China

^b Department of Electrical Engineering, NUST, College of Electrical and Mechanical Engineering, Rawalpindi 46000, Pakistan

^c Department of Electrical Engineering, Faculty of Computer and Electrical Engineering, UET Peshawar, Pakistan

ARTICLE INFO

Keywords:

Metasurfaces
Metamaterial antennas
Deep learning
Antenna design
Gain enhancement
Bandwidth
Size reduction
Hybrid optimization
Simulation
High-fidelity datasets
AI-driven methodologies
Deep learning (DL)
Machine learning (ML)

ABSTRACT

Metamaterials and metasurfaces have revolutionized antenna design by enabling unprecedented control over electromagnetic waves. This paper explores integrating deep learning (DL) techniques in designing and optimizing metamaterial and metasurface antennas, focusing on improvements in gain, bandwidth, and size reduction. The review considers modern methodologies, such as hybrid optimization techniques with DL combined with traditional methods such as genetic algorithms and evolutionary strategies. It also addresses the use of high-fidelity datasets generated from advanced simulations to train DL models for more efficient antenna design. The paper is structured into five main sections: an introduction to metamaterials and metasurfaces, a discussion on their electromagnetic behavior, a classification of different types, an overview of deep learning applications in antenna design, and a conclusion summarizing the current advances, challenges, and future directions. By emphasizing the potential of DL to streamline the design process and enhance antenna performance, this paper provides a valuable foundation for future research in electromagnetic metasurfaces.

1. Introduction

The term "metamaterial" comes from a Greek phrase that combines the words "meta" and "material," where "meta" means something that is advanced, changed, or beyond the ordinary. It is a synthetic substance created to have physical characteristics that are not present in natural materials. Rodger M. Walser of the University of Texas at Austin coined the word "metamaterial" in 1999 [1]. In order to create an optimal mix of two or more responses that are not found in nature, Walser described metamaterials as "macroscopic composites with a synthetic, three-dimensional, periodic cellular architecture [2]. Metamaterials (MTMs) possess exotic electromagnetic (EM) properties absent in natural materials and are also known as artificially engineered composite materials. This remarkable discovery of modern science has garnered significant research interest, particularly for microwave applications

over recent decades [3]. Metamaterials can be classified into various types: single negative (SNG), double negative (DNG), and double positive (DPS). SNG materials possess either negative permittivity (ϵ) or permeability (μ), while DNG materials have both parameters negative, and DPS materials have both positive. SNG metamaterials are further classified into epsilon-negative (ENG) and mu-negative (MNG) types. In 1968, Victor Veselago proposed the concept of a material exhibiting both negative permittivity and permeability, displaying properties contrary to those of ordinary materials [4]. In 2000, Smith et al. created a composite material with both negative permittivity and permeability, commonly referred to as "left-handed materials" (LHM) [5]. Unlike conventional materials, which only support forward wave propagation (right-hand wave propagation), metamaterials can support backward wave propagation, thus exhibiting left-handed properties. Additionally, modern studies on metamaterial properties have introduced a zero or

This work was partially supported by the Natural Science Foundation of China under Grant 62471211, and in part by Guangdong Provincial Key Laboratory of Integrated Circuits under Grant 2021KSY006 and Shenzhen Science and Technology Program under Grant JCYJ20220818100408018, 20231115204236001, and JCYJ20230807091814030.

* Corresponding author.

E-mail address: shereen@sustech.edu.cn (M.K. Shereen).

negative refractive index based on Snell's laws and the Doppler effect, which illustrates wave transfer between mediums [6]. In natural materials, rays refract along the interface's normal; however, in LHM, rays refract away from the normal, creating a focal point within the material. There are four main structural types of metamaterials: S-structure, symmetrical-ring structure, free split-ring structure, and omega structure. Meta-structures are specially designed to meet specific performance requirements with properties beyond those found in natural materials, and they can be distinguished by field, such as acoustics, mechanics, and electromagnetics [7]. Acoustic meta-structures [8] include Photonic crystals, acoustic metamaterials, and metasurfaces, offering novel methods for controlling acoustic and elastic waves, enabling functions such as wave blocking [9], absorption [10], focusing [11], robust energy harvesting, and negative refraction. Similar to electromagnetic metamaterials, Photonic crystals [12] exhibit bandgaps due to periodic distributions, blocking or attenuating mechanical waves. The development of locally resonant Photonic crystals introduced low-frequency hybridization bandgaps through resonances within the structure [13], spurring innovations in acoustic metamaterials with applications such as vibration and noise reduction, as well as properties like negative mass density, negative bulk modulus, and double-negative parameters [14]. In the last decade, aiming for efficient low-frequency acoustic/elastic wave control, researchers have developed acoustic metasurfaces by creating phase gradients based on generalized Snell's law. These metasurfaces offer functions like wave focusing, cloaking [15], and low-frequency absorption. Unlike Photonic crystals and acoustic metamaterials, metasurfaces are ultra-thin, planar, and highly designable, enabling compact acoustic devices. Recently, topological insulators in condensed matter physics have been applied to regulate mechanical waves within meta-structures [16]. Due to bandgaps, these meta-structures can act as mechanical insulators, with topological edge states allowing certain wave frequencies to propagate, showing properties like defect immunity and unidirectional waveguides [17]. Research on mechanical meta-structures focuses on elastic modulus, shear modulus, and Poisson's ratio for static performance enhancements [18]. Structures like origami [19], chiral, lattice, and honeycomb exhibit unconventional characteristics, such as negative stiffness, compression, and multi-stability, supporting applications in vibration suppression, impact resistance, and structural protection. Traditionally, designing meta-structures with specific properties relies on trial and error through experimental and computational methods, which are resource-intensive. Heuristic optimization methods like genetic algorithms [20], simulated annealing [21], and particle swarm optimization offer global search solutions but may lack stability. Advances in artificial intelligence (AI), particularly machine learning (ML) methods such as deep neural networks (DNNs) and reinforcement learning (RL), are overcoming these limitations, revolutionizing fields including materials science [22]. ML-based meta-structure design has become critical for addressing inverse problems, and recent reviews have outlined ML advances in meta-structure design across fields like nanophotonics [23], electromagnetic meta-structures [24], and mechanical meta-structures [25]. This review is defined by this comprehensive analysis of how deep learning techniques revolutionize metasurface-based antenna optimization and metamaterials. Even if there have been some references to applications of machine learning to materials science before, this paper is distinguished by the compilation of recent works on employing deep neural networks (DNNs), convolutional neural networks (CNNs), and GANs to direct and inverse antenna synthesis. The paper emphasizes how the tools enable multi-objective optimization, predictive models, gain, miniaturization, and bandwidth performance evaluation. In this way, this paper is an even-handed synthesis of the best current practices in electromagnetic, photonic, acoustic, and mechanical fields, with specialist consideration made to meta-structures with AI tools. The review is, therefore, an exhaustive and technically useful treatise to researchers developing AI applications for next-generation antenna and metamaterial systems. This review

highlights recent progress in ML inverse design of acoustic, elastic, and mechanical meta-structures, focusing on design objectives, summarizing progress in band structure design, wave propagation characteristics, and static characteristics, and concluding with future prospects for this interdisciplinary field.

This review paper is organized as:

1. Introduction
2. Properties Of Metamaterials/Metasurface
 - ENG
 - DPS
 - SNG
 - MNG
3. Deep Learning Categories
4. Metamaterial/Metasurface Classification
 - Electromagnetic Metamaterials (EM)
 - 1) Iterative Inverse Design Method
 - a) Topology optimization (TO)
 - b) Evolutionary algorithms (EAs)
 - 2) Direct Inverse Design Method:
 - a) DL-assisted inverse design:
 - b) Direct DL inverse design:
 - Photonic Metamaterials (PM)
 - 1) The basic principles of PnCs
 - 2) Neural network architecture and working principle
 - 3) Application of ML Algorithms in PnCs Design
 - a) PnCs Performance Prediction Using ML
 - b) Predicting Dispersion Relations of PnCs
 - c) Predicting Band Structures in PnCs
 - 5) Inverse Design and Topology Optimization of PnCs
 - Acoustic Metamaterials (AM)
 - 6) Properties and Applications
 - 7) Resonance-Based Acoustic Metamaterials
 - 8) Broadband Optimal Acoustic Absorption Structures
 - 9) Topological Acoustics and One-Way Edge States
 - 10) Noise Pollution Mitigation with Acoustic Metamaterials
 - 11) Advanced Phenomena and Practical Applications
 - 12) Basic principles of AMs
 - 13) Types of common AMs
 - 14) Optimization of metamaterial structures based on ML/DL models
 - Mechanical Metamaterials (MM)
 - 15) Design of static characteristics in mechanical meta-structures
 - 16. Application of Metamaterials
 - Metamaterial as Absorber
 - Metamaterial as Super-lens
 - Metamaterial as Cloaks
 - Metamaterial as Sensor
 - Metamaterial as Phase Compensator
 - 17. Metamaterials/Metasurface in Antenna Design (Effect of Metamaterials on Antenna Parameters)
 - Gain
 - Size Reduction
 - Bandwidth Enhancement
 - Multiband Antenna
 - Directivity Enhancement
 - Metamaterials For the Reduction of Specific Absorption Rate
 - 18. Lesson Learned: Deep Learning/Machine Learning Techniques for Metamaterial/Metasurface Antennas

2. Metamaterials/Metasurface properties

The behavior of electromagnetic fields in materials is described by Maxwell's equations. The electromagnetic properties of a material, specifically its dielectric permittivity (ϵ) and magnetic permeability (μ), determine how an electromagnetic wave interacts with it. The formula for the first of Maxwell's equations is

$$\nabla \times E = -j\omega\mu H \quad (1)$$

$$\nabla \times H = j\omega\epsilon E \quad (2)$$

where ϵ and μ stand for the permittivity and permeability of the material, respectively, and E and H for the electric and magnetic field vectors. The angular frequency is denoted by the symbol ω . The electric and magnetic fields for plane wave propagation are commonly expressed as follows:

$$E = E_0 e^{-j(kr-j\omega t)} \quad (3)$$

$$H = H_0 e^{-j(kr-j\omega t)} \quad (4)$$

In this case, k and r stand for the wave vector and position vector, respectively, and E_0 and H_0 are the amplitude vectors of the electric and magnetic fields. The Poynting power density vector S , which is separated into time-dependent $e^{j\omega t}$ and space-dependent e^{-jkz} components, is defined in order to evaluate the material qualities. The formula for the real part of the Poynting vector, which depicts the energy flow, is

$$S = (1/2)E \times H \quad (5)$$

The electric and magnetic fields for plane waves meet the following requirements:

$$k \times E = \omega\mu H; \quad (6)$$

$$k \times H = -\omega\epsilon E \quad (7)$$

The vectors E , H , and k constitute a right-handed coordinate system in a homogeneous medium where both ϵ and μ are positive. This is known as a right-handed medium (RHM), where the wave can propagate forward since the Poynting vector S and wave vector k are oriented in the same direction [26]. The equations can be rewritten as follows, though, if ϵ and μ are both negative, as they are for some metamaterials:

$$k \times E = -\omega|\mu|H \quad (8)$$

$$k \times H = \omega|\epsilon|E \quad (9)$$

Here, a left-handed coordinate system, known as a left-handed medium (LHM), is formed from the vectors E , H , and k . Backward waves, in which the energy and wavefronts move in opposing directions, can propagate in such a medium because the Poynting vector S points in the opposite direction to the propagation vector k . The triad models for left-handed (b) and right-handed (a) materials are shown in Fig. 1.

3. Metamaterials/Metasurface classifications

There are four types of metamaterials (as shown in Fig. 3), that can be classified depending on the value of permittivity (ϵ) and permeability (μ).

The materials are classified into four categories, as shown in Fig. 2, based on the values of ϵ and μ , which are described as follows:

- Electromagnetic Metamaterials: $\epsilon_r < 0, \mu_r < 0$

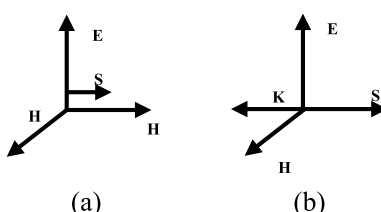


Fig. 1. The vectors E , H and k form a triplet in both right-handed (a) and left-handed (b) media.

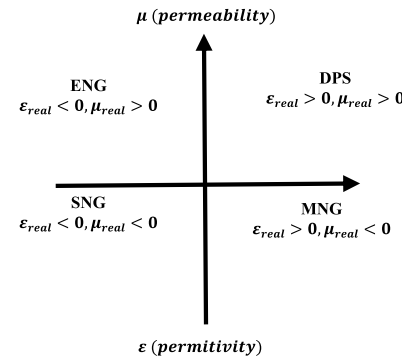


Fig. 2. Classification of Metamaterials.

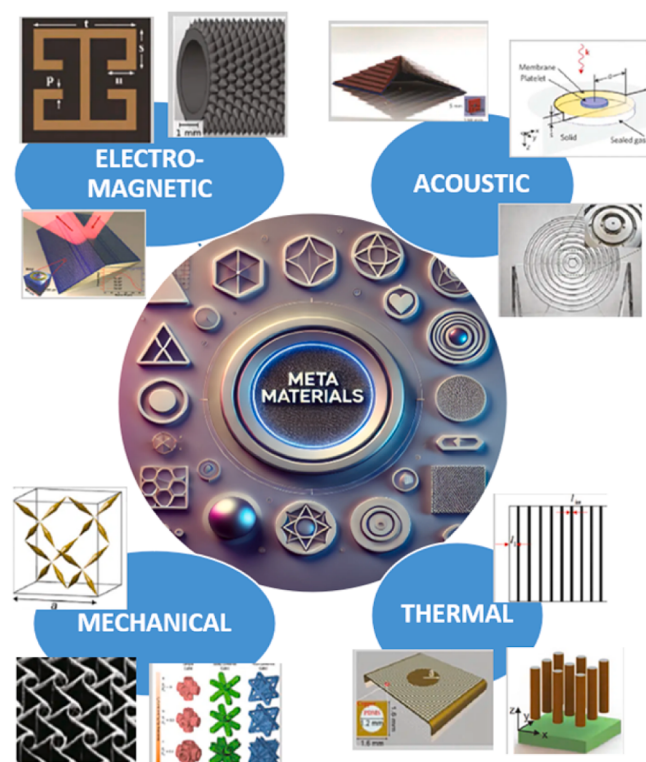


Fig. 3. Types of metamaterials.

- ϵ_r is the relative permittivity (dielectric constant), and μ_r is the relative permeability.
- Negative values for both parameters result in a negative refractive index, leading to unusual electromagnetic properties like reverse Doppler effect and reverse Cherenkov radiation

1. Photonic Metamaterials: $\omega_g = \frac{\pi c}{a}$
 - ω_g represents the photonic bandgap frequency.
 - c is the speed of light, and a is the lattice constant of the photonic crystal.
 - This equation determines the frequency range where light propagation is forbidden in the material.
2. Acoustic Metamaterials: $\rho_{eff} < 0, K_{eff} < 0$
 - ρ_{eff} is the effective density, and K_{eff} the effective bulk modulus.
 - Negative values for these parameters lead to negative refractive index for sound waves, allowing for unique acoustic properties like sound focusing and cloaking.
3. Mechanical Metamaterials: $E < 0, v < -1$
 - E represents Young's modulus, and v is Poisson's ratio.

- These unusual values indicate that the material contracts laterally when compressed axially, which is opposite to conventional materials.

4. Deep learning categories

Deep learning (DL) techniques can be broadly categorized into three main types: supervised learning, unsupervised learning, and reinforcement learning, as illustrated in Fig. 4. Supervised learning algorithms, such as multilayer perception (MLPs), convolutional neural networks (CNNs), recurrent neural networks (RNNs), and graph neural networks (GNNs), are highly effective for tasks like classification and regression, including property prediction in mechanical metamaterials. In contrast, unsupervised learning models, such as variational autoencoders (VAEs) and generative adverSARial networks (GANs), are primarily used for generating geometries in mechanical metamaterials. Reinforcement learning (RL) models, such as deep Q-networks (DQNs), promise to discover new mechanical metamaterials. When it comes to optimizing antenna parameters like gain, bandwidth, and size reduction, different

deep learning (DL) techniques have different strengths. Convolutional Neural Networks (CNNs) are great for classification and regression tasks, especially when dealing with geometrical features and predicting performance parameters like gain and bandwidth. They are good with structured data like images or electromagnetic field maps. Generative AdverSARial Networks (GANs) as unsupervised learning models are used to generate new antenna geometries to explore novel and innovative designs that may not be discovered through traditional methods. Reinforcement Learning (RL), particularly Deep Q-networks (DQNs), optimizes antenna designs by modeling the process as a decision-making task where the system adapts to the lesson learned from feedback. This allows dynamic parameter optimization in real-time. Each technique has its strengths: CNNs for pattern recognition in structured data, GANs for generating new designs, and RL for adaptive optimization. These can be combined for a holistic approach to antenna design and performance across multiple parameters. Table 1 comparing deep learning techniques such as CNNs, GANs, and reinforcement learning. It examines essential factors like data needs, accuracy, computational cost, strengths, and weaknesses of each method. This comparison helps choose the best

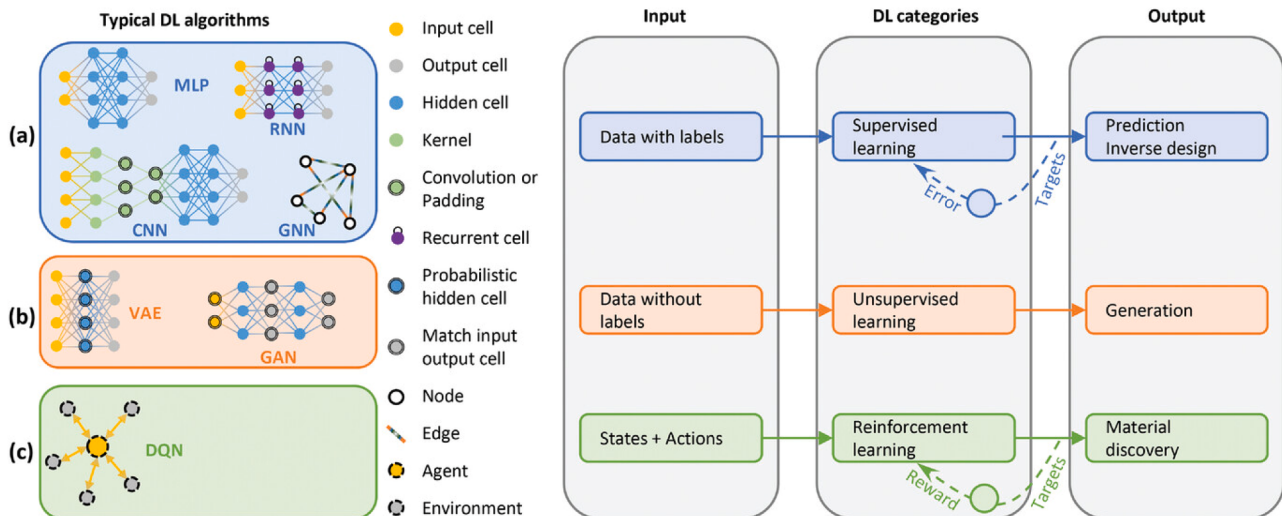


Fig. 4. Deep Learning (DL) Technique Classification: (a) Supervised Learning: This method uses a labeled dataset as input. In mechanical metamaterials, supervised learning is frequently employed for tasks like inverse design and property prediction. Multilayer perceptions (MLPs), convolutional neural networks (CNNs), recurrent neural networks (RNNs), and graph neural networks (GNNs) are examples of common supervised learning techniques. (b) Unsupervised Learning: An unlabeled dataset is used as input in this case. Mechanical metamaterials are usually generated using unsupervised learning. Generative adverSARial networks (GANs) and variational autoencoders (VAEs) are two well-known unsupervised learning algorithms. (c) Reinforcement Learning: States and actions are used as input in this technique. A strong tool for material discovery, reinforcement learning allows the model to maximize actions in dynamic contexts. Deep Q-networks (DQNs) are a well-known reinforcement learning algorithm. In 1986, the back-propagation algorithm enabled the MLP model to perform nonlinear processing [27]. Subsequent innovations introduced RNNs for time-series predictions [28] and CNNs for image processing [29]. As neural networks became more complex, training difficulties increased, but improved computational power eventually facilitated the deepening of models. By 2006, ANN research had entered the deep learning era, with open-source frameworks like TensorFlow and PyTorch simplifying algorithmic learning for beginners [30,31]. Over the last decade, diverse deep neural network (DNN) models have emerged, including GANs, conditional GANs (CGANs), and tandem neural networks (TNNS) [32–34]. Reinforcement learning, rooted in behaviorism [35], has gained traction alongside deep learning, achieving success in domains like autonomous driving and Go [36,37]. DNNs are particularly adept at learning implicit relationships from data, especially for nonlinear problems lacking clear functional relationships, as is often the case in metastructure design. Unlike forward problems (e.g., predicting properties from structural parameters), inverse design, which extrapolates structure from desired properties, can be challenging due to a lack of analytical solutions. Nevertheless, data-driven neural networks can use target properties as input to quickly determine design parameters [38]. For high-dimensional data, CNNs reduce computational complexity by limiting neuron connections. Autoencoders (AEs) can further extract features from high-dimensional property data for mechanical analysis. In the inverse design of metastructures, one property may correspond to multiple structural parameters, potentially causing training convergence issues. TNNS address this by freezing the pre-trained forward network and using it as a cascade in the inverse network. Additionally, transfer learning, which re-trains models from similar datasets, and GANs with CGANs can handle small-scale data situations [39,40]. In GAN-based solutions, the generator creates structures that the discriminator evaluates for authenticity, resulting in a model capable of generating target structures based on random vectors and specified properties. The integration of RL in metastructure inverse design treats structural parameters as agents. These agents adjust parameters based on feedback related to proximity to design goals, ultimately establishing an optimal parameter pathway. Fig. 1 summarizes ML applications in metastructure performance prediction and inverse design. Additionally, simpler ML algorithms like linear regression, logistic regression, and decision trees offer high performance in specific applications. For example, decision trees, which classify samples based on different attribute branches, can be grouped into random forests for enhanced performance and stability, albeit at a higher computational cost [41]. Finally, open-source DL frameworks, including TensorFlow [42] and PyTorch, make it easier for beginners to grasp ML concepts. These frameworks, integrated with Python, streamline the process by eliminating low-level coding requirements. For training, accessible datasets such as the Handwritten Digit Dataset, CIFAR10, and Fashion-MNIST are commonly used, along with MATLAB's neural network toolbox, which offers a user-friendly modeling interface.

Table 1
Comparison of deep learning techniques.

| Deep Learning Technique | Data Requirements | Accuracy | Computational Cost | Strengths | Limitations |
|--|---|---|--|--|--|
| Convolutional Neural Networks (CNNs) | High (requires large labeled datasets) | High (effective for spatial data, image processing) | Moderate to High (depends on network depth) | Excellent for pattern recognition, feature extraction in images | Requires large datasets, slow to train for complex models |
| Generative Adversarial Networks (GANs) | Very High (requires diverse data to generate realistic outputs) | High (capable of generating novel designs) | Very High (requires dual networks) | Can generate new antenna designs and geometries | Can suffer from mode collapse, difficult to train |
| Reinforcement Learning (RL) | Moderate (environment interaction required) | Moderate to High (depends on reward structure) | Very High (requires extensive training over many episodes) | Suitable for optimization, discovering novel designs through exploration | Slow convergence, requires high computational power |
| Multilayer Perceptrons (MLPs) | Moderate (large labeled datasets) | Moderate to High (suitable for regression and classification) | Moderate | Simple architecture, easy to train, good for classification tasks | Poor for spatial data, lacks interpretability in complex tasks |
| Graph Neural Networks (GNNs) | High (requires structured graph data) | High (effective for data with complex relationships) | High (complex model training) | Can handle data with relational structure (e.g., antenna components) | Difficult to scale, complex to train on large graphs |
| Variational Autoencoders (VAEs) | High (large and diverse datasets for feature generation) | Moderate (good for data generation but less accurate than GANs) | Moderate (depends on network depth) | Useful for generating new designs and learning latent representations | May generate blurry or unrealistic designs, less efficient than GANs |

technique for improving antenna features like gain and bandwidth and reducing their size.

In supervised and unsupervised learning, the model learns to identify and describe features from training data, whereas in RL, the model learns to determine optimal actions in specific situations [43]. Artificial intelligence (AI) aims to endow machines with human-like intelligence, with its origins tracing back to the Dartmouth Conference in 1956. Although the concept was formally proposed then, research in AI began earlier, progressing through phases such as symbolism, connectionism, and behaviorism [44]. Early AI research focused on expert systems, where human expertise was programmed into machines. However, while effective in logical environments (e.g., mathematical deduction), expert systems lack the ability to acquire new knowledge autonomously. Consequently, researchers turned to machine learning (ML) in the 1980s to enable machines to learn independently [45]. This shift marked the rise of connectionism, exemplified by the artificial neural network (ANN) algorithm, and led to significant advancements, including the perceptron model in 1958 [46].

5. Types of metamaterials

Metamaterials can be classified into four major types, as follows:

- A. Electromagnetic Metamaterials (EM)
- B. Photonic Metamaterials (PM)
- C. Acoustic Metamaterials (AM)
- D. Mechanical Metamaterials (MM)

5.1. Electromagnetic Metamaterials (EM)

Particles and traces incorporated in a dielectric matrix make up electromagnetic metamaterials (EM), which give them special electromagnetic characteristics like negative or zero refractive indices. Beam steering, radar antennas, modulators, lenses, microwave couplers, and bandpass filters are only a few of the many applications for these materials [47]. There are two primary categories of EM metamaterials: single-negative metamaterials that show either permittivity or negative permeability. Double-negative metamaterials have a negative refractive index because they exhibit both negative permittivity (ϵ) and negative permeability (μ) [48]. Because of their exceptional electromagnetic qualities, such as negative permittivity and permeability, which allow for greater control over wave propagation, metamaterials (MTMs) are especially preferred in antenna design. Electromagnetic metamaterials (EM) have special electromagnetic properties like zero or negative

refractive indices because they are made up of traces and particles embedded in a dielectric matrix. Beam steering, antenna radars, modulators, lenses, microwave couplers, and bandpass filters are only a few of the many applications for these materials [47]. Single-negative metamaterials, which have either negative permeability or permittivity, and double-negative metamaterials, which have both negative permittivity (ϵ) and negative permeability (μ), which results in a negative refractive index, are the two main categories into which EM metamaterials are generally divided [48]. Metamaterials (MTMs) are favoured in antenna design due to their unique electromagnetic properties, including negative permittivity and permeability, which enhance control over wave propagation. This results in a high degree of miniaturization while increasing antenna gain and bandwidth, thus addressing size and performance challenges in modern communication systems. Furthermore, MTMs reduce mutual coupling in MIMO antenna systems, significantly improving system efficiency and reliability [49]. These materials act as a bridge between the physical and digital realms by enabling dynamic manipulation of electromagnetic waves through digital coding and field-programmable metamaterials. Digital coding metamaterials, illustrated in Fig. 5, consist of coding elements that provide different phase responses by adjusting structural parameters. Each element includes a square metal patch as the top layer, a dielectric substrate as the middle layer, and a metal ground plane as the bottom layer [50]. Phase responses for coding states "0" and "1" are shown in Fig. 5(b), where the dashed and solid curves represent phase differences at 8.7 GHz and 11.5 GHz for a 1-bit coding scheme. This enables the generation of far-field scattered beams that vary according to coding patterns; for instance, patterns like "0" or "1" produce a single reflected beam, while alternating patterns such as "010101..." yield two symmetric beams, as illustrated in Fig. 5(c) and 5(d) [51].

Integrating artificial intelligence (AI) with information metamaterials has led to intelligent metamaterials capable of real-time, adaptive control over electromagnetic waves. This advancement extends traditional EM metamaterials into quantum information science, where they enable the manipulation of quantum states and interactions. Examples include space-time quantum metamaterials that control the spatial, spin, and spectral properties of quantum light [52]. Metamaterial absorbers, particularly those based on split-ring resonators (SRRs), are also useful for material detection due to their sensitivity to different dielectric constants, making them promising candidates for applications in sensing [53]. In the realm of artificial electromagnetic metamaterials (AEM), a common objective is to achieve specific scattered or guided wave states. This is often approached as an "inverse problem," where the desired scattering state (s) is specified, and an algorithm determines the appropriate AEM geometry (g) to produce it.

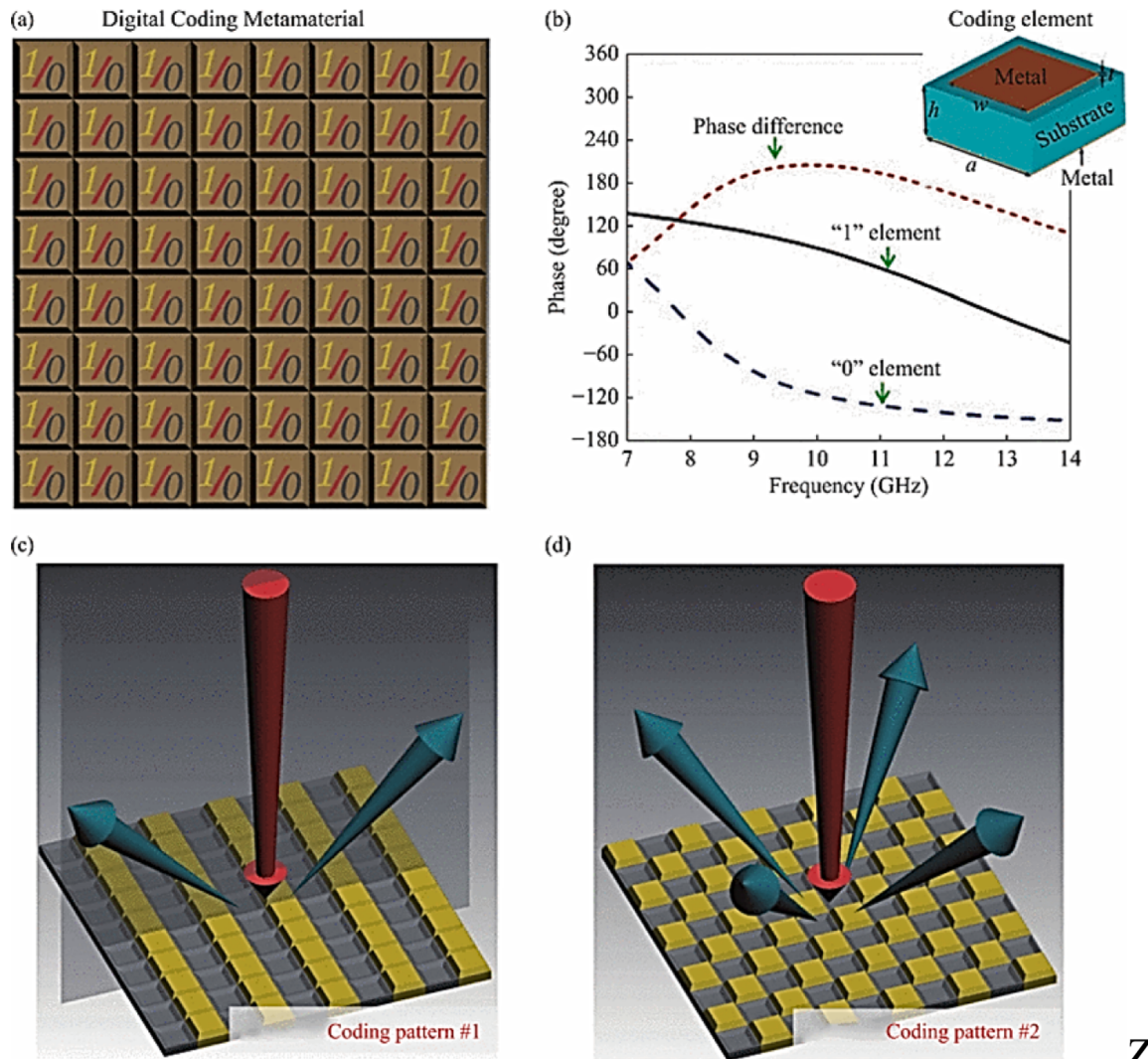


Fig. 5. "0" and "1" are the two types of elements that make up the digital coding metamaterial (a) schematic. (b) The coding element's geometry and the matching 1-bit reflection phases. Diagrammatic representations of beam scattering under various coding schemes are shown in (c) and (d) [48].

Although inverse problems have a rich history, rigorous mathematical approaches only emerged in the 20th century [54]. Hadamard established that a problem is “well-posed” if it satisfies three conditions: (1) existence of a solution, (2) uniqueness of the solution, and (3) stability, meaning the solution’s dependence on initial conditions [55]. A problem is considered “ill-posed” if it fails to meet any of these conditions [56]. Most direct problems in physics are well-posed, as they include initial and boundary conditions, which often guarantee a unique and stable solution. However, inverse problems are frequently ill-posed since they attempt to deduce the underlying cause from an observed effect or, more challenging, to find a cause that achieves a desired effect [57]. In AEM inverse design, issues arise when the specified target falls under three problematic cases: (M1) the target violates physical laws, (M2) it is achievable but not within the selected geometry domain, or (M3) it has multiple possible solutions. Cases M1 and M2 fail to satisfy the existence criterion (H1), while M3 fails the uniqueness criterion (H2). Thus, inverse problems in AEM often violate these Hadamard conditions, posing challenges for deep learning-based inverse modelling [58]. Violations of Hadamard conditions are illustrated in Fig. 6, which shows the interplay between input (S) and user-defined output (G) domains in AEM inverse problems. The inherent in inverse design means that standard neural networks, which approximate the inverse function $g^*=f^{-1}(s)$, may not reliably yield solutions. Ensuring that a solution exists for all s requires

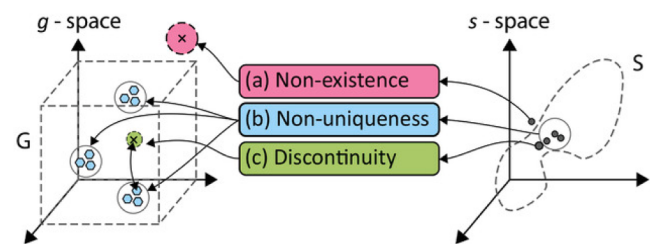


Fig. 6. An Example of Inverse Issues in Which the Three Hazard Conditions Might Not Be Fulfilled: (a) Non-existence: There isn't a solution; it only exists outside of the g -space and is shown as a dashed red circle. (b) Non-uniqueness for Certain s . The problem is one-to-many since there are multiple g solutions for a given spectrum. (c) Discontinuity: The problem is discontinuous when a negligible change in s -space causes a large change in g -space.

that each s belongs to S , a challenging and open problem in AEM inverse design, further discussed in Section 6 [59]. Non-unique solutions (H2 violations) in deep learning models can result in a one-to-many problem, where multiple configurations in G yield the same desired effect s , complicating deterministic modelling. This issue is well-documented and has led to the development of methods to either make models non-deterministic, identifying multiple solutions, or to adapt loss

functions to facilitate exploration of the solution space [60].

Recent investigations have as shown in Fig. 7 advanced DL-based inverse design in AEM, yet few frame these challenges through the lens of ill-posedness. Despite this, there is a universal desire to create models capable of addressing complex, user-defined scattering targets s that may not lie within S . Current work has explored a range of physically consistent yet custom targets, such as spectra variations derived from training data [61], Gaussian or Lorentzian profiles [62], real material responses (e.g., GaSb) [63], or hand-selected transmission points [64].

Deep learning (DL)-based techniques do not require large numerical simulations since they use pre-prepared data to determine the input-output relationship of the system's response. DL-assisted inverse design techniques rely on simulation data of the system's reaction with regard to structural configurations as the training dataset and employ standard algorithms as optimization solvers (as indicated in Table 2). On the other hand, direct DL inverse design uses inverse networks—like generative or tandem networks—to forecast workable architectures straight from the design goals. This method necessitates an additional dataset of simulation-derived optimum solutions. In order to forecast the solutions of partial differential equations (PDEs), physics-informed neural networks (PINNs) use labeled PDE data, boundary/initial conditions (BCs/ICs), and PDE residuals. This eliminates the need for simulation data.

5.1.1. Iterative Inverse Design Method

This optimization technique iteratively looks for workable structures to optimize an objective function. It consists of gradient-based topology optimization (TO) and gradient-free evolutionary algorithms (EAs). Physical simulation and optimization are its two main phases. It can be used alone or in conjunction with deep learning-based modeling for more accurate computations. The particular design and system needs will determine whether to use gradient-based or gradient-free techniques. Although gradient-based TO is dependable and effective, it is only applicable to continuous systems with differentiable goals, and it frequently produces local solutions for non-convex situations. On the other hand, even though EAs are computationally costly, they perform

well in situations when gradient information is not accessible, which makes them appropriate for simpler problems with fewer parameters. To take full advantage of EAs, computational approaches must advance. This section examines the uses of these techniques and covers recent studies on the EM metamaterial inverse design challenge.

5.1.1.1. Topology optimization (TO). A gradient-based inverse design technique called topology optimization (TO) modifies the distribution of materials in a design space to find the best structures. It has been shown to be a dependable instrument in both research and industry, and it is extensively used in many physical disciplines, including mechanics, optics, and electromagnetics. By iteratively improving the material layout to maximize a target function under certain constraints, TO solves optimization problems using numerical simulation techniques such as finite element analysis and finite-difference time-domain (FDTD). By offering directional information toward a local maximum, gradient-based algorithms—like the moving asymptotes method—direct the optimization process. The capacity of TO to manage intricate, expansive designs by dividing the design space into finely detailed components is one of its main advantages. This enables intricate structural personalization, but it can be computationally demanding, particularly for large-scale issues. TO is now able to optimize structures with a large degree of freedom thanks to advancements in approaches like adjoint methods, which have increased the efficiency of derivative calculations. However, TO has trouble striking a balance between design complexity and computing performance, especially when fine meshes are needed for large-scale designs. The optimization results depend on the initial estimate structures chosen, and it is prone to converge to local optima. Furthermore, adding manufacturing limitations may make computations more expensive. TO works well for continuous and differentiable systems, but it is less appropriate for discrete issues, where gradient-free techniques, such as evolutionary algorithms, might be more appropriate. Notwithstanding these difficulties, TO provides unparalleled adaptability in modifying device functionality and is still a potent instrument for inverse design, particularly when customized to meet particular design goals and limitations.

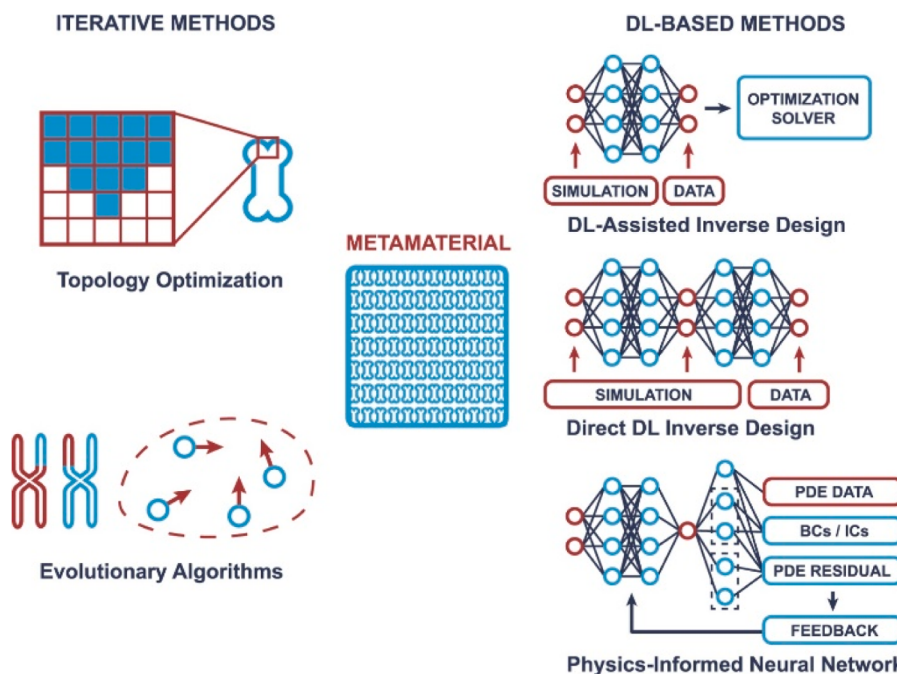
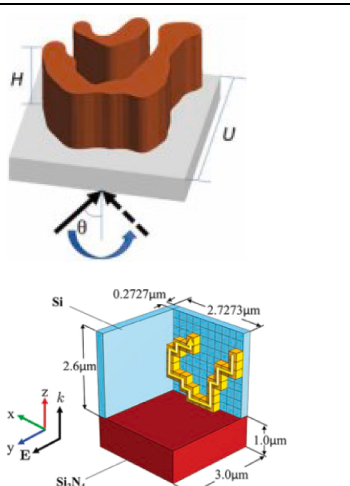
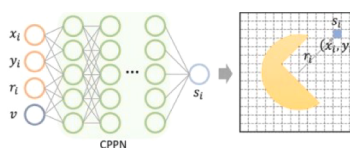
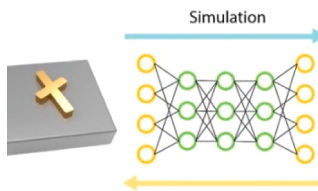
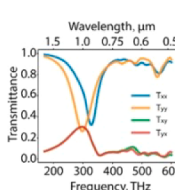
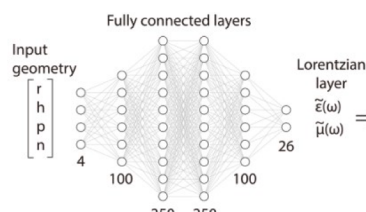
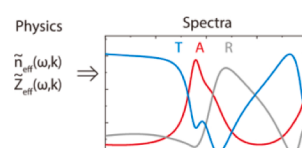


Fig. 7. Types of EM Metamaterial Inverse Design: Topology optimization (TO) and evolutionary algorithms (EAs) are the symbols for gradient-based and gradient-free iterative techniques to EM metamaterial inverse design, respectively. Throughout the design phase, optimization algorithms and numerical simulations collaborate.

Table 2

ML/DL in Electromagnetic Metasurface Design.

| Design Method | Network Type | Network Architecture/ Metamaterial Design and Performance | Description |
|--|---|--|---|
| Iterative Inverse Design Method: | Topology Optimization (TO), Finite Element Analysis (FEA), Finite-Difference Time-Domain (FDTD), Method of Moving Asymptotes (MMA), Adjoint Method, Aperiodic Fourier Modal Method, Gradient-based Algorithms [64–66], Evolutionary algorithms (EAs), (GA), Particle Swarm Optimization (PSO), Covariance Matrix Adaptation Evolution Strategy (CMA-ES), Simulated Annealing, Ant Colony Optimization (ACO), Artificial Bee Colony (ABC) [68–74,75] |  | The schematic of the optimized construction intended to have arbitrary shape birefringence [67]. |
| Direct Inverse Design Method | Deep Learning (DL)-based Surrogate Models, Artificial Neural Networks (ANNs), Deep Residual Network, Compositional Pattern-Producing Networks (CPPNs), Generative Neural Network (GLOnet), Transfer Learning-based Neural Networks, Cooperative Coevolution (CC) Algorithm, Genetic Algorithm (GA)-assisted Neural Networks, Particle Swarm Optimization (PSO)-assisted Neural Networks, Trust-Region (TR) Gradient Algorithm [77,78-79-81] Tandem Network, Generative Adversarial Network (GAN), Progressive Growing of GANs (PGGAN), Convolutional Neural Network (CNN), Artificial Neural Network (ANN), Deep Neural Network (DNN), Physics-Informed Neural Network (PINN) [83–85] |   | The improved nanoantenna trail is shown [76]. Compositional Pattern Producing Network (CPPN) schematic. The network uses a fully connected neural network to estimate the value (s_i) of each pixel after receiving as inputs the coordinates of a pixelated image (x_i, y_i, r_i) and a bias vector (v). Taken from [82]. Neural network-mediated inverse design replaces traditional trial-and-error methods; the suggested generative network architecture is displayed in the right column. Reprinted from [86] |
| Inverse Design Based on Physics-Informed Neural Networks | PINN, DLNN, ANN [87,88-89] |    | A Deep Learning Neural Network (DLNN) schematic diagram. The DLNN is trained using the complex scattering parameters (ω) that are derived from EM simulations. Taken from [90]. |

5.1.1.2. Evolutionary algorithms (EAs). Engineering problems are often non-convex, featuring multiple local optima, which poses challenges for gradient-based methods like Topology Optimization (TO). TO struggles with local optima and is unsuitable for non-differentiable, discrete problems. In contrast, gradient-free Evolutionary Algorithms (EAs) like Genetic Algorithms (GA), Particle Swarm Optimization (PSO), and Covariance Matrix Adaptation Evolution Strategy (CMA-ES) are more versatile. EAs simulate natural processes, exploring solutions without gradient information and are effective for complex design problems. GA encodes parameters as genotypes, using mutation, crossover, and selection for iterative improvements. It's well-suited for combinatorial optimization and can be combined with TO for complex structures. PSO, better for continuous problems, optimizes through particles sharing positional information to find the best solution. CMA-ES adapts a Gaussian distribution for high-dimensional optimization with less computational time. EAs are effective for solving inverse design challenges, particularly in metamaterials, but are computationally demanding as problem dimensions increase. They are often used with regular structures or small parameter sets. Strategies like surrogate models can help reduce computational costs, enhancing the efficiency of EAs.

5.1.2. Direct inverse design method

The direct inverse design method in neural networks offers a rapid, non-iterative approach to optimize structures directly from desired design parameters. This method typically employs artificial neural networks (ANNs) that are trained to learn the mapping between design inputs and optimal structures, bypassing the need for iterative optimization steps. Popular implementations include tandem networks and generative adversarial networks (GANs). Tandem Networks: Tandem networks involve a two-step training process where a forward model predicts physical responses and an inverse model predicts design parameters, which makes them suitable for high-precision applications. These networks are effective for scenarios where specific design constraints require precise tuning, and they often combine both forward predictions and adjustments to meet desired objectives accurately. Generative Networks: GANs and other generative models, such as Variational Autoencoders (VAEs), are trained to produce optimized structures directly from the input data. GANs, for instance, learn from datasets to generate high-dimensional, complex patterns, offering flexibility in creating diverse metamaterial and metasurface designs. While GANs require significant training data, they excel in applications with complex, non-linear design spaces, enabling rapid and efficient generation once training is complete. The direct inverse design method is advantageous due to its speed and the ability to handle complex geometries without iterative refinement. However, challenges include data-intensive training requirements, computational demands, and potential limitations in generalization across different design parameters. This approach is particularly valuable for high-dimensional metasurface and photonic designs where time-efficient and accurate solutions are crucial.

5.1.2.3. DL-assisted inverse design. A deep learning (DL) model was introduced to predict the optical response of metasurfaces, offering faster and more accurate predictions than traditional simulations. This DL-based surrogate model enables quick evaluations, making it suitable for complex design tasks. Although training data requirements remain a challenge, the approach demonstrates significant efficiency improvements. DL models have also been simplified to predict phase and group delays, with combinations of DL and evolutionary algorithms (EAs) like cooperative coevolution leading to more efficient inverse design of metasurfaces. DL techniques such as transfer learning and hybrid frameworks have reduced the need for extensive training data, enhancing optimization capabilities. DL models with EAs have been used to optimize meta-holography and physical meta-atom design,

addressing challenges like limited phase space and computational complexity. Other approaches have used DL-based surrogate models combined with gradient-based methods to accelerate optimization for metasurface designs, achieving significant bandwidth reductions for radar cross sections (RCS). A global topology optimization network, which integrates physics-based gradients into generative neural networks, has been developed to optimize the design of photonic devices. While DL-based methods can introduce errors when extrapolating beyond training data, their speed and ability to approximate complex physical simulations make them valuable for accelerating inverse design processes, particularly when combined with optimization techniques like EAs. Further refinement is needed to balance accuracy and computational efficiency, ensuring reliable results.

5.1.2.4. Direct DL inverse design. Direct inverse design in artificial neural networks (ANNs) allows for rapid, non-iterative prediction of optimal structures based on desired design characteristics, making it highly efficient. Popular implementations include tandem networks and generative networks. Tandem networks involve a two-step training process with a forward prediction model and an inverse model, which is useful for high-precision device design. Generative networks, such as GANs, learn from data to directly produce optimized structures, offering flexibility for complex, high-dimensional designs. Tandem networks have been applied for accurate predictions in metasurface design, while ANN-based approaches have been used to design visible band filters. Combining tandem neural networks with iterative algorithms has also proven efficient in optimizing metasurface designs. GANs enable the generation of diverse metamaterial patterns, though they require extensive training data and can encounter challenges such as high-dimensional interpolation. Improvements in GAN training, such as progressive growing of GANs (PGGANs) and self-attention layers, have enhanced the learning of complex structures, improving metasurface performance and showing promise for advanced design. Although these deep learning methods demand significant training data and computational resources, they offer rapid predictions once trained. Challenges include limited generalization when design parameters change and the need for validation to ensure physical feasibility. Despite these challenges, direct deep learning methods remain valuable tools for certain metasurface design tasks due to their speed and efficiency. A major challenge with using deep learning for inverse design is that these methods often have trouble when they encounter data different from what they learned during training. This can lead to designs that are not realistic or do not perform well. Because of this issue, examining these designs closely is essential to ensure they are correct. Additionally, applying rules based on physics principles can help ensure that the designs are valid and effective.

Deep learning (DL) has the potential to accelerate the inverse design of metamaterials and metasurfaces significantly, but some underlying challenges persist. One major limitation is the necessity for large, high-fidelity training data sets generated by numerically expensive full-wave simulations. Such reliance is an issue related to scalability because it tends to render the models susceptible to data inconsistencies. A second challenge is the DL models' generalizability; trained models generalize weakly to predict relatively different structures or parameter values out of the training dataset's range, limiting the models' capability to deal with actual world variations. DL models cannot satisfy physical laws or fabrication constraints, except by explicit inclusion at this stage, resulting in non-physics or unfeasible designs.

To address these constraints, researchers are currently exploring several promising avenues. One uses physics-based constraints to neural network learning, i.e., physics-informed neural networks (PINNs) [87], to enforce compliance with Maxwell's equations or other governing laws. The other is transfer learning, which is transferred across similar problems to reduce data demands and promote better generalization. Paradigms marrying DL to traditional optimization methods (e.g.,

topology optimization or evolutionary algorithms) offer an equitable trade-off between accuracy and efficiency. Generative models such as GANs and variational autoencoders (VAEs) can potentially search over large, diverse sets of designs, while active research remains to be explored to make them more convergent and stable to train. Such approaches continue to bring the power of DL to the design of high-performance, miniaturized, and customized metamaterial and metasurface antennas.

5.2. Photonic Metamaterials (PM)

Metamaterials designed for optical frequencies, particularly photonic metamaterials, represent an emerging research area in optics. Photonic metamaterials, characterized by zero refractive index, are artificially fabricated, subwavelength periodic structures engineered to interact with optical frequencies [91]. The sub-wavelength period differentiates photonic metamaterials from photonic band gap structures, offering unique functionalities. These materials enhance microscopy techniques by improving contrast and sensitivity, while metasurfaces enable advanced imaging methods such as ptychographic imaging, darkfield microscopy, and label-free biosensing [91]. Additionally, Photonic Crystal Enhanced Fluorescence (PCEF) advances fluorescence microscopy for applications including DNA microarrays and protein detection. Super-resolution microscopy techniques, such as STED, PALM, and SIM, leverage metamaterials to achieve nanoscale imaging beyond the diffraction limit, benefiting from nanofabrication methods like lithography and other cutting-edge nanotechnologies, leading to innovative devices for various applications (Fig. 8) [91].

Graphene, known for its exceptional electrical, thermal, mechanical,

and optical properties, shows promise for photonic and optoelectronic applications, though single-layer graphene (SLG) has limited optical absorption [92]. Researchers have addressed this by creating graphene metamaterials through stacking graphene with dielectric layers, enhancing light-matter interactions. These graphene-based metamaterials overcome fabrication challenges, paving the way for practical applications in energy, LEDs, optical communications, and spintronics (Fig. 8) [92]. Advanced engineering techniques also improve the performance of photonic metamaterial absorbers (PMAs) over conventional absorbers. Morphological engineering, including optimized impedance matching and resonance control, enhances absorption efficiency. Various approaches achieve near-unity absorption and broaden the absorption bandwidth, making PMAs suitable for solar energy, optical sensing, and gas detection. Moreover, advanced structures like plasmonic metasurfaces expand the functionality of PMAs, increasing their versatility across applications [93].

Recent studies have reported a photonic metamaterial analogue of a continuous time crystal: a two-dimensional array of plasmonic molecules supported on flexible nanowires, exhibiting long-range order in space and time and spontaneous oscillations driven by the plasmonic mode of the metamolecules [94]. This system demonstrates a spontaneous phase transition into a super-radiant-like state of oscillations in transmissivity, resulting from many-body interactions between the metamolecules. This long-range ordering, observed in both space and time, presents intriguing potential for studying dynamic classical many-body states with frequency conversion and temporal properties (Fig. 9) [94].

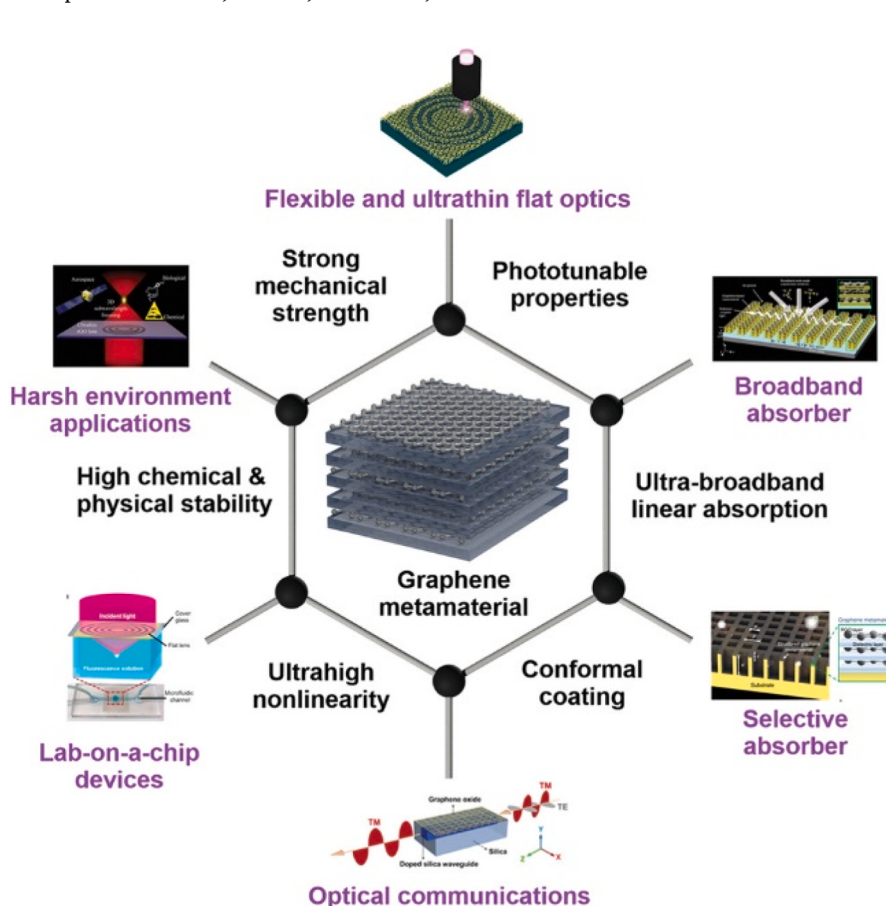


Fig. 8. Schematic Highlight of Unique Properties and Applications of Graphene Metamaterials: Graphene metamaterials possess unique properties that stem from the remarkable characteristics of graphene, such as its high electrical conductivity, flexibility, and tunability. These properties enable applications in various fields, especially in flexible and ultrathin flat optics. Graphene-based metamaterials are ideal for developing compact, lightweight, and flexible optical devices, such as beam steering elements, lenses, and waveguides, that can be integrated into portable or wearable technologies. Reproduced from [92].

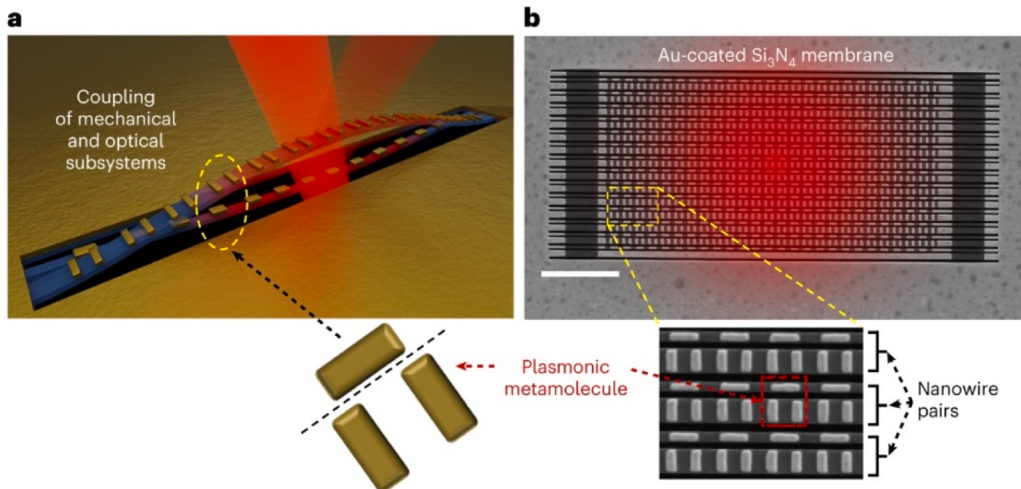


Fig. 9. Array of Plasmonic Metamolecules in Two Dimensions With the help of nanowires: a) Artistic Impression: Two silicon nitride nanowires embellished with plasmonic gold metamolecules form the fundamental building component of the crystal. b) Electron Scanning Microscope Picture: The picture displays the complete two-dimensional plasmonic metamolecule array. The apparatus enters a condition of continuous synchronized nanowire oscillations when illuminated with coherent light (seen by the schematically superimposed laser point). The scale bar is 5 μm in size. Taken from [94].

5.2.1. Basic principles of photonic crystals (PnCs)

Photonic Crystals (PnCs) are periodic materials designed to manipulate sound wave propagation by exploiting scattering and diffraction phenomena. The design of PnCs is based on two fundamental principles: Bragg scattering and the local resonance mechanism. *Bragg Scattering:* When sound waves encounter a periodic structure, they scatter in specific directions based on the periodic arrangement and properties of the scatterers. This scattering leads to the formation of photonic bandgaps frequency ranges where sound waves cannot propagate, creating a forbidden frequency band.

The scattering angle (θ) in Bragg scattering can be calculated by the equation:

$$\theta = \arcsin\left(\frac{\lambda}{2d}\right) \quad (10)$$

where: λ is the wavelength of the incident acoustic wave, and

d is the periodic spacing between the microstructures in the PnC. *Local Resonance Mechanism:* PnCs based on local resonance exhibit bandgaps at lower frequencies due to the resonance of the scatterers within the material. The resonance frequency (ω) for local resonance can be calculated by:

$$\omega = \sqrt{\frac{K}{m}} \quad (11)$$

where: K is the spring constant of the resonant unit, and m is the equivalent mass of the resonant unit. *Bloch–Floquet Theory:* According to Bloch–Floquet theory, the unit cell of a PnC must exhibit periodicity along the x and y axes. The displacement at the boundaries of the unit cell must satisfy the condition:

$$u(r+a) = e^{i(Ka)}u(r) \quad (12)$$

where: u is the displacement matrix for all nodes, a is the lattice constant of the structure, and K is the stiffness matrix of the unit cell. *Eigenfrequency of the Unit Cell:* The eigenfrequency (ω) of the unit cell can be derived from the following equation:

$$(K - \omega^2 M)u = 0 \quad (13)$$

where: M is the mass matrix of the unit cell, K is the stiffness matrix, and u is the displacement matrix of the nodes in the unit cell.

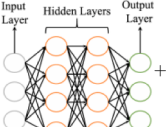
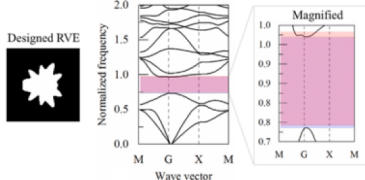
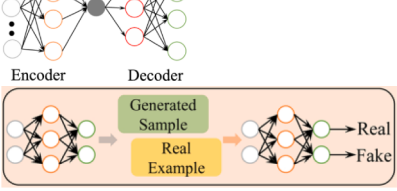
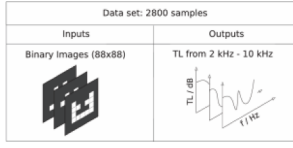
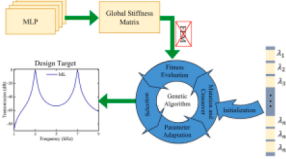
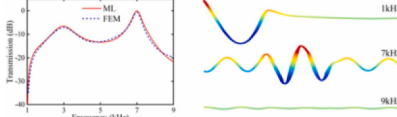
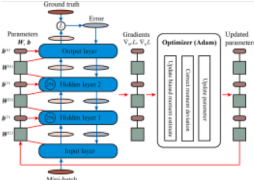
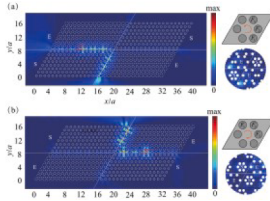
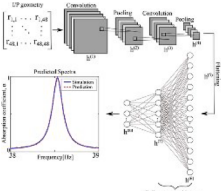
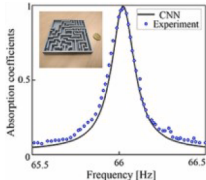
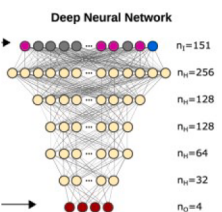
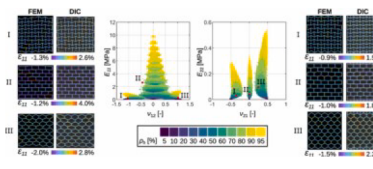
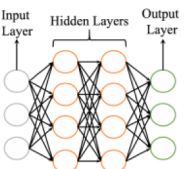
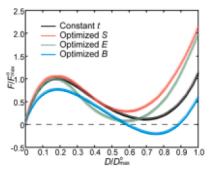
5.2.2. Neural network architecture and working principle

Machine learning (ML) and deep learning (DL) have been increasingly applied to the design and optimization of Photonic crystals (PnCs), with various approaches offering significant advancements as shown in Table 3. Li et al. [95] utilized a combination of multilayer perceptrons (MLPs) and convolutional neural networks (CNNs) for the inverse design of PnCs with magnified bandgaps, incorporating autoencoders (AEs) to extract topological features from randomly generated designs and establish relationships between geometric parameters and bandgap properties. Gurbuz et al. [96] employed conditional generative adversarial networks (GANs) to optimize the transmission loss of acoustic metasurfaces, generating unit-cell geometries that match target frequency responses. Chen et al. [91] demonstrated the integration of MLPs with genetic algorithms (GA) to inversely design multifunctional metabeams, leveraging MLPs as surrogate models for efficient bandgap prediction and optimization. He et al. [93] applied ML for the inverse design of metaplates with topological edge states, using the plane wave expansion method to generate datasets and train models for directional flexural wave propagation. Donda et al. [97] employed CNNs for feature extraction and performance optimization of acoustic metasurfaces, achieving subwavelength sound absorption and broadening the frequency range through systematic design. Pahlavani et al. [98] utilized DL to map the relationships between interface distributions and mechanical properties in planar lattices, facilitating rapid exploration of large design spaces. Liu et al. [99] applied ML to optimize curved beams for bistable energy absorption, predicting nonlinear mechanical properties such as stiffness and snapping forces. Finally, Wang et al. [100] employed variational autoencoders (VAEs) to encode PnC microstructures into a low-dimensional latent space, enabling systematic manipulation of designs and targeted optimization of bandgap properties. These studies collectively highlight the transformative role of ML/DL in advancing the design, optimization, and performance of PnCs.

5.2.3. Application of ML algorithms in PnCs design

5.2.3.5. PnCs Performance Prediction Using ML. Photonic Crystals (PnCs) are periodic materials with unique acoustic properties that can manipulate and control wave propagation. These materials rely heavily on intricate structural designs, and predicting their performance is one of the key challenges in advancing their applications. Machine learning (ML) algorithms provide a transformative approach by leveraging extensive datasets to predict the behavior of PnCs, reducing

Table 3
ML/DL in Photonic Metasurface Design.

| Network Type | Network Architecture | Metamaterial Design and Performance | Description |
|--------------|---|--|--|
| MLP + CNN |  |  | Inverse design of PnCs to broaden bandgap using autoencoders and FEA [95]. |
| GAN |  |  | Inverse design and optimization of PnC unit cells with GAN-guided transmission loss optimization [96]. |
| MLP + GA |  |  | Inverse design of multifunctional metabeams to control vibrational properties [91]. |
| MLP |  |  | Inverse design of topological metaplates and bandgap tuning [93]. |
| CNN |  |  | Design of metasurfaces with acoustic absorption beyond subwavelength scales [97]. |
| MLP/DNN |  |  | Advanced design of mechanical metamaterials using latent space exploration [98]. |
| MLP |  |  | Inverse design and optimization of mechanical beam [99]. |

(continued on next page)

Table 3 (continued)

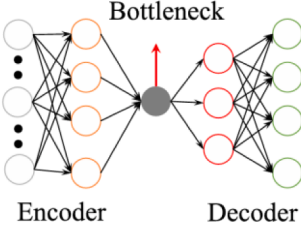
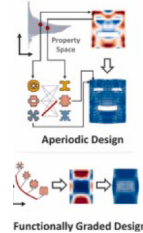
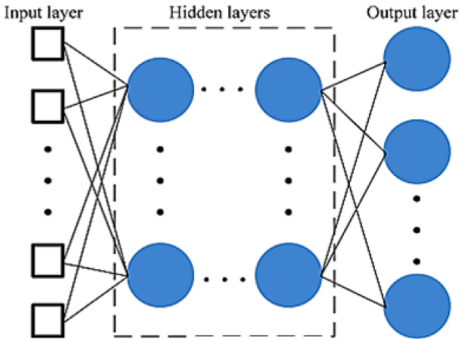
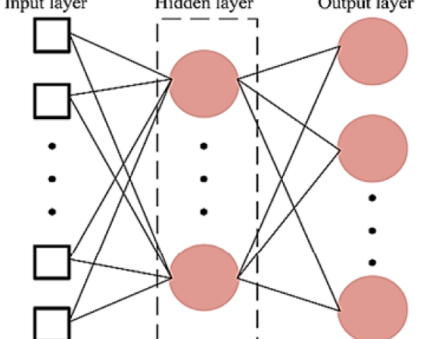
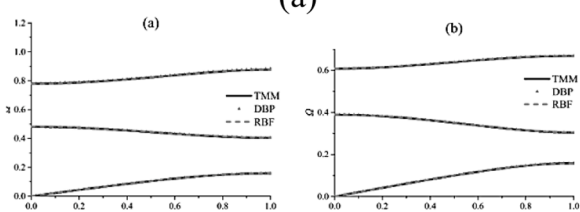
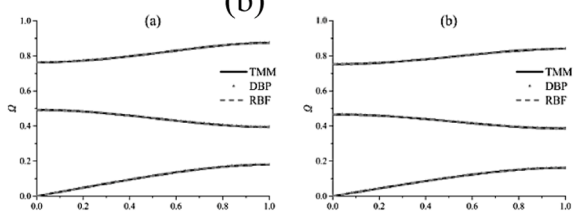
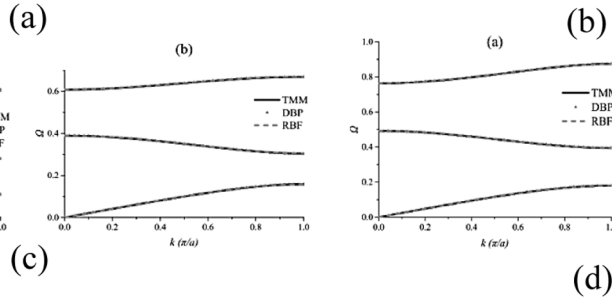
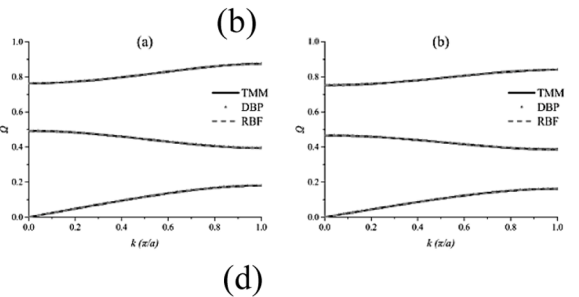
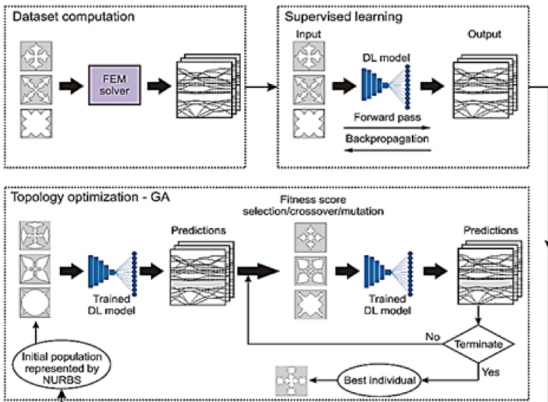
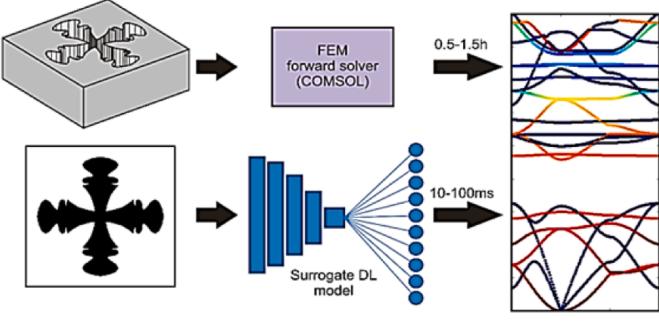
| Network Type | Network Architecture | Metamaterial Design and Performance | Description |
|--------------|---|--|--|
| AE |  |  | Optimization of PnC topologies through feature extraction [100]. |
| |  |  | |
| | (a)  | (b)  | |
| | (c)  | (d)  | |
| | (e)  | (f)  | |

Fig. 10. PnCs Design Framework Effect Diagram and Forecasted Dispersion Relationship: (a) Deep Backpropagation Neural Network (DBP-NN) create Framework: A diagram showing how to create photonic crystals (PnCs) using a DBP-NN. (b) Design Framework for Radial Basis Function Neural Networks (RBF-NN): A comparable diagram illustrating the RBF-NN-based design methodology for PnCs. (c) Diagram of the Single Parameter Prediction Effect: Results for the deep backpropagation neural network are shown on the left(a). Right(b): Outcomes that match the neural network's radial basis function. (d) Two-Parameter Prediction Effect Diagram: Deep backpropagation neural network results are shown on the left(a).Right(b): Outcomes that match the neural network's radial basis function. Reproduced from [101] with Springer Nature's permission. (e) Proxy Deep Learning (DL) Design Framework: A diagram showing how to anticipate dispersion relationships in PnCs using a proxy DL model. (f) Comparison of Prediction Times: A comparison between the time needed to simulate a dispersion curve using the traditional FEM (finite element model) and the time needed to forecast one using the proxy DL model. Reprinted from [102].

computational costs and enabling faster optimization. Traditional numerical simulations, like finite element analysis (FEA), are time-intensive and require significant computational resources, but ML techniques allow for predictive modeling that can bypass these constraints. By understanding the inherent relationship between physical parameters and acoustic properties, ML models can predict key performance metrics such as bandgap width, dispersion relations, and wave attenuation properties, significantly accelerating the design process and enabling comprehensive evaluation of PnC properties.

5.2.3.6. Predicting Dispersion Relations of PnCs. Phonon propagation in PnCs is influenced by Bragg scattering, which creates energy band gaps (BGs) in the dispersion relation. These BGs represent frequency ranges where wave propagation is impeded due to periodic structural interference. Accurate prediction of dispersion relations is vital to optimizing PnC properties and designing new materials. Dispersion relations illustrate how wave energy propagates through the material across various frequencies and wavevectors, revealing critical details about phonon-lattice interactions.

Liu and Yu [101] employed two neural network architectures—deep backpropagation neural networks (DBP-NNs) and radial basis function neural networks (RBF-NNs)—to predict dispersion relations in one-dimensional PnCs. Their study highlighted that RBF-NNs are highly efficient for single-parameter predictions, offering shorter training times and higher accuracy, whereas DBP-NNs excelled in multi-parameter scenarios due to their stability in high-dimensional spaces. The study demonstrated that neural networks could effectively map complex relationships between input parameters, such as lattice constants and elastic properties, to output dispersion characteristics. This approach replaces iterative numerical simulations with direct predictions, drastically reducing computation time while maintaining accuracy. Their results are summarized in Fig. 10 (a–d).

Kudela et al. [102] advanced this by integrating ML into a topology optimization framework for PnCs. Their approach involved three modules: dataset generation using finite element method (FEM) simulations, supervised learning to train a deep learning model, and topology optimization based on genetic algorithms (GAs). The trained ML model replaced traditional FEM solvers, reducing computation time for dispersion map predictions from hours to milliseconds (Fig. 10(f)). This ultrafast prediction capability enabled rapid iterations in topology optimization, allowing researchers to identify designs with optimized bandgap properties efficiently. The dispersion relation maps generated by the model provided detailed insights into frequency-wavevector relationships, enabling fine-tuned control over phonon propagation. Sadat and Wang [103] explored different ML algorithms, including logistic regression, artificial neural networks, and random forests, to predict the presence, center frequency, and width of bandgaps in PnCs. Random forests outperformed other models, achieving the highest accuracy in rapidly screening PnC structures for desired bandgap properties. This capability is particularly valuable in early design stages, where thousands of potential configurations need to be evaluated to identify promising candidates (Fig. 12).

5.2.3.7. Predicting Band Structures in PnCs. While dispersion relations provide critical insights into phonon propagation, the energy band structure offers a more comprehensive view of PnC properties, including detailed bandgap characteristics and wave attenuation capabilities. Predicting energy band structures is inherently more complex due to the higher dimensionality of the problem and the need to account for additional material and structural properties. Javadi et al. [104] utilized a data-driven approach to predict the energy band structure of thermoelastic waves in nanophonic beams. By preprocessing input data, optimizing hyperparameters, and employing both shallow and deep neural networks (DNNs), they developed a robust framework for classifying bandgaps and predicting PnC properties with high accuracy.

Their method significantly reduced computational costs while providing precise predictions of material behavior. Han et al. [105] combined generative adverSARial networks (GANs) with convolutional neural networks (CNNs) for both forward predictions and inverse design of energy band structures. By training a CNN on high-resolution spectral FEM data, they accurately predicted complex energy band structures, including topologies with high spatial attenuation. The GAN component enabled inverse design by generating PnC topologies with targeted bandgaps, making this framework ideal for applications in sound and vibration isolation. Their workflow and results are depicted in Fig. 11.

5.2.4. Inverse design and topology optimization of PnCs

Inverse design is a critical aspect of PnC research, focusing on generating structures that meet specific performance requirements, such as predefined bandgap widths or directional wave propagation. ML algorithms are particularly suited for this task due to their ability to learn from extensive datasets and uncover hidden patterns in design parameters.

Liu et al. [106] employed supervised neural networks (S-NN) and unsupervised neural networks (U-NN) for the inverse design of one-dimensional PnCs. By adjusting structural parameters such as filling ratio, shear modulus ratio, and mass density ratio, these networks achieved target bandgap requirements with high accuracy. U-NNs were particularly effective for multi-parameter designs, outperforming S-NNs in robustness and computational efficiency. Compared to traditional genetic algorithms (GAs), neural networks significantly reduced computation times while maintaining design accuracy. The framework and results are shown in Fig. 13.

Miao et al. [107] introduced a deep neural network (DNN) combined with a GA for inverse design of two-dimensional PnCs. The DNN predicted band boundaries with high precision, while the GA optimized structural parameters to meet target requirements. This hybrid framework generated optimized PnC structures within seconds, demonstrating both speed and accuracy in addressing complex design challenges. Reinforcement learning (RL) approaches, such as the Q-learning algorithm implemented by Luo et al. [108], further enhance inverse design capabilities. By defining states, actions, and rewards, RL algorithms can intelligently explore design spaces to maximize bandgap width or achieve specific energy band characteristics. Maghami and Hosseini [109,110] extended this approach with deep reinforcement learning (DRL), enabling real-time generation of design parameters without iterative searching. This method proved particularly effective for designing thermoelastic PnCs, where traditional optimization methods struggle with high-dimensional parameter spaces (Fig. 14). Advanced DL frameworks, such as conditional GANs and variational autoencoders, have also been applied to inverse design tasks [111,112]. These models enable probabilistic exploration of design spaces, offering solutions that maximize target performance metrics while accommodating uncertainties. For example, Lee et al. [113] demonstrated the use of conditional GANs for narrow band-pass filter design, achieving high transmittance at target frequencies with minimal computational effort.

5.3. Acoustic metamaterials (AM)

5.3.1. Properties and applications

Acoustic metamaterials are engineered using two or three distinct materials with varying mass densities and bulk moduli. These unique combinations enable the materials to achieve negative effective mass densities and bulk moduli, allowing precise control over sound wave behaviour. Designed for manipulation, regulation, and monitoring of sound waves in various media—such as liquids, solids, and gases—these materials achieve this by carefully tuning their bulk modulus and mass density. Li et al. [114] provide an in-depth review of acoustic metamaterials, covering resonance-based and topological approaches, supported by theoretical analysis and experimental validation.

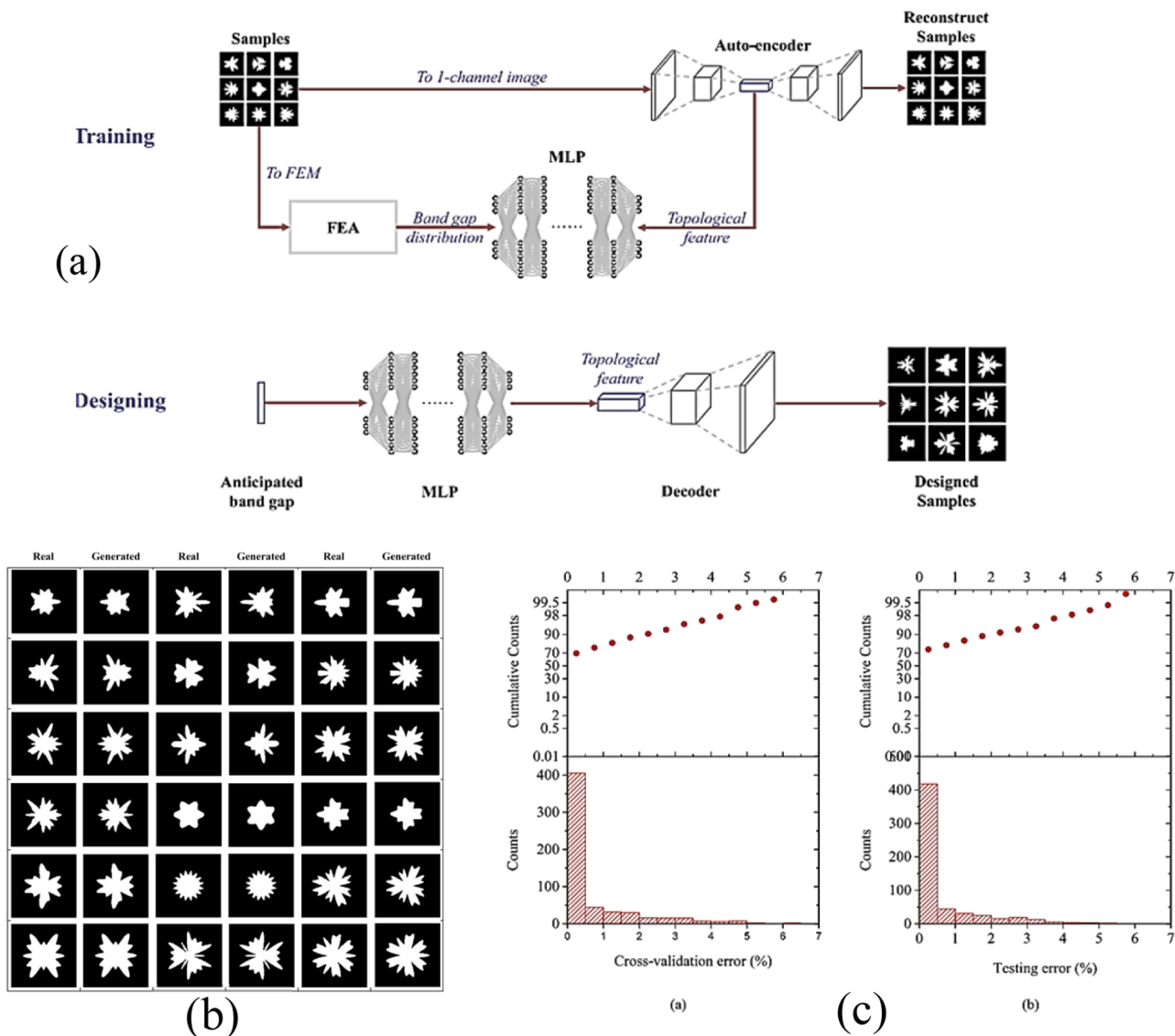


Fig. 11. Diagram of the Prediction Effect and the Deep Learning Framework Reprinted from [95], Elsevier-approved, Copyright 2019. (a) Diagram of the Deep Learning Design Framework: A schematic illustration of the deep learning design framework. (b) Test and Generated Samples: Topological representations of test samples and some generated samples, respectively. (c) Error Distribution: A visual representation of the distribution of test and cross-validation errors that emphasizes the framework's dependability and performance.

5.3.2. Resonance-Based acoustic metamaterials

Decorated membrane resonators (DMRs) are a key component of resonance-based acoustic metamaterials. These structures exhibit anti-resonance behaviour, which results in the total reflection of acoustic waves due to their divergent dynamic mass density. By increasing the curvature energy density through resonance, DMRs can achieve substantial acoustic absorption. However, their performance is constrained by the relatively thin membranes used in their construction.

5.3.3. Broadband optimal acoustic absorption structures

Achieving specific absorption spectra is influenced by causality constraints, which impose minimum thickness requirements. Fabry-Perot resonators are often utilized in integration schemes to achieve tunable broadband absorption spectra. While this approach enables a high degree of control, the absorption spectrum may remain below unity at the limiting line due to inherent material and structural limitations.

5.3.4. Topological Acoustics and One-Way Edge States

Acoustic metamaterials can also exploit topological properties, such

as one-way edge states and negative or zero refractive indices. Spatially coiling structures are capable of forming Dirac cones, enabling unique propagation behaviors. By introducing a spatially varying gauge field or pseudo-magnetic field within a photonic crystal, researchers can achieve Landau level quantization and one-way edge states. Additionally, breaking lattice symmetry can create topologically non-trivial bandgaps that support these edge states. For underwater applications, acoustic metamaterials show potential in areas like resource development, imaging, navigation, and communication. Despite their promise, challenges such as impedance mismatches and mode transitions remain significant. Techniques like acoustic invisibility and beam steering, achieved through locally resonant metamaterials and conformal transformation, address some of these issues. Future research may explore bioinspired transformation acoustics to improve directional emission and target detection. Effective underwater acoustic manipulation techniques have already been demonstrated experimentally, as reported in [115].

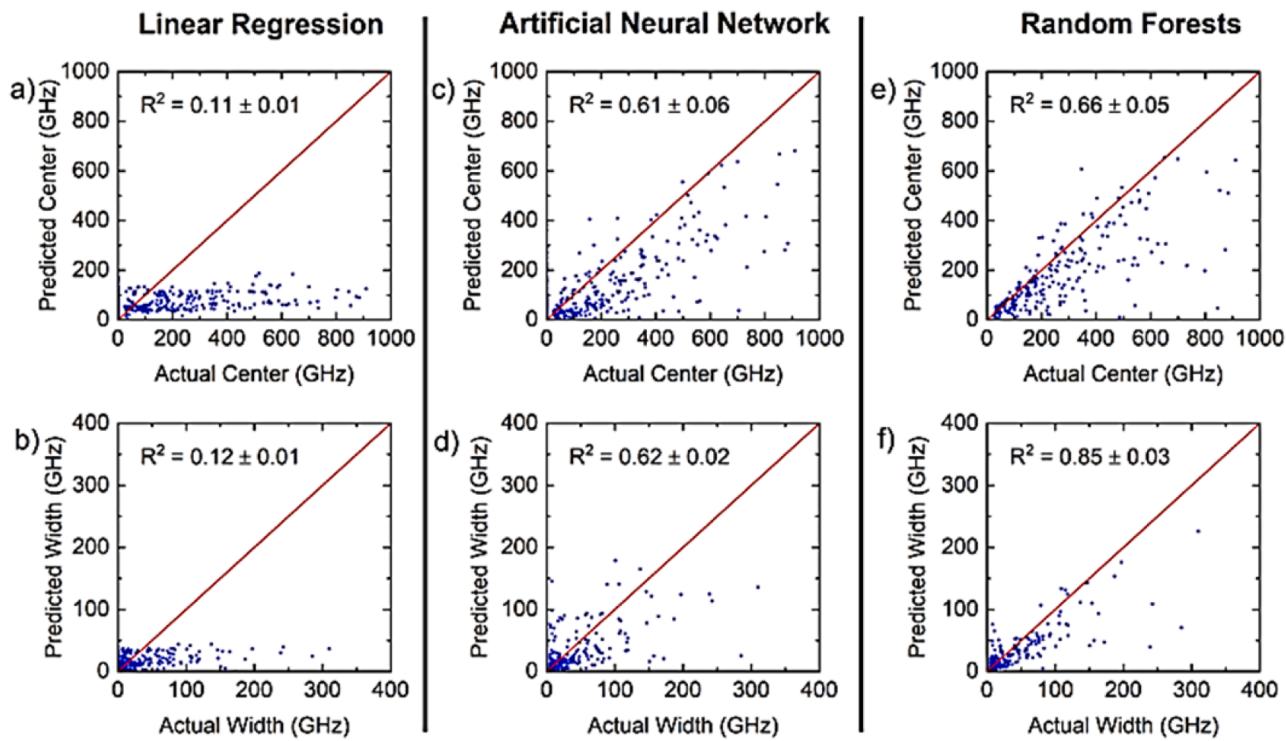


Fig. 12. Machine Learning Model Prediction Renderings with Known Bandgaps Reprinted from [103] with AIP Publishing's consent. Linear Regression Models (a) and (b): Prediction representations in relation to bandgap widths (b) and centers (a). Artificial Neural Network (ANN) Models (c) and (d): Prediction representations in relation to bandgap widths (d) and centers (c). Random Forest Models (e) and (f): Prediction outcomes for bandgap widths (f) and centers (e).

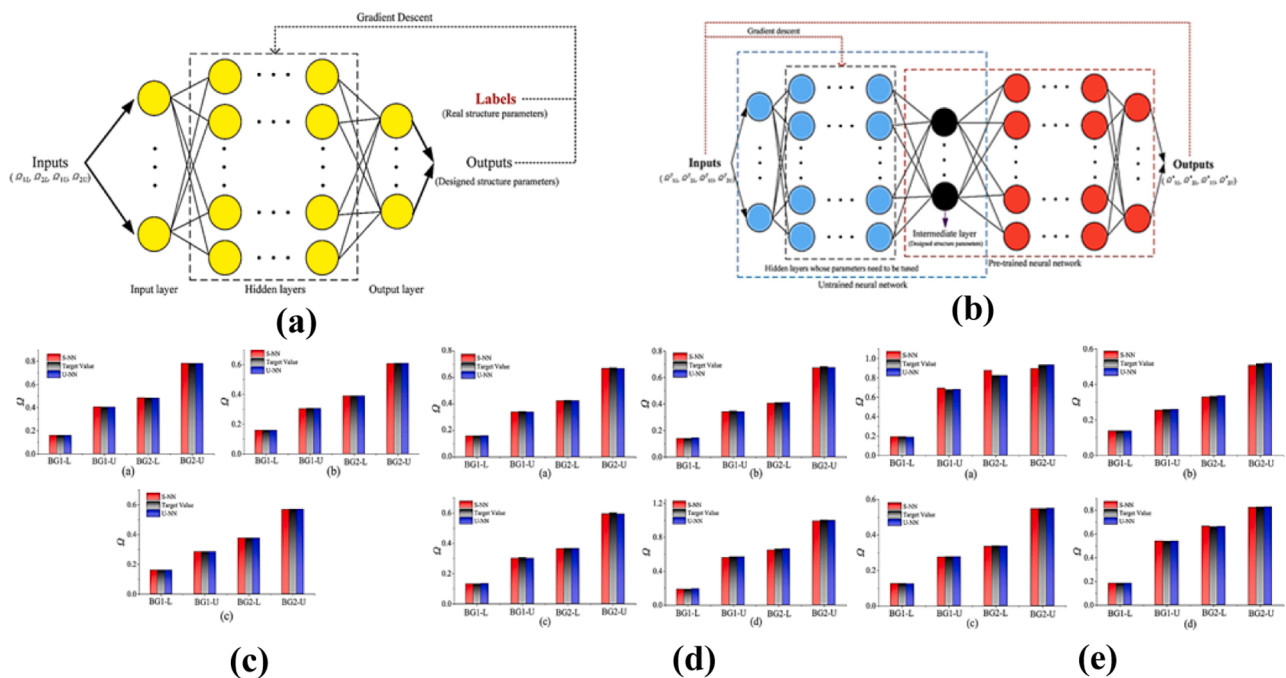


Fig. 13. Effect Diagram of Supervised and Unsupervised Neural Networks in Intelligent Reverse Design of One-Dimensional PnC Reprinted from [106] with AIP Publishing's consent. (a) Design Framework for Supervised Neural Networks (S-NN): A diagram showing the design framework under human supervision (b) Unsupervised Neural Network (U-NN) Design Framework: An illustration of the autonomous learning-driven design framework. (c) Single-Parameter Design Renderings: Findings showing how well the S-NN and U-NN models perform in terms of design for single-parameter predictions. (d) Results comparing S-NN and U-NN models for two-parameter predictions in two-parameter design renderings. (e) Three-Parameter Design Renderings: Outcomes demonstrating the S-NN and U-NN models' capacity for three-parameter forecasting.

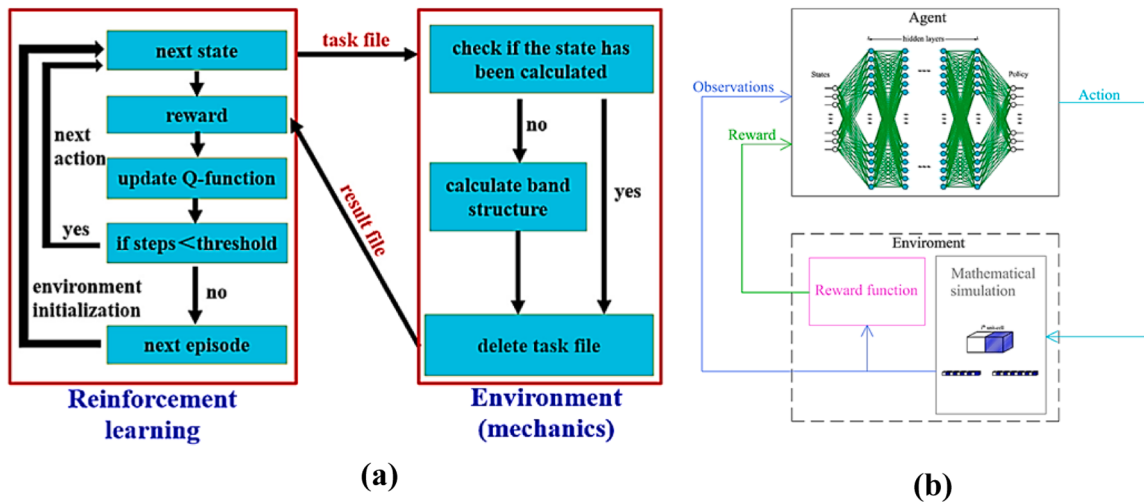


Fig. 14. Reinforcement learning design framework diagram (a) Reinforcement learning framework for layered photonic crystals (PnCs): A schematic illustration of the reinforcement learning framework used in PnC design. Reprinted from [108], Elsevier-approved, Copyright 2020. (b) Deep Reinforcement Learning Design Process for PnCs: A summary diagram showing how deep reinforcement learning is used in the design process to maximize photonic crystal qualities. Reprinted from [109].

5.3.5. Noise pollution mitigation with acoustic metamaterials

Acoustic metamaterials offer innovative solutions for noise control, particularly for low-frequency noise that traditional materials cannot effectively mitigate. These lightweight, compact materials are capable of manipulating sound waves through structural optimization. Gao et al. [116] provide an extensive review of the development and classification of acoustic metamaterials, detailing their physical mechanisms,

application scenarios, and current research trends in noise reduction. Active acoustic metamaterials, for example, adjust their acoustic parameters in response to external stimuli, making them suitable for dynamic noise environments. Active acoustic metamaterials can be categorized into sound-insulation and sound-absorption types. The sound-insulation category often employs mechanisms like piezoelectricity to regulate sound transmission and absorption. By fine-tuning



Fig. 15. Schematic of the general classification and application of acoustic metamaterials [116].

material properties, such as resonance elements and elastic matrices, these materials can achieve tunable acoustic characteristics. Designs like adaptive Photonic crystals and beam-type metamaterials enhance the versatility of these materials for adjustable sound insulation. The general applications of these materials are illustrated in Fig. 15.

5.3.6. Advanced phenomena and practical applications

Acoustic metamaterials demonstrate intriguing phenomena, including negative refraction, anomalous Doppler effects, and perfect sound absorption. Various designs have been proposed to harness these effects, with experimental prototypes showing significant promise. For instance, extraordinary transmission of sound waves can be achieved in systems featuring periodic air grooves and grating-copper plate structures. These curled spatial configurations are essential for producing the unique metamaterial properties required for extraordinary acoustic transmission. Practical applications of acoustic metamaterials include elastic wave isolation, acoustic cloaking, and sound absorption. Gao et al. [116] highlight advancements in both passive and active noise reduction, emphasizing the growing role of structural and material innovation. Moreover, experimental efforts continue to refine these materials for broader adoption, offering effective solutions to acoustic challenges in diverse fields. Further research into these structures promises enhanced performance and new possibilities for sound wave manipulation [117].

5.3.7. Basic principles of AMs

Acoustic metamaterials (AMs) control acoustic wave equations in a homogeneous medium, described as follows:

$$\frac{\partial^2}{\partial t^2} = \frac{K}{\rho} \nabla^2 p \quad (14)$$

where ρ is the mass density and K is the bulk modulus of the fluid medium. Here, p represents the sound pressure, and t is time. The acoustic wave velocity, which controls wave direction changes at interfaces, is given by:

$$c = \sqrt{\frac{K}{\rho}} \quad (15)$$

Acoustic impedance (Z_0) is defined as the ratio of the pressure in the wave to the fluid velocity, expressed as $Z_0 = p/v = K\rho$. Impedance controls the amplitude of reflection and transmission at the interface. Compared to traditional acoustic materials, the properties of AMs and Photonic crystals (PnCs) are often represented by transmission loss $TL(\theta)$ and sound absorption coefficient. Transmission loss at an incident angle θ is calculated as:

$$TL(\theta) = 10 \log \left[1 + \left(\frac{\omega m_s \cos^2 \theta}{\rho c} \right) \right] \quad (16)$$

where m_s is the mass per unit area, ω is the angular frequency of the sound wave, and ρ and c are the density and speed of sound in air, respectively.

The sound absorption coefficient (α) measures the sound absorption performance of acoustic materials, reflecting the material's ability to absorb sound. It is calculated as:

$$\alpha = \frac{E_i - E_r}{E_i} = 1 - \frac{E_r}{E_i} \quad (17)$$

where E_i is the incident sound energy, and E_r is the reflected sound energy. When sound waves strike the surface of the AM structure perpendicularly, the acoustic impedance Z_0 can be used to represent the reflection coefficient, and the sound absorption coefficient becomes:

$$\alpha = 1 - |r|^2 = 1 - \left| \frac{Z_0 - \rho c}{Z_0 + \rho c} \right|^2 \quad (18)$$

In evaluating AMs and PnCs, additional factors such as negative refractive index, phonon bandgap, and other unique properties are also essential. For negative index materials, equivalent parameters are given by:

$$n_{eff} = \frac{n}{c_0} \quad (19)$$

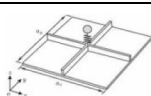
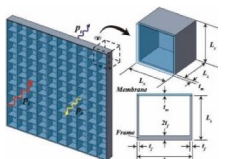
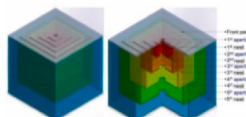
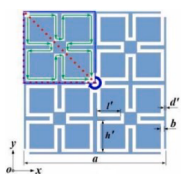
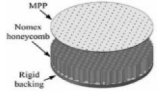
where n_{eff} is the equivalent refractive index of the negative index material, n is the speed of light in a vacuum, and c_0 is the phase velocity in the negative index material.

Calculating the phonon bandgap involves using Brillouin zone theory and numerical simulations. The Brillouin zone boundary is defined based on the PnC lattice structure, with the bandgap frequency range determined by analyzing phonon dispersion relations within the Brillouin zone. Various numerical simulation methods—such as the transfer matrix method, plane wave expansion method, finite difference time domain method, and multiple scattering method—are employed to solve the acoustic wave equation or dynamic equations. These methods model the PnC structure, calculate the frequency and mode of phonons, and ultimately determine the phonon bandgap by analyzing the propagation modes within the specified frequency range.

5.3.8. Types of common AMs

Different types of AMs can be seen in Table 4. Resonant acoustic metamaterials (AMs) incorporate resonant structures, such as helical springs and mass-spring resonators, into their microstructures, exhibiting unique acoustic properties like negative impedance and elastic modulus within specific frequency ranges. These properties facilitate phenomena such as negative refraction and phonon band gaps through local resonance effects, requiring precise adjustments to geometry, size, and material parameters. Xiao et al. [118] developed locally resonant thin plates on homogeneous thin plates, using the Plane Wave Expansion method to evaluate bandgap attenuation performance. Nouh et al. [119] proposed metamaterial plates with periodic cells and built-in local resonances. Xi-Xi et al. [120] introduced stiffened plates with spring-vibrator resonance units to expand Bragg bandgaps, while Jian et al. [121] enhanced low-frequency bandgap generation using double cantilever structures. Membrane-type AMs, also known as thin-film AMs, employ thin films combined with mass units to manipulate acoustic waves through dynamic mass effects, enabling selective sound transmission or reflection. Mei et al. [122] designed asymmetric lamella-decorated thin films for low-frequency sound absorption, while Zi-Hou et al. [123] embedded piezoelectric elements in elastic membranes for tunable acoustic properties. Zhou et al. [124] presented distributed thin-film AMs for acoustic isolation in the 20–1200 Hz range, and Jang et al. [125] created box-frame thin-film AMs capable of blocking sound waves across specific frequency bands. Helmholtz AMs leverage resonators consisting of cavities and necks to modulate sound waves via mass-spring-damping mechanisms. Fang et al. [126] introduced periodic Helmholtz resonators with acoustic inductance and capacitance properties, while Duan et al. [127] proposed hexagonal cellular resonators for broadband underwater absorption. Yang et al. [128] designed parallel Helmholtz AMs with multiple cavities for broader absorption, and Yang et al. [129] later developed nested Helmholtz resonators for suppressing narrowband noises. Space-coiling AMs feature coiled structures that extend sound wave propagation paths, offering properties like double negativity and high refractive index. Traditional space-coiling unit cells [130] have evolved into tapered labyrinthine designs [131], symmetric coiled structures [132], and quasi-fractal geometries [133]. Composite structural AMs combine diverse components to achieve tunable acoustic properties. Lee et al. [134] integrated membranes with Helmholtz resonators for negative density and modulus, while Fok and Zhang [135] combined resonating structures for double-negative AMs. Fei et al. [136] used micro-perforated panels (MPP) and Fabry-Perot channels for up to 99%

Table 4
Types of Acoustic Metamaterial.

| Type | Fig. s | Description | Citation |
|------------------------------|---|--|-----------|
| Resonant-Type AMs |  | Locally resonant stiffened plates. | [118–121] |
| Membrane-Type AMs |  | Box frame thin-film AM for frequency-specific noise control. These AMs exploit the dynamic mass effect for efficient low-frequency isolation. | [122–125] |
| Helmholtz Resonance-Type AMs |  | Modular nested Helmholtz resonators for multiple noise suppression. These AMs offer precise sound modulation through tailored resonance. | [126–129] |
| Space-Coiling AMs |  | Quasi-fractal geometries for recursive substructures. These AMs provide high refractive index and double-negative properties but face size and fabrication challenges. | [130–133] |
| Composite Structural AMs |  | Honeycomb core with MPP structure for 99% resonance frequency absorption. | [134–137] |

sound absorption below 500 Hz, and Xie et al. [137] incorporated honeycomb cells with MPPs, forming Helmholtz resonators for enhanced sound absorption.

5.3.9. Optimization of metamaterial structures based on ML/DL models

Machine learning (ML) and deep learning (DL) have transformed the field of acoustic metamaterials (AMs) by enabling precise optimization and innovative design methodologies (Table 5). Neural networks, as general ML models, have been widely utilized in AM structure optimization due to their ability to learn nonlinear relationships and represent features from input data. Deep neural networks (DNNs), with their multiple hidden layers, provide advanced capabilities for abstract and high-level feature representations, improving the performance and expressiveness of models for AM design [138–147]. Cheng et al. [148] implemented the inverse design of composite acoustic absorber units, combining Helmholtz resonant cavities and porous materials using DNNs and deep self-encoder networks to improve design efficiency and accuracy. Similarly, Liu et al. [149] addressed challenges in the design of phonon plate metamaterials by employing DNNs and combining them with multi-objective optimization algorithms to create a framework that enhances the efficiency of AM design processes. Du and Mei [150] further demonstrated the use of DNNs in the intelligent design of acoustic retroreflectors, achieving efficient reflection functions across wide and continuous ranges of incidence angles. Convolutional neural networks (CNNs), designed for processing spatial and image data, have also been extensively used in AM optimization. These networks analyze the relationships between acoustic properties and structural parameters based on two-dimensional cellular maps of metamaterials. For instance, Zhao et al. [151] introduced a dual-CNN framework for designing hypersurfaces, achieving regional acoustic field control and providing significantly higher accuracy than traditional genetic algorithms. Donda et al. [97] utilized CNNs to simulate broadband absorption responses for ultrathin surface absorbers, feeding geometric inputs into the CNN for prediction and optimization, which proved effective in resolving

bandwidth limitations of conventional acoustic absorption materials. Wu et al. [152] proposed a multi-fidelity complex CNN model for predicting high-dimensional scattered sound fields with low data costs, reducing the computational time to just 8% of traditional genetic algorithms. Reinforcement learning (RL) and deep reinforcement learning (DRL) further contribute to AM structure optimization by allowing algorithms to autonomously learn and optimize acoustic properties [153]. Shah et al. [154] proposed a semi-analytical approach using DRL to suppress acoustic scattering by optimizing the design parameters of cylindrical scatterers, utilizing a double deep Q-learning network (DDQN) to minimize total scattering cross sections (TSCS). Shah and Amirkulova [155] extended this framework to optimize design parameters, such as position, radius, and material properties, for metamaterials to minimize scattering effects. Generative DL models represent another critical advancement in AM design by expanding training datasets and generating new structures with desired properties. Amirkulova et al. [156] combined variational self-encoders, supervised learning, unsupervised learning, and Gaussian processes to approximate and minimize acoustic wave scattering in the design of 2D acoustic cloaks. Gurbuz et al. [96] employed a conditional generative adversarial network (CGAN) to design soundproofing unit cells for AMs, achieving tailored designs based on input acoustic properties. Lai et al. [157] utilized conditional Wasserstein GANs (WGANs) combined with CNNs to simulate TSCS in rigid cylindrical configurations, demonstrating efficient computational performance. ML also facilitates the prediction of AM properties, significantly enhancing the design process [158–160]. Ding et al. [161] proposed a DL algorithm for modelling nonlocal hypersurfaces, enabling accurate multi-channel reflection predictions with a relative error of less than 1%. Ciaburro and Iannace [162] constructed a regression tree model to predict sound absorption coefficients, providing detailed sensitivity analyses for various input variables. Tran et al. [163] used a CNN model to simulate multiple acoustic wave scatterings in cylindrical structures, achieving efficient inverse design of scatterer configurations. Thang et al. [164] developed

Table 5
Role of ML/DL.

| Role of ML/DL | Mechanism | Description | Citation |
|--|-----------|---|--------------------|
| Metamaterial Structure Optimization Using DNN and CNN Models | | Du and Mei combined DNNs with multi-objective optimization for designing retroreflectors. CNNs are specialized for spatial data | [97, 144–151] |
| Structure Optimization Using DRL Models | | Shah and Amirkulova expanded this approach to optimize metamaterial design parameters, improving performance beyond traditional optimization methods. | [154,155] |
| Generative DL Models for Metamaterial Design | | Amirkulova et al. combined generative models with multiple scattering theory to minimize acoustic scattering. | [96,156,157] |
| Prediction of AM Properties Using ML | | Regression tree prediction model framework | [161–164, 171] |
| Reverse Design of AMs Using DL | | Yinggang et al. used DL to predict vibration transmission properties, achieving on-demand design. | [167–170, 172–174] |

a predictive ML framework for optimizing meta-structures and designed cylindrical cloaks to minimize TSCS, combining a variational self-encoder with Gaussian processes. Reverse design has become a critical area of interest, with ML enabling on-demand development of AMs with specific acoustic properties [165,166]. Zhang et al. [167] constructed a forward and backward network framework to design metamaterials based on target sound absorption curves, achieving high accuracy and generalization performance. Hou et al. [168] employed DL to create a neural network for reverse design, reducing the time required to solve inverse problems by using wavelength-refraction curves to predict desired structures. Yinggang et al. [169] proposed a DL-based method for the intelligent prediction and design of acoustic ultra-material bundles, utilizing fully connected networks to achieve on-demand reverse designs. Miao et al. [170] extended this approach by

proposing the inversion design of megapixel holograms based on acoustic metasurfaces, reconstructing configurations with high precision.

We use various methodologies to address the variation of simulation results from experiments while formulating deep learning (DL) models for actual applications of the designs of metamaterials so that models can be utilized reliably for actual applications. They include data augmentation to introduce variability to generalize the model better, using experimental data with simulation data to address actual shortcomings, and transferring learning to transfer the models to actual applications through fine-tuning. A blending of physics-based methods with DL is also utilized for conforming to the underlying physics laws and leveraging the versatility of deep learning. Uncertainty quantification is introduced into the training to address the discrepancies better,

make the model even more reliable, and make the model function better under actual scenarios. These methodologies play an essential role in overcoming the challenges of bridging the translation of simulation to experiments to the actual implementation of designs of metamaterials.

5.4. Mechanical metamaterials (MM)

Mechanical metamaterials are artificial composite materials designed to exhibit unique mechanical properties, such as a negative Poisson's ratio, negative elastic modulus, zero shear modulus, and frictional properties. These materials are often constructed with the inclusion of secondary materials or controlled porous structures, enabling them to achieve properties not found in traditional materials. Mechanical metamaterials, or architected materials, form an advanced

class of composites engineered for applications ranging from sports-shoe soles to deployable space structures. Other commercial applications include acoustic sound absorbers and vibration isolators, while scientific applications extend to gravitational-wave detection and seismic protection. Key properties of mechanical metamaterials include backward wave propagation, topological band gaps, unidirectional sound propagation, and elastic wave polarization. However, two critical research questions remain: determining the effective elastic properties and optimizing microstructural design. These metamaterials could find wider applications by integrating mechanical properties with optical, electrical, and thermal functionalities [98]. The field of mechanical metamaterials focuses on innovative microstructural designs that enable new mechanical properties and highlight the potential for multifunctional integration, such as sensing, energy harvesting, and actuation. These

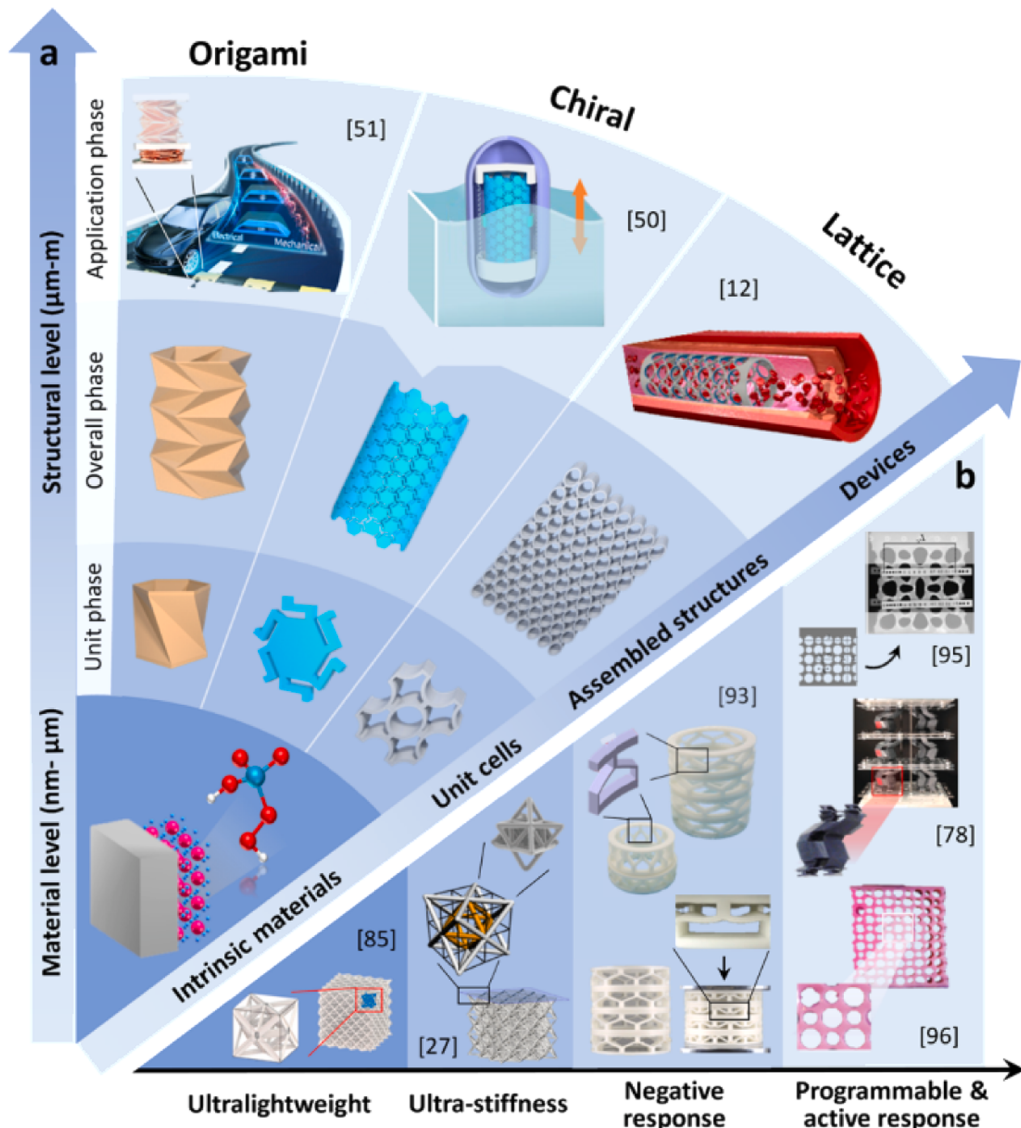


Fig. 16. Mechanical Metamaterial Formation: Transitioning from Material to Structural Levels: A hierarchical design procedure that moves from the material level to the structural level creates mechanical metamaterials. Because of their meticulously designed microstructures, these materials have special qualities. Types of Mechanical Metamaterials Metamaterials made of origami: These incredibly flexible structures, which can be folded into small forms, were inspired by origami principles. They are extensively used in energy absorption and deployable systems. Chiral Metamaterials: These materials, which have chiral microstructures, are made for uses where torsional stiffness and negative Poisson's ratios are necessary. Metamaterials on Lattices: These metamaterials, which are frequently utilized in ultra-lightweight and high-strength applications including automotive and aerospace components, are composed of periodic lattice structures. Extraordinary Mechanical Properties: Mechanical metamaterials exhibit remarkable qualities like as Ultra-lightweight: Perfect for situations where weight is a concern, this product has a low density and excellent performance. Extremely stiff: Exceptional stiffness in relation to weight. Negative Response: Displaying characteristics such as negative stiffness or negative Poisson's ratio. Programmable Response: The ability to modify mechanical behavior to meet particular functional requirements. adapted from [175].

features could support the development of intelligent systems capable of environmental adaptation. Additionally, the paper identifies challenges in current research and emphasizes the role of data-driven approaches, particularly artificial intelligence, in optimizing the design and functionality of mechanical metamaterials for future applications. Mechanical metamaterials, with their tailored microstructures, provide mechanical properties beyond those of conventional materials. Current research primarily explores passive mechanical metamaterials, while there is a growing drive toward developing active and functional systems. Integrating advanced functionalities such as sensing, actuation, and energy harvesting could transform these materials into intelligent systems. Data-driven methods, especially artificial intelligence, hold significant potential for optimizing designs and enhancing multi-functionality. Emerging applications for mechanical metamaterials include energy harvesting devices, smart sensors, and soft robotics. These materials can be classified by their microstructural design, such as origami, chiral, and lattice metamaterials (Fig. 16) [175]. Advances in mechanical metamaterials demonstrate their exceptional static and dynamic properties. Early developments included static mechanical metamaterials with unusual elastic characteristics, such as auxetics and Penta modes, which are used in ultra-lightweight deployable structures for space exploration and compact acoustic and vibration absorbers for vehicles. They also have scientific applications, including vibration isolation in optical interferometers and seismic waveguides for building protection. Dynamic mechanical metamaterials, also known as acoustic or elastic metamaterials, are increasingly used to control mechanical energy in unconventional ways, enabling diverse applications, such as:

- Acoustic Cloaking: Metamaterials that render regions invisible to acoustic waves without altering their inherent properties.
- Mechanical Energy Barriers and Isolators: Structures designed to dissipate, confine, or convert mechanical energy, useful in sound attenuation and vibration isolation.
- Wave Beam Steering and Wave Guiding: Systems that redirect energy flow without energy loss, applicable in areas like ultrasonic imaging.
- Acoustic Black Holes: Metamaterials that trap and absorb sound waves by simultaneously controlling the direction and magnitude of energy flow.

Despite these advances, manufacturing challenges remain, as many mechanical metamaterials are large and costly for applications such as traffic noise and seismic wave shielding. Recent nanofabrication advancements open new possibilities. Currently, microscale (GHz or THz) and even nanoscale Photonic crystals and acoustic metamaterials with ultra-high working frequencies are under development. These could lead to optical and thermal devices for signal processing and sensing. Emerging technologies, such as "phoxonic crystals," combine acoustic, optical, and electromagnetic wave manipulation, potentially offering even more versatile functionalities for dynamic metamaterials [100].

5.4.1. Design of static characteristics in mechanical meta-structures

Mechanical meta-structures, with their extreme static performance, are a growing focus in ML-enabled design. By leveraging machine learning (ML), high-performance meta-structures can be optimized by altering components, allowing for unique mechanical properties. Typically designed and optimized on planes for specific shapes or material compositions. Convolutional Neural Networks (CNNs) are widely used

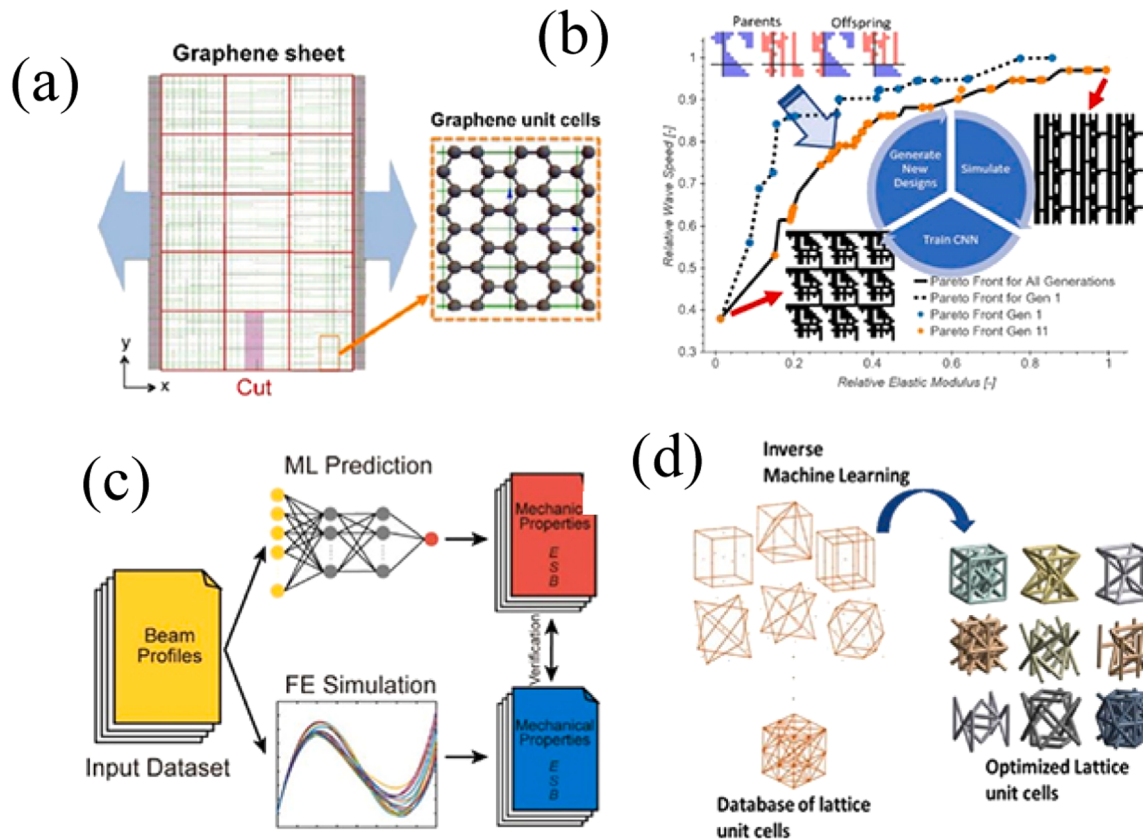


Fig. 17. Using Machine Learning to Design Static Properties for Mechanical Meta-Structures: (a) Graphene Kirigami Design: To maximize stretching performance, graphene kirigami is optimized through the gradual training of a CNN [177]. Reproduced from Ref [177] with permission. (b) Lattice Metamaterial Design: CNN and a genetic algorithm (GA) are combined to create lattice metamaterials that satisfy the limitations of additive manufacturing [180]. (c) Curved Beam Design: To create curved beams with the best mechanical qualities, optimization techniques and a multilayer perceptron (MLP) are used [99]. (d) Lightweight Lattice Structures: Using a GAN-based inverse design framework to create lightweight lattice structures [181].

for image feature extraction in such designs. Gu et al.: Developed a self-learning CNN model that iteratively learns patterns from high-performance structures, achieving designs superior to the training set [176]. Hanakata et al.: Designed stretchable graphene kirigami (Fig. 17(a)) with controllable cutting density and positions to optimize elastic stretchability. Their CNN was trained to predict stretchability via yield strain and further refined through molecular dynamics-calculated datasets. They later proposed a supervised autoencoder (AE) for improved designs [177,178]. Kollmann et al.: Used CNNs to optimize 2D metamaterials for bulk modulus, shear modulus, or minimized Poisson's ratio. Their dataset was generated via topology optimization with periodic boundary conditions [179].

To achieve optimal 2D designs with superior mechanical properties, machine learning (ML) techniques such as CNNs, GANs, and GAs are often combined, as summarized in Table 6. *Combining CNN with GAN or GA:* Tan et al.: Developed a deep convolutional GAN (DCGAN) to generate candidate structures adhering to geometric constraints, with a CNN mapping microstructure to their properties. The combined models enable inverse design of microstructural materials with targeted mechanical properties [182]. Garland et al.: Integrated CNN and GA for structural lattice metamaterials, meeting additive manufacturing constraints (Fig. 17(b)) [180]. Wang et al. and Chang et al.: Applied this paradigm to inverse design of shell-based metamaterials and auxetic metamaterials with zero Poisson's ratio, respectively [183,184]. Tian et al.: Combined CNN and GAN to design meta-structures with customized Poisson's ratios. The CNN predicts global Poisson's ratio responses, while GAN performs inverse structural design through adverSARial training [185]. *Design and Optimization of One- and Three-Dimensional Meta-Structures:* Liu et al.: Designed curved beams with optimal mechanical properties (stiffness, forward snapping force, backward snapping force) using an MLP-based framework (Fig. 17(c)). The MLP predicts mechanical properties based on thickness distributions and integrates into an optimization cycle to refine beam design [99]. Challapalli et al.: Proposed a GAN-based inverse design framework for lightweight lattice structures (Fig. 17(d)). This framework incorporates initial and boundary conditions and forward regression for distinguishing real data, iteratively training GAN to generate structural units with enhanced mechanical performance [181].

Applying deep learning (DL) to metamaterial and metasurface antenna design faces several critical challenges that need to be addressed for optimal performance. One key challenge is the availability of high-quality, comprehensive datasets, which are essential for training DL models. To overcome this, future research could focus on creating robust datasets through improved data collection methods, including simulations and leveraging transfer learning for smaller datasets. Another significant challenge is ensuring that models generalize well to unseen designs, which could be addressed by developing hybrid models [82, 186,187] that combine data-driven DL approaches with physics-based models. Additionally, the computational cost of training DL models in high-dimensional spaces remains a concern, and future efforts could explore more computationally efficient algorithms, such as model pruning or surrogate models, to reduce resource requirements. The interpretability of DL models is also a pressing issue, and future research could focus on improving explainability through techniques like explainable AI (XAI) or attention mechanisms. Finally, translating optimized DL designs into manufacturable structures remains a challenge, which could be mitigated by integrating advanced manufacturing techniques, such as 3D printing, into the design process. Addressing these challenges will drive future advancements in the field and enable more practical and efficient designs for metamaterials and metasurfaces.

6. Application of metamaterials

6.1. Metamaterial as absorber

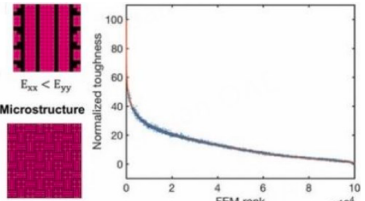
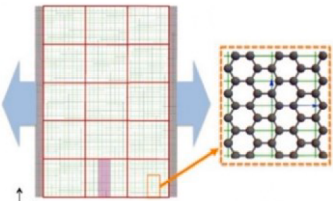
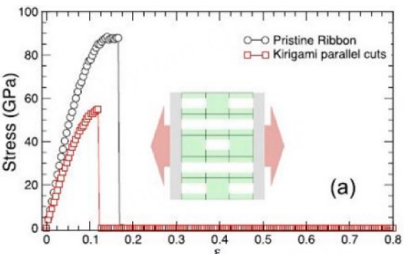
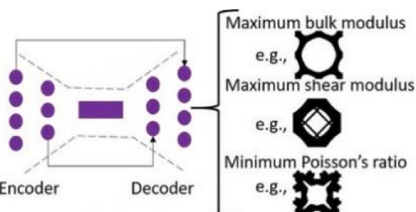
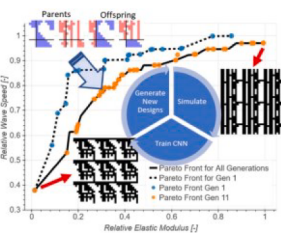
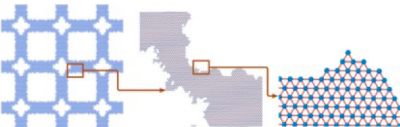
Metamaterial absorbers are advanced structures designed to

efficiently absorb electromagnetic radiation, finding applications in emitters, photodetectors, sensors, infrared camouflage, wireless communication, and solar photovoltaics. By leveraging the effective medium design of metamaterials and loss components of permittivity and magnetic permeability, they achieve high electromagnetic absorption. Recent innovations include a tungsten-based absorber with over 90% absorption across 400–750 nm and 70% absorption at oblique angles up to 60°, ideal for photovoltaics and thermal emitters [188]. Another design, featuring a three-layer metal-dielectric-metal structure, achieves 96.77% average absorption from 389.34 to 697.19 nm and nearly 99.99% at 545.73 nm, with ultra-broadband absorption for both TE and TM polarizations, making it highly suitable for solar energy harvesting and optical sensors [189]. An ultrathin metasurface absorber composed of tungsten nanowires demonstrates perfect absorption in the UV range (~350–400 nm) and ~85% in the visible range of 400–750 nm. Effective medium theory validates its high absorption rate of 95% and operating bandwidth of 450 nm, making it suitable for biosensing, solar cells, and thermal emitters [190]. Another design, a simple Al/SiO₂/Al sandwich structure, acts as a hybrid dual-resonator absorber, achieving over 95% absorption from 450 to 600 nm. Electric and magnetic field studies, along with an inductance-capacitance circuit model, help explain its geometry-dependent absorption characteristics. This structure is useful for optical management and photovoltaic applications, with tunable absorption across different frequency regions [191]. An ultra-thin film absorber made of Ni/SiO₂ achieves high absorption rates of over 96% for transverse electric polarization and 92% for transverse magnetic polarization, remaining effective at angles from 0° to 80° with a half-cylinder cross-section. Its robustness against fabrication errors makes it suitable for thermal emitters, optical energy harvesting, and thermal detectors [192]. Lastly, a new ultrathin, two-layer absorber based on diamond dielectric arrays on a metal substrate achieves an average absorption rate of 93.3% in the visible range. This design, resulting from electromagnetic dipole and lattice resonances, is polarization-independent and angle-insensitive, offering potential for light energy acquisition, optoelectronics, and sensing devices [193].

6.2. Metamaterial as super-lens

The diffraction limit is a fundamental constraint of conventional lenses and microscopes that limits their resolution, preventing the transmission of evanescent waves, which are non-propagating components carrying fine-scale details. One approach to overcome this limitation is to increase the refractive index, though this is restricted by the availability of high-index materials. The super lens improves resolution by enhancing and recovering these evanescent waves, enabling the capture of information at very small scales. Optical imaging systems, such as microscopes and space telescopes, rely heavily on refractive lenses to extend human vision, enhancing our ability to observe objects beyond the capabilities of the naked eye. These systems can be cumbersome and complex, with limitations on achieving super-resolution beyond the diffraction limit. Techniques like STED and STORM have advanced resolution but rely on resource-intensive computational methods. In the early 2000s, metamaterials introduced a new perspective by altering optical properties through subwavelength structures. This led to the development of negative index materials and super lenses with theoretically unlimited resolution by amplifying evanescent waves, though practical applications remain limited due to high losses and fabrication challenges. Recent advancements in flat lenses, such as metalenses and multi-level diffractive lenses, demonstrate their potential in creating compact and high-performance imaging devices. A new polarization-insensitive metalens design based on anisotropic TiO₂ nanofins achieves achromatic performance from 460 to 700 nm while maintaining diffraction-limited resolution. This design features a single layer of nanofins with a numerical aperture of 0.2 and a diameter of 26.4 μm, making it suitable for applications from imaging to

Table 6
ML/DL in mechanical meta-structures.

| Design type | Algorithm | Meta-structure and performance | Description | Year |
|--------------|---------------|---|---|------|
| 2D structure | CNN |  | Greatly reduces computational time compared to traditional finite element methods [176]. Inverse design of high-toughness hierarchical structures | 2018 |
| | CNN |  | Achieves optimal designs under given yield strain and stress conditions [177]. Optimal cutting mode for stretchable graphene kirigami structures | 2018 |
| | Supervised AE |  | Allows exploration of new structures but may bias mechanical performance predictions beyond the dataset [178]. Generates structures by passing potential variables to the decoder | 2020 |
| | CNN |  | Robust in accuracy and inference time [179]. Predicts 2D metamaterials with the best mechanical properties. | 2020 |
| DCGAN, CNN, | |  | Efficiently controls geometric constraints with high design flexibility [182]. Combines DCGAN and CNN for designing microstructures | 2019 |
| CNN, GA | |  | Identifies Pareto-optimal designs using small datasets and handles complex nonlinear constraints [180]. Combines CNN and GA for structural design | 2021 |
| CNN, GAN | |  | Generates structures beyond the dataset and mimics real structural responses [185]. Inverse design of 2D metamaterials with predefined Poisson's ratio | 2022 |

(continued on next page)

Table 6 (continued)

| Design type | Algorithm | Meta-structure and performance | Description | Year |
|-----------------|-----------|--------------------------------|---|------|
| 1D/3D structure | MLP | | Efficiently achieves optimized mechanical properties for various objectives [99]. Accurate prediction and optimization of variable thickness curved beams | 2020 |
| | GAN | | Generates and experimentally verifies lattice designs with superior mechanical performance [181]. Lightweight lattice structures with high load-bearing performance | 2021 |

virtual and augmented reality [194]. Another recent development is a light-field camera utilizing a metalens array of gallium nitride nanoantennas for broadband achromatic imaging. This camera, featuring a 60×60 array of meta lenses each $21.65 \mu\text{m}$ in diameter, provides diffraction-limited resolution of $1.95 \mu\text{m}$. It captures light intensity and direction, allowing refocusing and depth reconstruction for applications in robotic vision, autonomous vehicles, and virtual/augmented reality [195]. Progress in metalenses has led to the development of Hybrid Achromatic Metalenses (HAMLs) with refocusing capabilities that correct chromatic aberration. Using recursive ray tracing and a phase library, HAMLs achieve diffraction-limited numerical apertures of 0.27, 0.11, and 0.06, with efficiencies between 60% and 80%. Fabricated with low-index materials via multi-photon lithography or molding, HAMLs can be adapted to larger diameters and numerical apertures for enhanced functionality [186]. Computational wavefront coding in metalenses, achieved through simple circular or square nanopillars, enables polarization-insensitive and broadband achromatic imaging by designing focal depths to overlap at a specified focal plane. Particle swarm optimization in the optical communication band (1300–1700 nm) has optimized the PIA-ML, providing stable focusing and imaging across a large wavelength range [196]. Traditional lens design suggests that correcting chromatic aberrations requires multiple surfaces. However, [197] demonstrates how a single diffractive flat lens can achieve correction across a wide bandwidth using a phase-only, lossless pupil function. This lens, with a 3 mm diameter and 5 mm focal length (numerical aperture of 0.3, f/1.59), functions achromatically from 450 nm to 1 μm (NIR) and has been experimentally characterized for point spread functions and off-axis aberrations. In another advancement, [198] illustrates chromatic aberration control with a single diffractive surface, eliminating the need for multiple optical elements. The designed MDL is $\leq 10 \mu\text{m}$ thick, $\sim 1 \text{ mm}$ in diameter, with an 18 mm focal length, sustaining consistent focal length across wavelengths from 0.45 μm (blue range) to 15 μm (long-wave infrared). Experiments and simulations verify this method's high NA and its potential to simplify imaging systems by avoiding refractive lenses. A novel approach using optimized light coherence has enabled large-scale achromatic multi-level diffractive lenses within a new design framework. Polymer lenses from 1 to 10 mm in diameter have been fabricated, showing superior performance over a broad wavelength range (400–1100 nm). This technique has significantly improved white-light imaging performance over conventional refractive lenses, paving the way for practical planar optical devices [199]. The diffraction limit is a fundamental constraint in conventional lenses and microscopes, restricting their resolution by

preventing the transmission of non-propagating evanescent waves, which carry fine-scale information. One way to enhance resolution is by increasing the refractive index, but this approach is limited by the availability of high-index materials. The super lens overcomes this limitation by amplifying and recovering evanescent waves, allowing the capture of information at nanoscale levels. Optical imaging systems, like microscopes and space telescopes, are essential for extending human vision, but they are often complex and struggle to achieve super-resolution beyond the diffraction limit. While techniques like STED and STORM improve resolution, they are computationally expensive. In the early 2000s, metamaterials provided a breakthrough by modifying optical properties through subwavelength structures, offering a new approach to surpassing the diffraction limit and enabling super-resolution imaging. This led to the development of negative index materials and super lenses with theoretically unlimited resolution by amplifying evanescent waves, though practical applications remain limited due to high losses and fabrication challenges. Recent advancements in flat lenses, such as metalenses and multi-level diffractive lenses, demonstrate their potential in creating compact and high-performance imaging devices. A new polarization-insensitive metalens design based on anisotropic TiO₂ nanofins achieves achromatic performance from 460 to 700 nm while maintaining diffraction-limited resolution. This design features a single layer of nanofins with a numerical aperture of 0.2 and a diameter of 26.4 μm , making it suitable for applications from imaging to virtual and augmented reality [194]. Another recent development is a light-field camera utilizing a metalens array of gallium nitride nanoantennas for broadband achromatic imaging. This camera, featuring a 60×60 array of meta lenses each $21.65 \mu\text{m}$ in diameter, provides diffraction-limited resolution of $1.95 \mu\text{m}$. It captures light intensity and direction, allowing refocusing and depth reconstruction for applications in robotic vision, autonomous vehicles, and virtual/augmented reality [195]. Progress in metalenses has led to the development of Hybrid Achromatic Metalenses (HAMLs) with refocusing capabilities that correct chromatic aberration. Using recursive ray tracing and a phase library, HAMLs achieve diffraction-limited numerical apertures of 0.27, 0.11, and 0.06, with efficiencies between 60% and 80%. Fabricated with low-index materials via multi-photon lithography or molding, HAMLs can be adapted to larger diameters and numerical apertures for enhanced functionality [186]. Computational wavefront coding in metalenses, achieved through simple circular or square nanopillars, enables polarization-insensitive and broadband achromatic imaging by designing focal depths to overlap at a specified focal plane. Particle

swarm optimization in the optical communication band (1300–1700 nm) has optimized the PIA-ML, providing stable focusing and imaging across a large wavelength range [196]. Traditional lens design suggests that correcting chromatic aberrations requires multiple surfaces. However, [197] demonstrates how a single diffractive flat lens can achieve correction across a wide bandwidth using a phase-only, lossless pupil function. This lens, with a 3 mm diameter and 5 mm focal length (numerical aperture of 0.3, f/1.59), functions achromatically from 450 nm to 1 μm (NIR) and has been experimentally characterized for point spread functions and off-axis aberrations. In another advancement, [72] illustrates chromatic aberration control with a single diffractive surface, eliminating the need for multiple optical elements. The designed MDL is $\leq 10 \mu\text{m}$ thick, ~1 mm in diameter, with an 18 mm focal length, sustaining consistent focal length across wavelengths from 0.45 μm (blue range) to 15 μm (long-wave infrared). Experiments and simulations verify this method's high NA and its potential to simplify imaging systems by avoiding refractive lenses. A novel approach using optimized light coherence has enabled large-scale achromatic multi-level diffractive lenses within a new design framework. Polymer lenses from 1 to 10 mm in diameter have been fabricated, showing superior performance over a broad wavelength range (400–1100 nm). This technique has significantly improved white-light imaging performance over conventional refractive lenses, paving the way for practical planar optical devices [199]. These innovations collectively address the challenges of chromatic aberration, efficiency, and miniaturization in optical imaging, pushing the boundaries of what is possible with flat lens technology. Performance metrics for these systems include diffraction efficiency, J_ω (F) and parameter P relative to the effective height H_{eff} . Here, H_{eff} is defined as $(n-1)H$, where H represents the structural height and n is the refractive index [199]. Efficiency values are normalized by calculating diffraction efficiency and adjusting for transmittance and polarization conversion ratio (PCR). There is a strong positive correlation between comprehensive performance metrics and effective height H_{eff} , indicating that increasing H_{eff} enhances lens performance. Diffraction efficiency can, in principle, be calculated and is usually slightly higher than overall efficiency, as transmittance is less than unity. In highly transmissive cases, the diffraction efficiency may approach the theoretically calculated value and the experimentally measured one. For metasurfaces with polarization rotation based on PB phase design, the polarization conversion ratio should be considered together with the transmission efficiency [200].

6.3. Metamaterial as cloaks

In the realm of metamaterial research focused on cloaking applications, several innovative methodologies have been introduced by different research groups. Singh et al. (2021) proposed a novel approach utilizing a metamaterial structure with unique geometric configurations to achieve broadband invisibility in the microwave frequency range, effectively manipulating electromagnetic waves to reduce the radar cross-section (RCS) of objects [201]. Similarly, Wang et al. (2019) developed a zero-refraction metamaterial composed of periodic arrangements that demonstrated enhanced stealth performance by guiding electromagnetic waves around an object, thereby reconstructing the wavefront to avoid detection [202]. Meanwhile, Zhang and Liu (2021) focused on a tunable metamaterial cloak that leverages adjustable parameters to achieve dynamic cloaking over a range of frequencies, offering potential applications in adaptive stealth technologies [203]. In another study, Fernandez et al. (2020) designed a metamaterial-based cloak using a transformation optics approach, which minimizes scattering by effectively bending light around an object, providing near-perfect cloaking within a specified bandwidth [204]. Lastly, Gupta and Sharma (2018) presented a comprehensive analysis of metamaterial-based cloaks that utilize layered structures to achieve multi-band cloaking, which could be crucial for next-generation stealth materials in defense applications [205].

6.4. Metamaterial as sensor

Recent advancements in metamaterials have significantly impacted the development of highly sensitive sensors across various applications. Alrayes and Hussein (2020) designed a metamaterial-based sensor incorporating a split-ring resonator (SRR) and a Hilbert fractal curve to enhance sensitivity in biomedical applications, specifically for distinguishing between different types of cancer cell lines based on their electrical properties [206]. Similarly, Sharma et al. (2021) developed a terahertz metamaterial sensor with multi-resonance characteristics, providing high sensitivity for detecting trace gases and environmental pollutants. Their sensor design, characterized by a periodic arrangement of unit cells, exhibited an enhanced response in the terahertz frequency range, demonstrating potential for environmental monitoring [207]. Meanwhile, Liu et al. (2020) explored a metamaterial sensor based on a graphene-covered dielectric substrate, achieving tunable resonances and high sensitivity suitable for chemical and biological sensing applications [208]. Kim and Park (2018) focused on a metamaterial-inspired optical sensor designed for detecting biochemical substances, utilizing a nano-patterned array structure to achieve high sensitivity and specificity in the visible spectrum [209]. Lastly, Wang et al. (2019) proposed a planar metamaterial sensor optimized for ultra-sensitive detection of glucose concentrations in biomedical samples, demonstrating the ability to provide real-time monitoring with minimal sample preparation [210].

6.5. Metamaterial as phase compensator

Metamaterials have revolutionized the development of phase compensators, enabling precise control over electromagnetic wave propagation and opening up new possibilities in optical and photonic applications. Lee et al. (2018) designed electrically tunable multifunctional metasurfaces based on hyperbolic metamaterial substrates, demonstrating dynamic control of phase and amplitude modulation for next-generation ultracompact integrated optical systems [211]. Droulias et al. (2019) explored loss compensation and amplification in metallic metamaterials, presenting new approaches for enhancing electromagnetic wave interactions at the nanoscale, which is crucial for phase modulation applications [212]. Meanwhile, Kildishev et al. (2020) introduced a metamaterial-based phase compensator that utilizes an array of nano-antennas to achieve precise phase control and tunable waveform manipulation, highlighting its potential for adaptive optics and beam shaping applications [213]. In another study, Yang and colleagues (2021) developed an all-dielectric metamaterial structure capable of achieving broadband phase compensation by manipulating Mie resonances, which offers significant advantages in reducing optical losses and improving device performance in various optical applications [214]. Finally, Zhang et al. (2019) presented a phase compensator using a metamaterial absorber-based design, optimizing phase response across a wide frequency range for high-capacity imaging and sensing applications, demonstrating the versatility and functionality of metamaterials in practical applications [215].

7. Metamaterials/Metasurface in antenna design (effect of metamaterials on antenna parameters)

Metamaterial coatings have significantly enhanced the performance of electrically small electric and magnetic dipole antennas, boosted radiated power and improved radiation and matching properties. For instance, the latest metamaterial antenna can radiate up to 95% of the input radio signal at 350 MHz, with a design as compact as one-fifth of the wavelength. Metamaterial coverings on patch antennas improve directivity, and a zero-index metamaterial flat aperture on a flat horn antenna demonstrates enhanced directivity as well. Zero-index metamaterials, when used in antennas, maintain a constant phase across all points in the field, resulting in improved gain and reduced return loss.

Research has shown that metamaterials can enhance antenna parameters such as gain, bandwidth, directivity, suppression of off-side lobes and back lobes, and overall efficiency. These advancements have led to reduced antenna sizes, better gain, wider bandwidth, and the development of multiband antennas, marking significant progress in antenna technology.

7.1. GAIN

Low gain is a significant limitation of small planar antennas, particularly in transceiver devices where maximizing energy efficiency is critical. To overcome this, incorporating metamaterials has emerged as an effective solution. Metamaterials, such as artificial magnetic

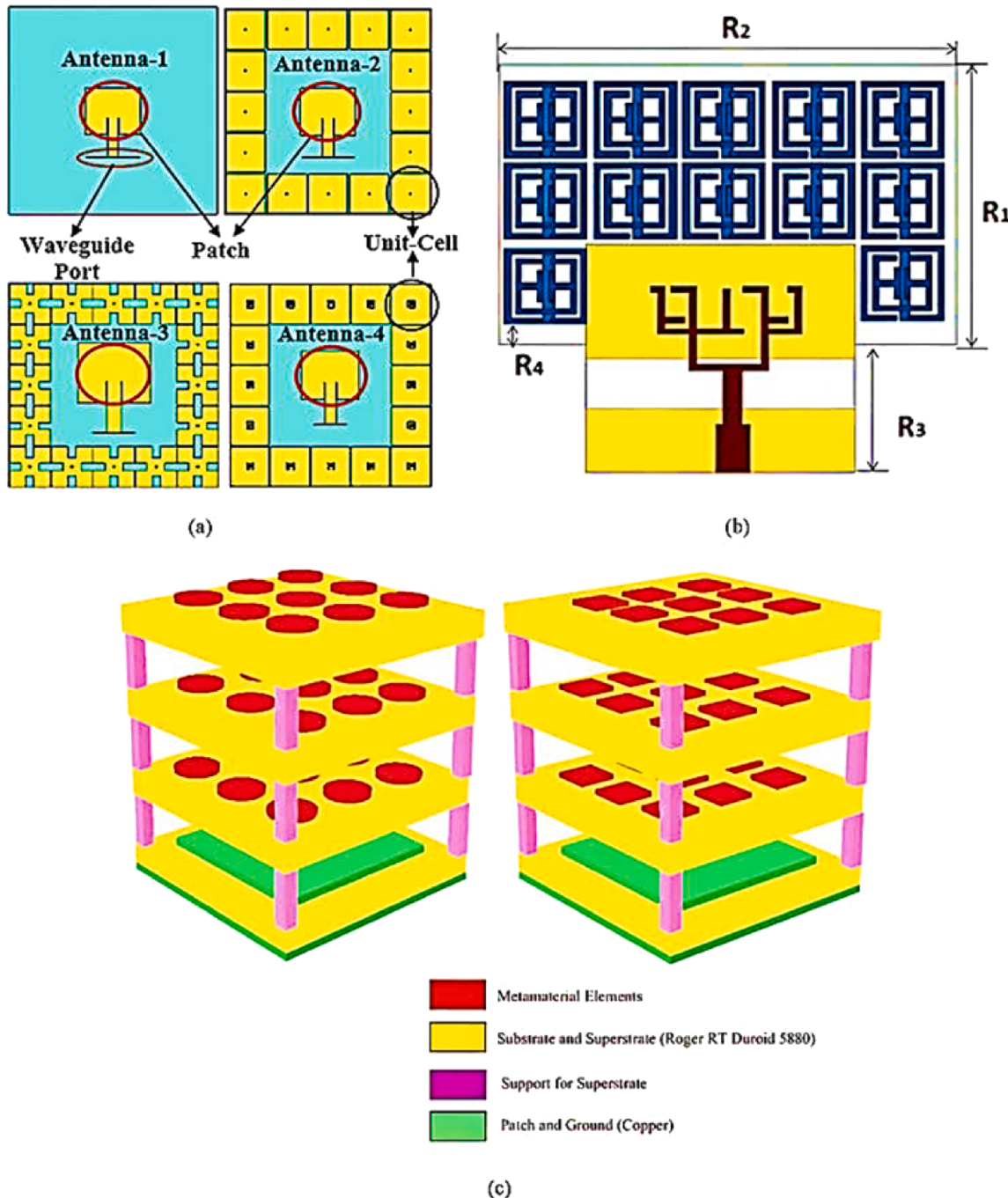


Fig. 18. Through a variety of design combinations, metamaterials can greatly increase antenna gain. In antenna design, metamaterials are frequently used in three ways: (a) Radiating Element Encircled by Unit Cells: To improve performance, metamaterial unit cells can be placed around the antenna's radiating elements. This will increase radiation efficiency and reflect surface waves. Significant gain enhancement is possible with this configuration, especially if the metamaterial unit cells are precisely engineered to resonate with the operating frequency of the antenna [216]. (b) Metamaterials for Antenna Loading: Metamaterials can be incorporated into the antenna's body or positioned next to it to serve as loading structures. By changing the field distribution and assisting the antenna in producing a more focused and effective radiation pattern, loading metamaterials into antennas can aid to improve their overall performance [217]. (c) Metamaterial as a Superstrate: In this arrangement, a metamaterial is positioned above the radiating elements on a different dielectric layer and functions as a superstrate. By increasing directivity, decreasing reflection losses, and reflecting waves back toward the antenna, this superstrate can increase the gain of the antenna. The number of superstrates, the number of metamaterial unit cells, and the distance between the superstrate and the radiating elements are some of the variables that affect performance [216,217].

conductors (AMCs) or artificial magnetic materials (AMMs), can be integrated into the antenna environment in various ways. This includes arranging metamaterial unit cells around the radiating elements, adding superstrates above or below the radiating elements, or using metamaterials as loading structures for the antenna. The improvement in antenna power gain is influenced by factors like the number of superstrates, the type of unit cell, and the gap between the radiating elements and the superstrate. When metamaterials are applied as superstrates, they are placed on a separate dielectric layer above the radiating elements, with the gap playing a crucial role in performance. This setup enhances power gain, although it may increase the antenna's size and thickness. The gain improvement also depends on how the metamaterial unit cells are arranged, either surrounding the radiating elements or on the sides of the substrate [216]. To effectively enhance performance, the unit cells must resonate with the antenna's operating frequency. AMCs, for instance, can provide zero-degree reflection at the operating frequency when etched onto the antenna [217]. Metamaterials can reflect

surface waves and improve gain, especially when integrated with traditional antenna designs. Surrounding a traditional antenna with metamaterial unit cells can significantly increase its gain [218]. The number of unit cells and the distance between the superstrate and radiating elements are key factors that affect gain and directivity, as demonstrated in Fig. 18 [219].

Fig. 19

The application of metamaterials in enhancing antenna gain has been a significant focus in recent research, with various studies demonstrating their effectiveness in different antenna configurations. Nguyen Ngoc Lan and Vu Van Yem (2019) investigated a novel MIMO antenna design incorporating a metamaterial structure on the ground plane, which resulted in significant gain enhancement and reduced mutual coupling between antenna elements. This metamaterial configuration contributed to a peak gain of 9.2 dBi and improved isolation, demonstrating the potential of these materials to increase radiation efficiency and bandwidth in MIMO systems [220]. Hedi Sakli et al. (2021)

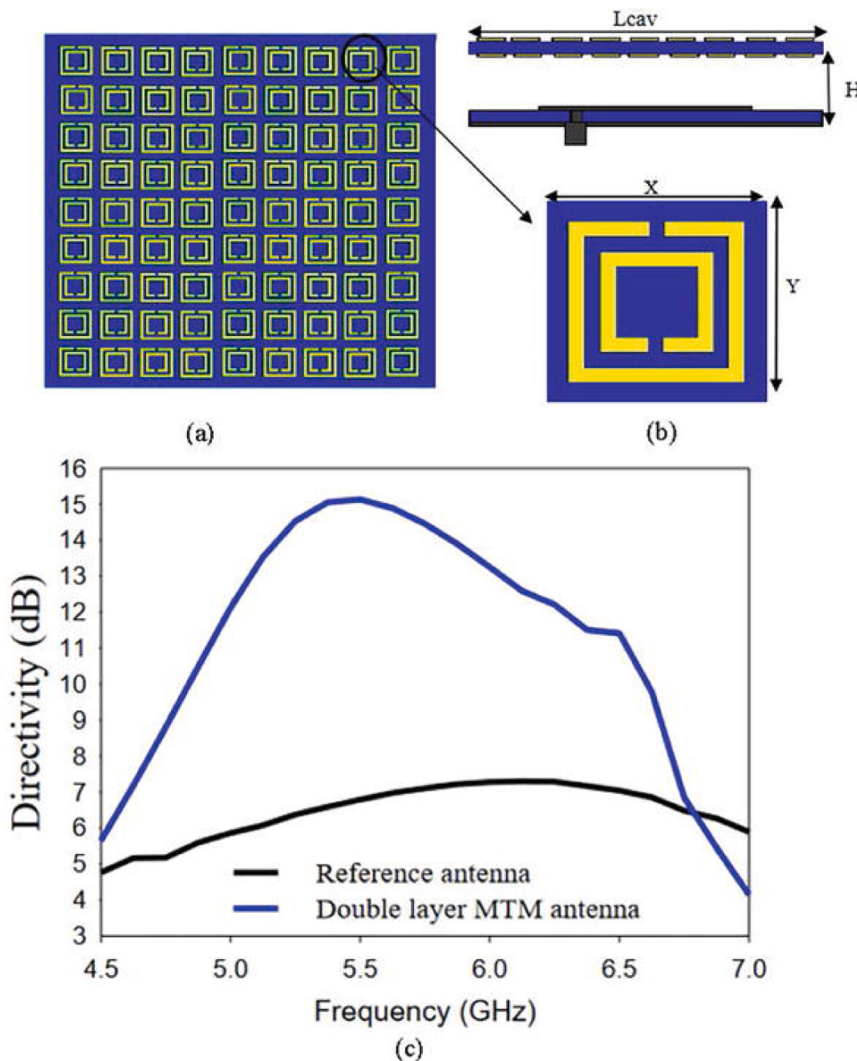


Fig. 19. The following elements are essential to the construction of a patch antenna with a double-layer metamaterial superstrate: (a) Antenna Front and Top View: A metamaterial superstrate is positioned atop the patch antenna, which is usually of the microstrip variety. By altering the wave propagation properties and enhancing the radiation pattern, the double-layer superstrate improves the antenna's performance. The antenna and superstrate layer layouts are shown in the front and top views. (b) SRR (Split-Ring Resonator) Unit Cell: SRRs, which are designed to resonate at particular frequencies, are commonly found in the unit cell of the metamaterial superstrate. With characteristics like negative permeability and high resonant frequencies, SRRs are useful for managing electromagnetic waves. By placing these unit cells in the metamaterial superstrate, the antenna's gain is increased and its radiation properties are altered. (c) Directivity with/without Superstrate: As seen by the comparison of the antenna's performance with and without the superstrate, the addition of the double-layer metamaterial superstrate greatly increases the antenna's directivity. By concentrating the radiated energy, the metamaterial superstrate raises the antenna's gain and guarantees more effective signal transmission in a specific direction. When the superstrate is added, the directivity graph shows how the radiation patterns and signal strength improve [219].

explored the use of split-ring resonators (SRRs) in enhancing the performance of ultra-wideband (UWB) MIMO antennas. Their results indicated that metamaterials could effectively reduce mutual coupling and improve critical parameters, such as S-parameters and diversity gain, essential for 5 G and IoT applications [221]. In another study, Tadesse and Abdu (2020) reviewed advancements in planar antenna design over the past two decades, highlighting the role of metamaterial loading in achieving substantial gain performance improvements. They discussed various metamaterial configurations and their impact on antenna performance, showcasing the broad applicability of these materials in modern communication systems [222]. Moreover, Ramakrishna et al. (2020) developed a metamaterial-based antenna for MIMO applications, demonstrating significant gain enhancement through a novel metamaterial superstrate design that optimized the phase distribution and minimized mutual coupling crucial for efficient signal transmission and reception in complex environments [223]. Finally, Li and Huang (2021) presented a comprehensive overview of metamaterial-inspired designs for gain enhancement in planar antennas, emphasizing the use of metamaterial arrays and surfaces to achieve desired electromagnetic properties, such as reduced back-lobe radiation and increased directivity, which are vital for high-performance antenna systems [224].

7.2. Size reduction

For constructing compact antennas, various technological approaches have been explored, such as high-permittivity dielectric microstrip substrates, shorting pins, shorting partitions, structural disturbances, and fractal geometry. Recently, metamaterials have been effectively used as defected ground structures (DGS) to further reduce antenna size. In these designs, the unit cells of metamaterials exhibit unique properties at the antenna's resonance frequency, with their dimensions often matching the removed sections in the DGS. The application of metamaterials in compact antenna design has become a major focus, leveraging their ability to introduce distinctive characteristics at the resonance frequency. For instance, in recent designs, metamaterials configured as a DGS have shown significant compactness. Fig. 20 depicts the geometry of an antenna with metamaterial loading on the bottom layer. The simulated S11 results, as shown in Fig. 14, reveal that the original antenna operates at 7 GHz. However, after introducing a metamaterial layer composed of multiple parallel rings, the resonance frequency shifts to 4 GHz, achieving a significant reduction in antenna size, as illustrated in Fig. 21 [225,226].

Metamaterials have been instrumental in achieving significant size reductions in antenna designs without compromising performance. Surendrakumar Painam and Chandramohan Bhuma (2019) developed a

compact microstrip antenna that utilizes a complementary split ring resonator (CSRR) with nonuniform metasurfaces on the ground plane, resulting in a 74% size reduction compared to conventional designs. This approach-maintained performance metrics such as gain and efficiency, making it ideal for indoor base-station antennas [227]. Similarly, Yajuan Han et al. (2020) explored reducing the radar cross section (RCS) of patch antennas by using dispersion-engineered metamaterial absorbers (MAs). By fine-tuning the geometric parameters of the MA, they achieved significant RCS reduction while preserving antenna functionality, demonstrating its potential for stealth applications [228]. In another study, Gupta et al. (2021) utilized metamaterial-inspired techniques to miniaturize a planar antenna for IoT applications, achieving a compact design with a 60% size reduction. Their design optimized current distribution on the antenna surface, resulting in enhanced bandwidth and radiation patterns [229]. Furthermore, Liu and Chen (2020) proposed a dual-band antenna with a metamaterial superstrate, achieving a compact structure with reduced physical dimensions and improved impedance bandwidth, demonstrating its effectiveness for 5 G and satellite communication systems [230]. Lastly, Wang and Li (2019) introduced a novel metamaterial-based approach to reduce the size of a broadband antenna, focusing on enhancing its operational frequency range while minimizing its footprint. Their design incorporated a periodic metamaterial structure, providing effective miniaturization and high radiation efficiency—crucial for modern wireless communication applications [231].

7.3. Bandwidth enhancement

Compared to conventional patch antennas, metamaterial-loaded antennas exhibit significantly higher bandwidth. Metamaterials can be integrated into antennas in several ways, including as components of the antenna itself or as a superstrate mounted above the radiating surface. This method is similar to the approach used for enhancing antenna gain. Metamaterial unit cells can be positioned either on top or below the superstrate, and both the number of unit cells and the distance between the radiating element and the superstrate are crucial factors that affect the antenna's impedance bandwidth. In addition to improving gain and directivity, metamaterials also enhance the impedance bandwidth of antennas. To achieve this, metasurfaces can be incorporated either as part of the antenna or as a superstrate placed over the main radiating element. As discussed earlier in relation to gain enhancement, the placement of the superstrate—either above or below the metamaterial unit cells—plays a significant role in the antenna's impedance bandwidth. Fig. 22 illustrates the configuration of the antenna with a superstrate and shows the simulated reflection coefficient (S11) with

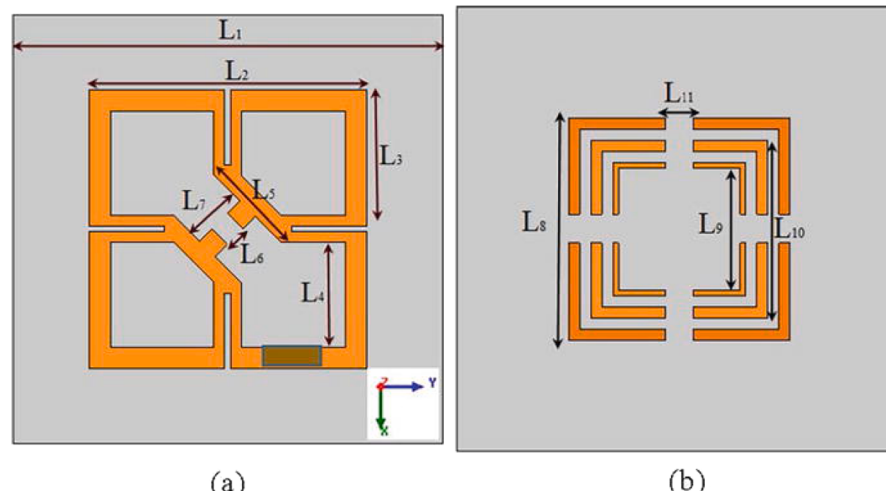


Fig. 20. Geometry of the antenna: (a) top view, and (b) MMT load at the bottom layer [37].

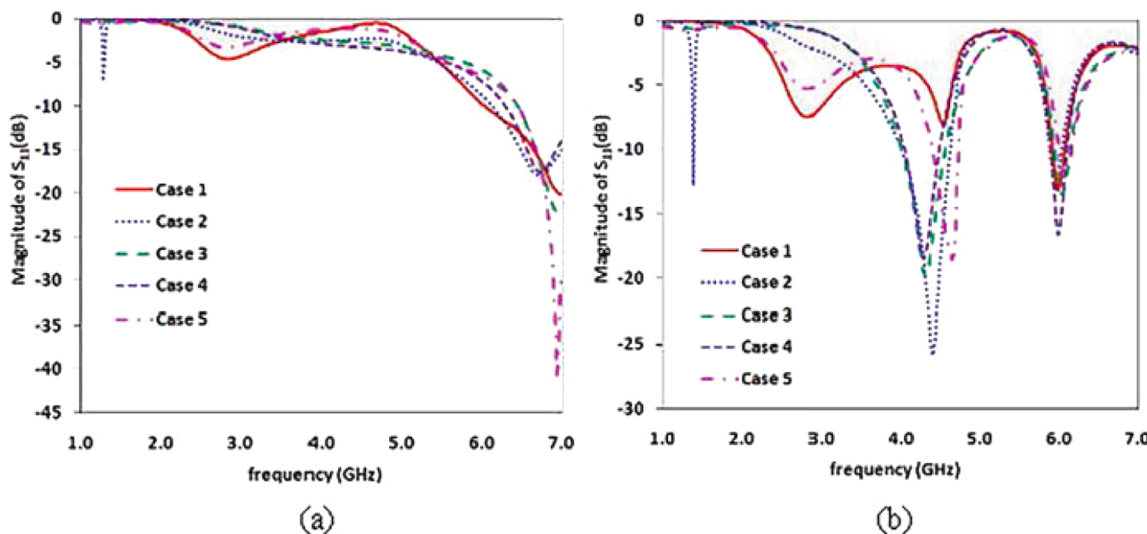


Fig. 21. Reflection coefficient ($S_{11}S_{11}$): (a) without metamaterial, and (b) with metamaterial [226].

and without metamaterials. The addition of metamaterials leads to a substantial increase in bandwidth, particularly for the higher frequency band, where the bandwidth increases from 9.35% to 28%. The bandwidth of the third band also increases to 27.81%, with a slight shift to a higher frequency. Additionally, incorporating metamaterial unit cells improves impedance matching in the lower band, enhancing overall antenna performance [232].

Metamaterials have played a pivotal role in enhancing the bandwidth of antennas, a crucial factor in modern communication systems. Ali Hanafiah Rambe et al. (2018) investigated the use of left-handed metamaterials (LHM) in rectangular patch microstrip antennas operating at 2.4 GHz. Their study showed that the inclusion of LHM on an FR4 substrate significantly increased the antenna's bandwidth by up to 175.7 MHz, representing a 213.75% enhancement over conventional designs, along with improved return loss performance [233]. Similarly, Omid Borazjani et al. (2020) demonstrated that integrating an electromagnetic band gap (EBG) structure into planar antennas for X-band applications could expand the antenna bandwidth by up to 1.6 GHz. This approach, using a metallic ring structure on a Rogers 4003C substrate, effectively improved bandwidth without degrading far-field radiation [234]. In another study, D. S. Ramakrishna et al. (2021) focused on the use of metamaterial loading on an L-shaped slot antenna to achieve dual-band operation with significant bandwidth enhancement. Their design achieved a considerable increase in impedance bandwidth, making it suitable for modern wireless communication applications like Wi-Fi and WLAN [235]. S. W. Loke et al. (2019) presented a metamaterial-inspired approach to broaden the bandwidth of compact antennas, using a novel metasurface design that achieved a 45% bandwidth enhancement in the 5 G frequency spectrum. This study highlighted the advantages of metamaterial surfaces in managing electromagnetic waves to improve antenna performance [236]. Finally, T. M. Le and Q. H. Vuong (2020) developed a wideband planar antenna with a metamaterial superstrate that provided enhanced bandwidth performance for satellite communications. Their innovative design optimized the antenna's radiation pattern and impedance matching, significantly broadening its operational bandwidth and improving its suitability for high-frequency applications [237].

7.4. Multiband antenna

Metamaterials have greatly contributed to the development of multifrequency-band antennas, enabling compact and efficient designs that operate across multiple frequency bands. These metamaterial unit

cells can serve as radiation elements, components of the antenna structure, or as loaded elements in the antenna's ground plane. At their resonant frequencies, symmetric metamaterial pairs can support negative refraction indexes, facilitating the creation of smaller, more compact antennas compared to traditional designs. By integrating metamaterials with conventional or fractal microstrip antennas, multiband antennas can be achieved, where the overall size of the antenna is primarily determined by the lowest operating frequency. This innovation allows for high-performance antennas that maintain functionality across a range of frequencies, while significantly reducing their physical size. Metamaterials have greatly enhanced multiband antenna performance across multiple frequency bands while maintaining compactness and efficiency. Ali et al. (2017) presented a comprehensive study on multiband frequency reconfigurable antennas using metamaterial design techniques, demonstrating how metamaterials enable frequency selectivity and size reduction. Their approach utilized fractal and slot techniques to achieve multiband functionality, making the antennas suitable for various wireless standards with improved gain and reduced interference [238]. Similarly, David et al. (2021) introduced a multiband antenna design incorporating novel metamaterial structures like SCSRR and CSSRR, which support WiMAX and WLAN applications by independently controlling resonance frequencies to provide stable radiation characteristics across multiple bands [239]. Tanweer Ali and colleagues (2020) explored the use of metamaterials to enhance gain and directivity in multiband antenna designs, focusing on zero-index properties to create compact and efficient antennas suitable for various communication standards [240]. Kim et al. (2020) investigated miniaturized multiband metamaterial antennas with dual-band isolation enhancement, demonstrating significant bandwidth improvements while maintaining a small form factor. Their work highlighted the potential of metamaterials for applications requiring high isolation and multiband operation [241]. Nguyen et al. (2019) developed a reconfigurable multiband metamaterial antenna with a unique metasurface design, achieving broad tunability and improved bandwidth across multiple bands, making it effective for modern wireless communication systems [242]. Lastly, Zhang et al. (2021) proposed a metamaterial-based structure that enhances antenna bandwidth and achieves multiband operation, showcasing the flexibility of metamaterials in managing electromagnetic properties for various design requirements [243].

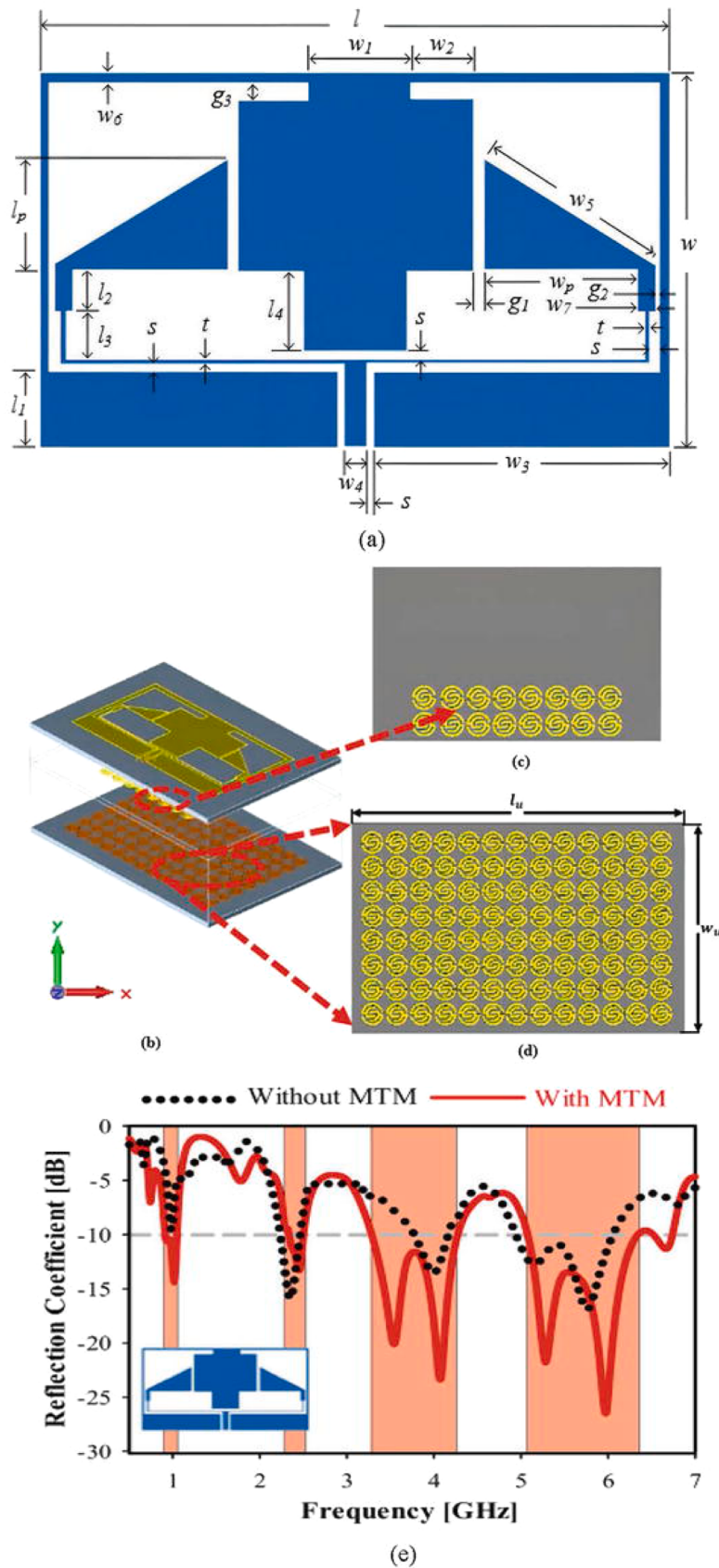


Fig. 22. The metamaterial-loaded antenna's configuration consists of: (a) Front view: Shows the metamaterial unit cells and radiating elements. (b) 3D view: Displays the location of the metamaterial layer and the antenna structure. (c) Back view: Shows the antenna's back, including any extra ground planes or metamaterial components. (d) Suspended Separator MTM Layer: To improve performance, a metamaterial layer is positioned between the antenna and substrate. (e) S11 with and without metamaterial: Displays the reflection coefficient, showing that the use of metamaterial improves bandwidth and impedance matching [232].

7.5. Directivity enhancement

DNG (Double Negative) materials enhance the directive properties of antennas by concentrating electromagnetic radiation in a small angular domain around the normal to the surface. Metamaterials, with their inherent ability to control the direction of electromagnetic radiation, are valuable in improving the directivity of antennas—a critical parameter for strengthening signals and reducing interference in wireless communication systems. Mourad Elhabchi, Mohamed Nabil Srifi, and Raja Touahni (2021) demonstrated the use of a Near Zero Refractive Index (NZIM) metamaterial superstrate to enhance the directivity and gain of a UWB elliptical metamaterial antenna. Their research indicated significant performance improvements, with gains of up to 6 dB and an increase in directivity by 5.42 dB, effectively channeling incident radiated waves towards the normal direction over a broad frequency range of 3.1 GHz to 20 GHz [244]. Similarly, Bilal Tütüncü, Hamid Torpi, and S. Taha İmeci (2019) explored the application of inverse refraction metamaterials as a lens to enhance the directivity of microstrip antennas. They found that a single omega-shaped metamaterial (OSM) layer could boost directivity by 2.74 dB, with a second lens layer further enhancing it to 4.08 dB, demonstrating the effectiveness of metamaterial lenses in compact antenna designs [245]. In another study, Das et al. (2019) investigated directivity enhancement in wire monopole antennas using magnetic metamaterials. By employing an array of magnetic metamaterial unit cells to manipulate the electromagnetic field distribution around the antenna, they achieved a directivity increase of up to 5 dB without altering the antenna's physical size, underscoring the versatility of magnetic metamaterials in antenna design [246]. J. Y. Huang and C. W. Hsu (2020) examined various metamaterial structures, such as split-ring resonators and mushroom-type structures, for enhancing antenna directivity. Their findings showed that incorporating these elements effectively focused the radiated energy, improving directivity an essential feature for satellite and radar applications [247].

Lastly, Wang et al. (2021) proposed a novel metamaterial-based antenna design featuring a multilayered superstrate, achieving a peak directivity improvement of 6.5 dB. This design provided a robust solution for high-frequency applications, highlighting the role of metamaterial superstrates in modern antenna engineering [248].

7.6. Metamaterials for the reduction of specific absorption rate

Wireless Body Area Networks (WBANs) are increasingly used in applications such as mobile communication, military operations, medical diagnostics, and rescue services, where antennas operate in close proximity to the human body. However, this closeness can lead to backward radiation being absorbed by human tissues, posing potential health risks. The Specific Absorption Rate (SAR) quantifies the rate at which electromagnetic energy is absorbed by tissue per unit mass [249]. International standards set SAR limits for devices like mobile phones to ensure safety: the U.S. standard is 1.6 W/kg averaged over 1 g of tissue, while the EU standard is 2.0 W/kg averaged over 10 g of tissue [250]. To mitigate SAR risks, various methods like reflectors, RF shielding with ferrite and conductive materials, and highly directional antennas have been used [251–253]. Recently, metamaterials such as Artificial Magnetic Conductors (AMC), Split-Ring Resonators (SRR), and Electromagnetic Bandgap (EBG) structures have emerged as effective solutions to block electromagnetic waves from reaching the human body, thus reducing SAR exposure [254].

Fig. 23

In a study, a metamaterial structure was used as a shield to protect the human head from harmful radiation emitted by a mobile phone. Simulation results showed that, without metamaterial shielding, the SAR for mobile phones at L, S, and C-band frequencies exceeded safe limits, with a value of 7.78 W/kg, surpassing the FCC's safe limit of 1.6 W/kg for 1 g of tissue. In contrast, integrating a metamaterial-based antenna reduced the SAR to 0.028 W/kg, well below the safe

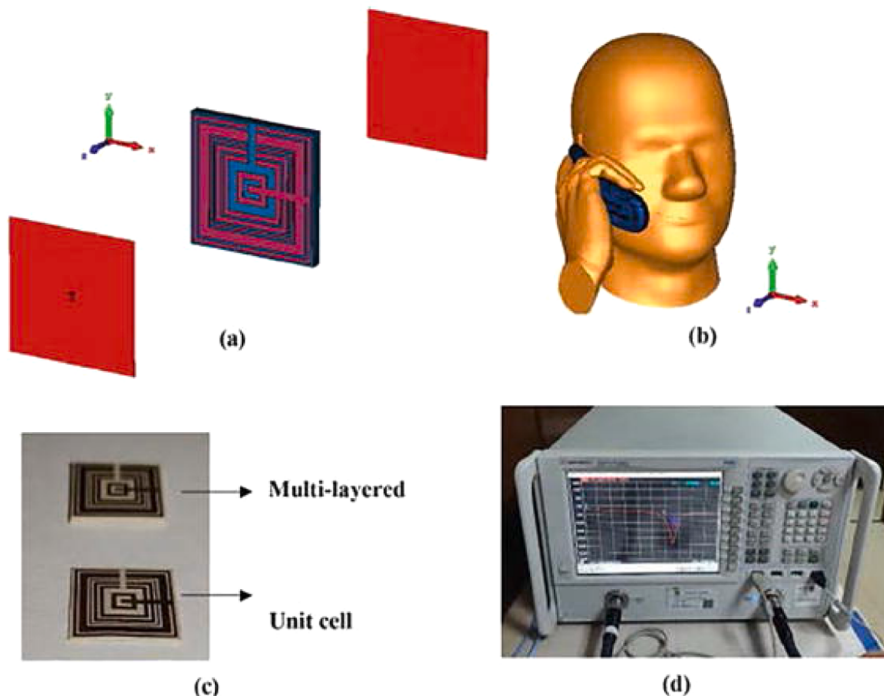


Fig. 23. Configuration and Layout of the Simulation (a) Metamaterial Structure: The metamaterial structure's design is optimized to reduce SAR values and shield electromagnetic radiation. (b) Voxel Model: This simulation model, which is used to analyze SAR exposure when the device is operating close to a human body, includes a human hand and head. (c) Fabricated Metamaterial Structure: The metamaterial's tangible realization, showcasing its usefulness for practical uses. (d) Agilent N5227A VNA: A vector network analyzer that evaluates the metamaterial structure's performance and confirms that it is efficient in lowering SAR and backward radiation [255].

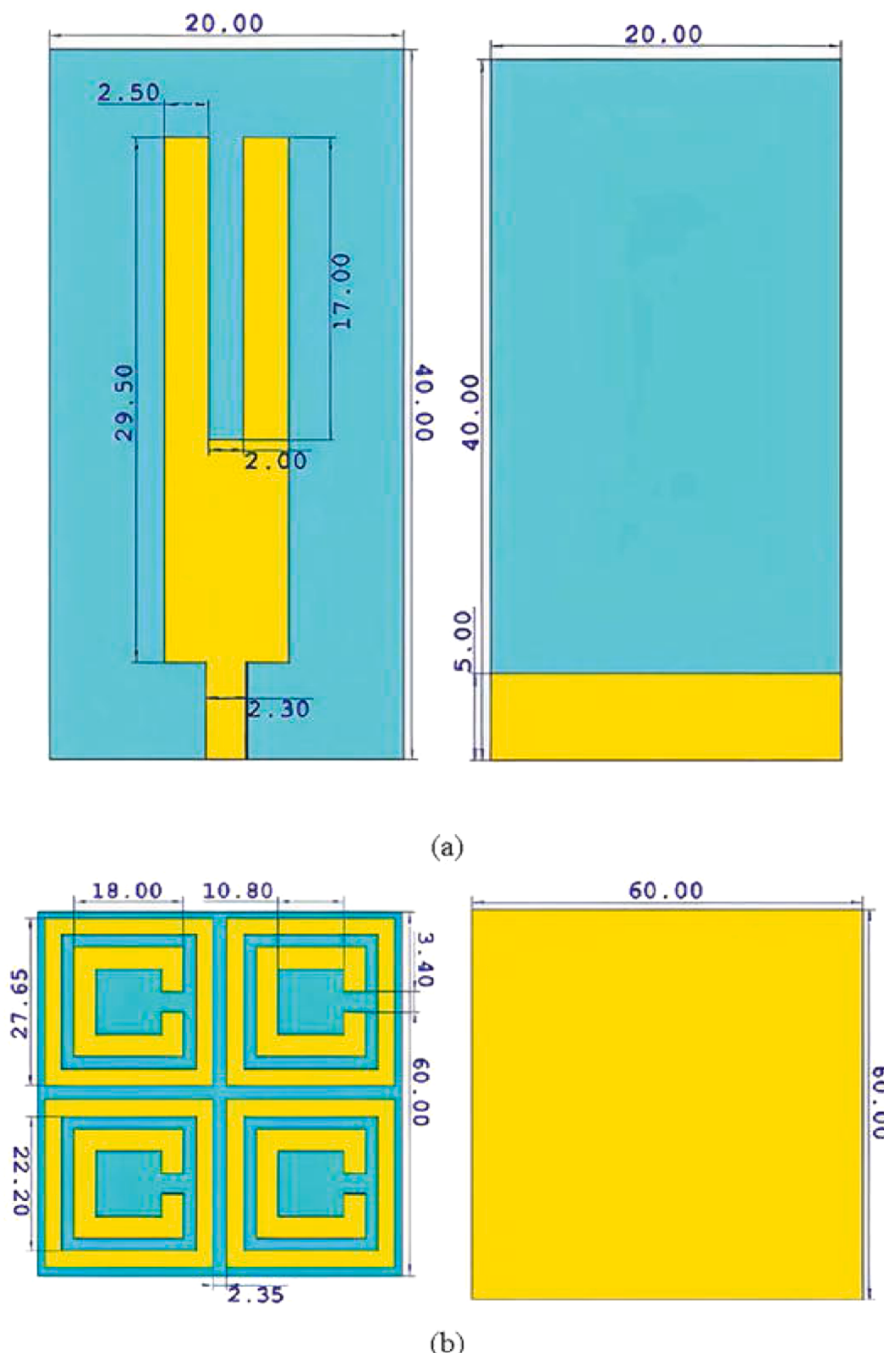


Fig. 24. Design Layout (a) U-shaped Fabric Antenna: Usually used in wearable or portable electronics, a U-shape antenna is made on a flexible fabric substrate. WBAN (Wireless Body Area Networks) applications benefit greatly from the U-shape's ability to produce effective radiation patterns and resonance at particular frequencies. Key U-shape proportions that are optimized for the target frequency band—typically the ISM band—are included in the configuration. (a) Fabric Material Metamaterial: To improve the performance of the antenna and lower SAR, a metamaterial layer is incorporated into the fabric. In order to prevent harmful radiation from entering the human body, the metamaterial design may incorporate features such as artificial magnetic conductors (AMC) or electromagnetic band gaps (EBG). The metamaterial layer serves as a shield to lessen electromagnetic exposure while preserving antenna efficiency and can be applied directly to the fabric or as a superstrate. Details of the metamaterial pattern and how it aligns with the cloth substrate for best results are included in the layout [256].

threshold, achieving a 98% reduction in SAR exposure [255,256]. This demonstrates the effectiveness of metamaterial integration in making antennas safer when used near the human body by significantly reducing SAR, ensuring compliance with international safety standards

Fig. 24

Fig. 25

Metamaterials have emerged as a promising solution to reduce the Specific Absorption Rate (SAR) in antenna applications, ensuring safer

electromagnetic exposure levels for users. Imaculate Rosaline et al. (2022) introduced a metamaterial slab composed of pentagonal split rings integrated with a compact triple-band antenna designed for WLAN and WiMAX applications. This approach not only enhanced the antenna's gain but also achieved an 84.5% reduction in SAR by optimizing the antenna-slab distance, demonstrating the potential of metamaterials in developing high-performance, low-SAR antennas for portable devices [257]. Similarly, Saif Hannan and colleagues (2021) developed a

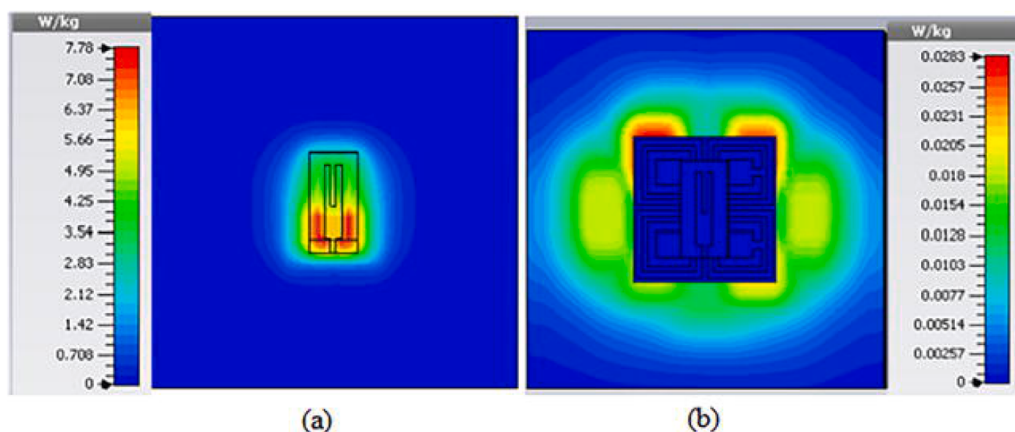


Fig. 25. Simulated SAR of the Proposed U-Shaped Antenna (a) Without Metamaterial: When the U-shaped antenna works near the body without metamaterial shielding, the SAR simulation shows that human flesh absorbs a large amount of electromagnetic radiation. Potential health risks are highlighted when the SAR value beyond the safe limit established by international standards (such as the FCC limit of 1.6 W/kg for 1 g of tissue). (b) With Metamaterial: The SAR value is significantly decreased when a metamaterial layer is integrated into the U-shaped antenna. Backward radiation is efficiently blocked by the metamaterial structure, which also ensures that safety regulations are followed (e.g., SAR well below 1.6 W/kg for 1 g of tissue) [256].

co-polarization-insensitive metamaterial absorber for 5 G n78 mobile devices operating at 3.5 GHz, which demonstrated a significant SAR reduction of at least 33%. This design is particularly effective for array implementations in next-generation mobile devices, highlighting the role of metamaterial absorbers in mitigating SAR while ensuring robust communication capabilities [258]. Additionally, Xiang et al. (2022) explored the use of metamaterial-inspired radiofrequency (RF) shields for ultra-high-frequency (UHF) MRI applications. Their study demonstrated that incorporating these RF shields could effectively lower SAR levels by controlling the distribution of electromagnetic fields, thereby improving both safety and imaging quality in medical diagnostics [259]. In another study, Wang et al. (2022) investigated a metamaterial-based design for wearable antennas, achieving significant SAR reduction while maintaining high radiation efficiency, proving beneficial for applications in body-centric wireless communications [260]. Finally, Alves et al. (2021) examined the effects of metamaterials on SAR reduction in dual-band antennas for mobile communication. Their results showed a marked decrease in SAR values without compromising antenna performance, emphasizing the versatility and efficacy of metamaterials in various communication settings [261].

8. Lesson learned: deep learning/machine learning techniques for metamaterial/metasurface antennas

The application of deep learning and machine learning to metamaterial antenna design has led to significant advancements in optimizing antenna performance and enabling innovative functionalities. Recent advancements in these techniques have significantly transformed the design and optimization of metamaterial and metasurface antennas, leading to improved performance across various electromagnetic applications (Table 7). Artificial intelligence (AI) has arrived as a transformative tool in materials science, facilitating accelerated discovery, design, and optimization of functional materials for the next generation. Recent reviews have highlighted the capacity of AI to uncover complex structure-property relations, handle high-dimensional data sets, and reduce the computational cost associated with traditional modeling and simulation methods. Xu et al. (2021) point to the growing impact of AI across scientific disciplines, particularly materials science, where it enables efficient mapping of vast design spaces and facilitates predictive modeling of new material systems [262]. Similarly, a review paper by Wu et al. (2023) points to using AI algorithms in electronic materials, demonstrating how machine learning can guide experimental synthesis and optimize device-level performance prediction [263]. These

developments constitute a strong foundation for applying deep learning to engineer metamaterial and metasurface antennas, in which electromagnetic properties are sensitively dependent on subwavelength structure variations. Employing AI allows researchers to attain multi-objective optimization of key parameters of the antenna, such as gain, bandwidth, and miniaturization, that matter in upcoming wireless communication technology.

Lin et al. (2021) introduced a smart metasurface with adaptive control capabilities utilizing a Q-learning algorithm, enabling real-time beam steering and encrypted communication. Their approach demonstrated the potential of AI in dynamically adjusting antenna parameters for optimized performance under varying conditions [264]. Similarly, Tiwari et al. (2020) leveraged machine learning models, such as random forest and decision tree regressors, to optimize microstrip patch antennas, achieving significant enhancements in bandwidth and gain with reduced computational resources [265]. In another innovative approach, Liu et al. (2022) employed deep learning models to predict and optimize S-parameters for coding metamaterials, allowing for rapid adjustments to electromagnetic properties in response to environmental changes. This method enhances the flexibility and efficiency of metamaterial antennas in dynamic settings [266]. Zhang et al. (2021) developed a convolutional neural network (CNN) to design circularly polarized 3D-printed lens antennas, demonstrating the model's capability to handle complex geometrical and material parameters for enhanced antenna performance [267]. Moreover, Hodge et al. (2022) explored the use of generative adversarial networks (GANs) for creating novel metamaterial designs with specific electromagnetic characteristics, showcasing the potential of deep learning in innovating antenna design processes by automatically generating optimized metamaterial configurations [268]. Zhao et al. (2020) utilized deep learning for terahertz data extraction and analysis, which is critical for developing high-performance metamaterial-based sensors and imaging systems [269]. Li et al. (2020) applied reinforcement learning to optimize metasurface designs for adaptive antenna radiation patterns, effectively minimizing interference and maximizing signal quality in wireless communication systems [270]. Wang et al. (2021) employed a knowledge-based artificial neural network (ANN) to fine-tune circularly polarized antennas, resulting in significant improvements in gain and efficiency, which are vital for satellite communication applications [271]. Alibakhshikenari et al. (2020) demonstrated the effectiveness of using machine learning algorithms to optimize metasurface designs for broadband and multiband antenna applications, enhancing the overall electromagnetic performance across diverse frequency ranges [272].

Table 7

overview of design based Deep learning/machine Learning Techniques for metamaterial/metrasurface antennas.

| Authors / Reference / Year | Method/Technique of Deep Learning / Machine Learning Used | Technical Samples, Levels, Layers, Other Technical Aspects | Worked for Antenna |
|----------------------------|---|--|-----------------------------------|
| [250] | Random Forest, Machine Learning | Optimized polarization converter metasurfaces for enhanced bandwidth; focused on reducing computational cost | Bandwidth Enhancement |
| [251] | XGBoost, ANN, Random Forest | Optimized design parameters for terahertz fractal antennas with metamaterial FSS; aimed at gain enhancement across terahertz frequencies | Antenna Gain |
| [252] | Deep Learning, Equivalent Circuit Theory | Accelerated generative metasurface design using deep learning; employed circuit models for optimization | Metasurface Design Optimization |
| [253] | Intelligent Antenna Synthesis Using Machine Learning | Developed multi-layer neural networks to synthesize antennas with specific radiation patterns | Antenna Design Optimization |
| [254] | Machine Learning for On-Demand Metasurface Construction | Utilized AI to optimize electromagnetic properties of metasurfaces; facilitated rapid prototyping | Antenna Directivity and Gain |
| [255] | Machine Learning for Bandwidth Enhancement | Used machine learning for optimizing a metasurface polarization converter; achieved significant bandwidth performance improvements | Bandwidth Enhancement |
| [256] | Deep Learning for Generative Metasurface Design | Applied deep learning to explore the metasurface design space for optimal electromagnetic wave manipulation | Electromagnetic Wave Manipulation |
| [257] | AI Framework for Intelligent Antenna Synthesis | Developed a machine learning framework for synthesizing intelligent antennas with enhanced performance | Antenna Gain, Efficiency |
| [258] | Efficient ANN for Metasurface Design | Implemented ANN models with hidden layers to optimize metasurface parameters | Metasurface Optimization |
| [259] | High-Quality Data Acquisition for ML-Based Electromagnetic Design | Developed a data acquisition method to improve ML-based design accuracy for | Electromagnetic Structure Design |

Table 7 (continued)

| Authors / Reference / Year | Method/Technique of Deep Learning / Machine Learning Used | Technical Samples, Levels, Layers, Other Technical Aspects | Worked for Antenna |
|----------------------------|--|--|--|
| [260] | CNN-LSTM-DNN Framework for Metasurface State Recognition | electromagnetic structures | Multiband Antenna Performance |
| [261] | DNN and CNN for Inverse Metasurface Design | Combined CNN, LSTM, and DNN to optimize state recognition and element mapping in digital metasurfaces | Metasurface Design Optimization |
| [262] | Reinforcement Learning for Metasurface Optimization | Utilized deep neural networks for the inverse design of metasurfaces to achieve desired electromagnetic properties | Reconfigurable Metasurface Performance |
| [263] | Knowledge-Based ANN for Circularly Polarized Antenna Design | Implemented RL to enhance adaptability of STCDME in dynamic environments | Circular Polarization and Gain |
| [264] | Inverse Extreme Learning Machine for Metasurface Design | Developed ANN to design circularly polarized antennas; automated design process | Scattering Optimization |
| [265] | Machine Learning for Polarization Converter Metasurfaces | Applied inverse ELM to optimize scattering properties of metasurfaces | Bandwidth Enhancement |
| [266] | AI-Based Framework for Antenna Synthesis | Employed ML methods to enhance bandwidth of polarization converter metasurfaces | Antenna Gain, Efficiency |
| [267] | Deep Learning for Real-Time Metasurface Characterization | Leveraged ML for synthesizing antennas with improved gain and efficiency | Electromagnetic Characterization |
| [268] | ML Techniques for Broadband and Multiband Antenna Design | Used DL to characterize metasurfaces in real-time, improving design accuracy and speed | Multiband Antenna Performance |
| [269] | Knowledge-Based ANN for Satellite Communication Antennas | Explored ML algorithms to optimize broadband and multiband metasurface designs | Antenna Gain, Efficiency |
| [270] | Reinforcement Learning for Adaptive Antenna Radiation Patterns | Employed ANN to optimize circularly polarized antennas for satellite communications | Radiation Pattern Optimization |
| [271] | Equivalent Circuit Theory and Deep Learning | Applied RL for optimizing metasurfaces for adaptive antenna radiation patterns | Metasurface Design Optimization |
| [272] | AI for On-Demand Metasurface Design | Integrated DL with circuit theory for rapid metasurface design | Metasurface Design |

(continued on next page)

Table 7 (continued)

| Authors / Reference / Year | Method/Technique of Deep Learning / Machine Learning Used | Technical Samples, Levels, Layers, Other Technical Aspects | Worked for Antenna |
|----------------------------|--|---|---|
| [273] | Inverse ELM for Metasurface Design | Deployed inverse ELM to optimize scattering properties | Scattering Property Optimization |
| [274] | ANN for Metasurface Design | Applied ANN models with hidden layers to model complex electromagnetic behavior | Metasurface Optimization |
| [275] | High-Quality Data Acquisition for Electromagnetic Design | Introduced high-quality data acquisition methods to support ML-based design | Electromagnetic Structure Design |
| [276] | Machine Learning for Antenna Optimization | Developed ML models to optimize the design parameters of antennas, focusing on size reduction and performance | Antenna Size Reduction |
| [277] | Generative Adversarial Networks (GANs) for Metasurface Synthesis | Used GANs to synthesize metasurfaces with specific electromagnetic characteristics | Metasurface Design |
| [278] | Reinforcement Learning for Metasurface Control | Applied RL to dynamically control metasurface elements to achieve desired responses | Metasurface Control |
| [279] | Support Vector Machine (SVM) for SAR Reduction in Metamaterial-Enhanced Antennas | Used SVM to predict and reduce specific absorption rate (SAR) in antennas with metamaterial coatings | SAR Reduction |
| [280] | Deep Reinforcement Learning for Smart Metasurfaces | Utilized deep RL to optimize the state of smart metasurfaces in real-time applications | Metasurface Optimization |
| [281] | Supervised Learning for Metamaterial-Based Sensing Antennas | Implemented supervised learning algorithms to enhance the sensitivity of metamaterial-based antennas for sensing applications | Antenna Sensitivity Enhancement |
| [282] | Convolutional Neural Networks (CNNs) for Metamaterial-Inspired Antennas | Deployed CNNs to optimize the design of antennas inspired by metamaterial structures | Antenna Design Optimization |
| [283] | Transfer Learning for Efficient Metasurface Optimization | Applied transfer learning to leverage existing models and improve the efficiency of metasurface optimization processes | Metasurface Design Optimization |
| [284] | Deep Neural Networks for Antenna Size and Bandwidth Optimization | Developed DNN models to optimize antenna size and bandwidth, achieving significant improvements | Antenna Size Reduction, Bandwidth Enhancement |
| [285] | Decision Trees and Random Forest for Antenna Parameter Optimization | Used decision trees and random forest algorithms to optimize antenna | Antenna Parameter Optimization |

Table 7 (continued)

| Authors / Reference / Year | Method/Technique of Deep Learning / Machine Learning Used | Technical Samples, Levels, Layers, Other Technical Aspects | Worked for Antenna |
|----------------------------|---|---|--------------------------------|
| [187] | Hybrid Neural Networks for Multiband Antenna Design | parameters for specific use cases Employed hybrid neural networks to design multiband antennas, focusing on performance optimization across multiple frequency bands | Multiband Antenna Design |
| [286] | Recursive Neural Networks (RNNs) for Metasurface Control | Applied RNNs to control the dynamic states of metasurface elements for achieving desired electromagnetic responses | Metasurface State Control |
| [287] | Gradient Boosting Machines (GBM) for Metasurface Design and Control | Utilized GBM for designing and controlling metasurfaces with specific radiation characteristics | Metasurface Design and Control |
| [288] | Genetic Algorithms (GA) for Metasurface Optimization | Employed GA to optimize the physical parameters of metasurfaces for enhancing electromagnetic performance | Metasurface Optimization |

Yan et al. (2020) focused on a deep learning framework for real-time electromagnetic characterization of metasurfaces, significantly speeding up the design process while achieving high accuracy in parameter optimization [273]. The integration of deep learning and machine learning techniques has revolutionized the design and optimization of metamaterial and metasurface antennas, facilitating more efficient and innovative approaches. Zhou et al. (2023) applied artificial neural networks (ANNs) to optimize the design of metamaterial power dividers by predicting geometrical configurations that achieve desired physical responses, addressing the limitations of traditional electromagnetic simulations in bandwidth enhancement [274]. Chen et al. (2022) explored the use of deep neural networks (DNNs) and CNNs for the inverse design of metasurfaces with specific electromagnetic properties, demonstrating significant improvements over conventional trial-and-error methods [275]. Li et al. (2021) introduced a reinforcement learning framework for optimizing space-time coding digital metasurfaces (STCDME) in reconfigurable intelligent surfaces (RIS) applications, enhancing the adaptability and efficiency of metasurfaces in dynamic environments [276]. Hodge et al. (2022) also developed a knowledge-based ANN model to design circularly polarized 3D-printed lens antennas, showcasing the potential of machine learning in automating and refining antenna design processes [277]. Wang et al. (2022) introduced a smart metasurface based on a Q-learning algorithm, allowing real-time adaptation to changing electromagnetic conditions, thus improving performance and functionality [278]. Kim et al. (2021) implemented efficient ANN models for the inverse design of metasurfaces, exemplifying machine learning benefits in achieving rapid and accurate design optimizations [279]. Wang et al. (2020) used an inverse extreme learning machine model to design metasurfaces with optimized scattering properties, simplifying complex design tasks [280]. Ali et al. (2021) applied CNN-LSTM-DNN frameworks for state recognition and mapping in space-time coding digital metasurfaces, illustrating the versatility of machine learning in metamaterial research [281]. Lin et al. (2023) presented high-quality data acquisition methods for machine

learning-based design, while Lee et al. (2023) provided an overview of AI applications in meta-optics, reflecting the broad scope of this interdisciplinary field [282,283]. Recent advancements by Chatzichristodoulou et al. (2024) in polarization converter metasurfaces using machine learning achieved over 90% conversion efficiency across a wide frequency range, reducing computational costs and accelerating the design process for reconfigurable intelligent surfaces (RIS) [284]. Babu et al. (2024) utilized machine learning algorithms, including XGBoost, ANN, and Random Forest, to optimize a terahertz fractal antenna with a metamaterial frequency-selective surface, demonstrating improvements in antenna gain and efficiency for terahertz applications [285]. In another study, Zhang et al. (2023) employed a deep learning-based equivalent circuit theory to accelerate the generative design of metasurfaces, making it a valuable tool for the rapid development of advanced electromagnetic devices [187]. Wang et al. (2022) introduced an intelligent antenna synthesis method based on machine learning, significantly reducing the design cycle and computational requirements, ideal for real-time applications [286]. Singh et al. (2023) explored the use of machine learning in the rapid on-demand construction of metasurfaces, demonstrating how AI-driven techniques can optimize metasurface designs to meet specific electromagnetic criteria [287]. Li et al. (2024) employed machine learning techniques to develop a novel metasurface polarization converter, achieving significant bandwidth enhancement and demonstrating the potential of AI to optimize metasurface performance across multiple frequency bands [288]. Zhao (2022) investigated deep learning in the generative design of metasurfaces, focusing on optimizing electromagnetic wave manipulation properties [289]. Lastly, Bai et al. (2023) developed a framework for synthesizing intelligent antennas with enhanced performance metrics, exemplifying the transformative impact of AI in electromagnetic design [290].

Recent advances in large foundation models, such as generative models like Generative Adversarial Networks, Variational Auto-encoders (VAEs), and transformer-like models, have revolutionized computational materials science and inverse-design tasks. Such large-scale pre-trained models on high-dimensional electromagnetic simulation databases or synthetic databases generated through full-wave solvers can learn challenging nonlinear mappings between structural geometry and material response. In metasurface and metamaterials design, such geometries can enable automated synthesis of sub-wavelength unit-cell structures with target spectral responses, such as negative refractive index, anisotropic phase shift, or frequency-selective behavior, under fabrication constraints. Large models enable efficient surrogate modeling by substituting expensive finite-element or FDTD computation with efficient inference from learned networks, significantly reducing optimization times. In addition, diffusion models and conditional generative architectures can be utilized to enable controllable synthesis of shapes from prescribed electromagnetic targets, thus offering room for real-time, closed-loop optimization with the inclusion of reinforcement learning agents. Multimodal learning, such that the geometry, spectrum, and fabrication parameters are encoded in concert, benefits the models to be more generally applicable to other classes of metamaterials. Extension of such model-based systems to metasurface antenna designs not only simplifies parametric sweeps and search over topology but is worthwhile for scalable, data-efficiency-enabled approaches to the discovery of next-generation reconfigurable, broadband and miniaturized antenna structures for 6 G and beyond.

9. Conclusion

Metamaterials and metasurfaces have revolutionized antenna design with an exceptional ability to manipulate electromagnetic waves. Their structural design versatility, electrical characteristics, and remarkable achievements in antenna performance gains, bandwidth improvement, miniaturization, and directivity were made apparent through this review. Combining deep learning (DL) and machine learning (ML)

techniques with the design and optimization procedure has proven to be a powerful trend, enabling automated, accurate, and multi-objective optimization of complex antenna structures. Hybrid techniques combining AI with conventional optimization algorithms enhance the efficiency even more.

However, several challenges must be overcome. These are the unavailability of standardized, widely available high-fidelity datasets, the high cost of computation required for training deep models, and the inferior generalizability of AI models to novel materials or design conditions. Additionally, deployment in real systems is typically degraded by fabrication tolerances and environmental variability that simulation-trained models may not always be equipped to handle.

In the future, metamaterial antenna design will significantly rely on advanced AI-based paradigms. Some key areas of future directions include the development of physics-informed neural networks, real-time adaptive optimization paradigms, and open-access data sets for rapid innovation. The collaboration between computational scientists, RF engineers, and material scientists will be the linchpin to break through the existing bottlenecks and realize the complete potential of DL-enabled metamaterial technologies. Such technologies are expected to play a vital role in the construction of future wireless systems like 6 G, IoT networks, and satellite communication.

CRediT authorship contribution statement

Muhammad Kamran Shereen: Writing – review & editing, Writing – original draft, Visualization, Project administration, Formal analysis, Data curation, Conceptualization. **Xiaoguang Liu:** Supervision. **Xiaohu Wu:** Software, Resources. **Salah Ud Din:** Visualization, Methodology, Investigation. **Ayesha Naseem:** Writing – review & editing. **Shehryar Niazi:** Visualization, Validation. **Muhammad Irfan Khattak:** Writing – review & editing.

Declaration of competing interest

The authors declare the following financial interests/personal relationships which may be considered as potential competing interests:

Muhammad Kamran Shereen reports financial support was provided by Southern University of Science and Technology. Muhammad Kamran Shereen reports a relationship with Southern University of Science and Technology that includes: employment and funding grants. If there are other authors, they declare that they have no known competing financial interests or personal relationships that could have appeared to influence the work reported in this paper.

Acknowledgment

This work was partially supported by the Natural Science Foundation of China under Grant 62471211, and in part by Guangdong Provincial Key Laboratory of Integrated Circuits under Grant 2021KSY006 and Shenzhen Science and Technology Program under Grant JCYJ20220818100408018, 20231115204236001, and JCYJ20230807091814030.

Data availability

No data was used for the research described in the article.

References

- [1] R.M. Walser, Electromagnetic metamaterials, in: Proc: SPIE 4467 Complex Mediums II: Beyond Linear Isotropic Dielectrics, San Diego, USA, 2001, pp. 1–15.
- [2] C. Caloz, T. Itoh, Application of the transmission line theory of left-handed (LH) materials to the realization of a microstrip LH line, in: Proceedings of the IEEE Antennas and Propagation Society International Symposium, 2002, pp. 412–415, <https://doi.org/10.1109/APS.2002.1016111>.

- [3] I.B. Vendik, O.G. Vendik, Vendik, O. Vendik, Metamaterials and their application in microwaves: a review, *Tech. Phys.* 58 (1) (2013) 1–24, <https://doi.org/10.1134/S1063784213010234>.
- [4] V.G. Veselago, The electrodynamics of substances with simultaneously negative values of ϵ and μ , *Sov. Phys. Usp.* 10 (4) (1968) 509–514, <https://doi.org/10.1070/PU1968v01m04ABEH003699>.
- [5] D.R. Smith, W.J. Padilla, D.C. Vier, S.C. Nemat-Nasser, S. Schultz, Composite medium with simultaneously negative permeability and permittivity, *Phys. Rev. Lett.* 84 (18) (2000) 4184–4187, <https://doi.org/10.1103/PhysRevLett.84.4184>.
- [6] S.H. Lee, C.M. Park, Y.M. Seo, C.K. Kim, Reversed doppler effect in double negative metamaterials, *Phys. Rev. B Condens. Matter Mater. Phys.* 81 (24) (2010) 241102, <https://doi.org/10.1103/PhysRevB.81.241102>.
- [7] R. Kumar, M. Kumar, J.S. Chohan, S. Kumar, Overview on metamaterial: history, types and applications, *Mater. Today, Proc.* 56 (2022) 3016–3024, <https://doi.org/10.1016/j.matpr.2021.11.423>.
- [8] G. Ma, P. Sheng, Acoustic metamaterials: from local resonances to broad horizons, *Sci. Adv.* 2 (2016) e1501595, <https://doi.org/10.1126/sciadv.1501595>.
- [9] X. Yu, J. Zhou, H. Liang, Z. Jiang, L. Wu, Mechanical metamaterials associated with stiffness, rigidity and compressibility: a brief review, *Prog. Mater Sci.* 94 (2018) 114–173, <https://doi.org/10.1016/j.pmatsci.2017.12.003>.
- [10] T. Cui, Electromagnetic metamaterials - from effective media to field programmable systems, *Sci. Sin. Inf.* 50 (10) (2020) 1427, <https://doi.org/10.1360/SSI-2020-0123>.
- [11] Y. Jin, Y. Pennec, B. Bonello, H. Honarvar, L. Dobrzynski, B. Djafari-Rouhani, et al., Physics of surface vibrational resonances: pillared phononic crystals, metamaterials, and metasurfaces, *Rep. Prog. Phys.* 84 (8) (2021) 086502, <https://doi.org/10.1088/1361-6633/abdab8>.
- [12] X. Wu, Z. Wen, Y. Jin, T. Rabczuk, X. Zhuang, B. Djafari-rouhani, Broadband Rayleigh wave attenuation by gradient metamaterials, *Int. J. Mech. Sci.* 205 (2021) 106592, <https://doi.org/10.1016/j.ijmecsci.2021.106592>.
- [13] L. Cao, Z. Yang, Y. Xu, S.-W. Fan, Y. Zhu, Z. Chen, et al., Flexural wave absorption by lossy gradient elastic metasurface, *J. Mech. Phys. Solids* 143 (2020) 104052, <https://doi.org/10.1016/j.jmps.2020.104052>.
- [14] S. Huang, Z. Zhou, D. Li, T. Liu, X. Wang, J. Zhu, et al., Compact broadband acoustic sink with coherently coupled weak resonances, *Sci. Bull.* 65 (5) (2020) 373–379, <https://doi.org/10.1016/j.scib.2019.11.008>.
- [15] Y. Jin, W. Wang, A. Khelif, B. Djafari-rouhani, Elastic metasurfaces for deep and robust subwavelength focusing and imaging, *Phys. Rev. Appl.* 15 (2) (2021) 024005, <https://doi.org/10.1103/PhysRevApplied.15.024005>.
- [16] H. He, C. Qiu, L. Ye, X. Cai, X. Fan, M. Ke, et al., Topological negative refraction of surface acoustic waves in a WEYL phononic crystal, *Nature* 560 (7716) (2018) 61–64, <https://doi.org/10.1038/s41586-018-0367-9>.
- [17] H. Zhou, W. Fu, Y. Wang, Y. Laude, C. Zhang, Ultra-broadband passive acoustic metasurface for wide-angle carpet cloaking, *Mater. Des.* 199 (2021) 109414, <https://doi.org/10.1016/j.matdes.2020.109414>.
- [18] X. Fang, X. Wang, Y. Li, Acoustic splitting and bending with compact coding metasurfaces, *Phys. Rev. Appl.* 11 (6) (2019) 064033, <https://doi.org/10.1103/PhysRevApplied.11.064033>.
- [19] X. Zhang, M. Xiao, Y. Cheng, M. Lu, J. Christensen, Topological sound, *Commun. Phys.* 1 (1) (2018) 97, <https://doi.org/10.1038/s42005-018-0094-4>.
- [20] M.S. Kushwhaha, P. Halevi, L. Dobrzynski, B. Djafari-Rouhani, Acoustic band structure of periodic elastic composites, *Phys. Rev. Lett.* 71 (13) (Sep. 27 1993) 2022–2025, <https://doi.org/10.1103/PhysRevLett.71.2022>.
- [21] Z. Liu, X. Zhang, Y. Mao, Y.Y. Zhu, Z. Yang, C.T. Chan, et al., Locally resonant sonic materials, *Science* 289 (5485) (2000) 1734–1736, <https://doi.org/10.1126/science.289.5485.1734>.
- [22] Z. Yang, J. Mei, M. Yang, N.H. Chan, P. Sheng, Membrane-type acoustic metamaterial with negative dynamic mass, *Phys. Rev. Lett.* 101 (20) (2008) 204301, <https://doi.org/10.1103/PhysRevLett.101.204301>.
- [23] N. Fang, D. Xi, J. Xu, M. Ambati, W. Srituravanich, C. Sun, et al., Ultrasonic metamaterials with negative modulus, *Nat. Mater.* 5 (6) (2006) 452–456, <https://doi.org/10.1038/nmat1644>.
- [24] C. Ding, L. Hao, X. Zhao, Two-dimensional acoustic metamaterial with negative modulus, *J. Appl. Phys.* 108 (7) (2010) 074911, <https://doi.org/10.1063/1.3493155>.
- [25] S.H. Lee, C.M. Park, Y.M. Seo, Z.G. Wang, C.K. Kim, Composite acoustic medium with simultaneously negative density and modulus, *Phys. Rev. Lett.* 104 (5) (2010) 054301, <https://doi.org/10.1103/PhysRevLett.104.054301>.
- [26] R. Marques, F. Martin, M. Sorolla, *Metamaterials with negative parameters: theory, design and microwave applications*. Wiley Series in Microwave and Optical Engineering, Wiley-Blackwell, 2008, pp. 123–145.
- [27] D.E. Rumelhart, G.E. Hinton, R.J. Williams, Learning representations by back-propagating errors, *Nature* 323 (6088) (1986) 533–536, <https://doi.org/10.1038/323533a0>.
- [28] J. Elman, Finding structure in time, *Cogn. Sci.* 14 (2) (1990) 179–211, https://doi.org/10.1207/s15516709cog1402_1.
- [29] Y. LeCun, L. Bottou, Y. Bengio, P. Haffner, Gradient-based learning applied to document recognition, *Proc. IEEE* 86 (11) (1998) 2278–2324, <https://doi.org/10.1109/5.226791>.
- [30] G.E. Hinton, S. Osindero, Y.W. Teh, A fast learning algorithm for deep belief nets, *Neural Comput.* 18 (7) (2006) 1527–1554, <https://doi.org/10.1162/neco.2006.18.7.1527>. PubMed.
- [31] I. Goodfellow, J. Pouget-Abadie, M. Mirza, et al., Generative adverSARial nets. *Proc. 27th Int. Conf. Neural Information Processing Systems*, MIT Press, Montreal, Canada, Cambridge, 2014, pp. 2672–2680. Dec. 8–13.
- [32] M. Mirza and S. Osindero, "Conditional generative adverSARial nets," Available from: <https://arxiv.org/abs/1411.1784> [Accessed: 2023].
- [33] D. Liu, Y. Tan, E. Khoram, Z. Yu, Training deep neural networks for the inverse design of nanophotonic structures, *ACS Photonics* 5 (4) (2018) 1365–1369, <https://doi.org/10.1021/acsphotonics.7b01377> (DOI).
- [34] L.P. Kaelbling, M.L. Littman, A.W. Moore, Reinforcement learning: a survey, *J. Artif. Intell. Res.* 4 (1996) 237–285, <https://doi.org/10.1613/jair.301>. Available: <https://arxiv.org/abs/cs/9605103>. Accessed Aug. 14, 2023.
- [35] D. Silver, J. Schrittwieser, K. Simonyan, I. Antonoglou, A. Huang, A. Guez, et al., Mastering the game of GO without human knowledge, *Nature* 550 (7676) (Oct. 18 2017) 354–359, <https://doi.org/10.1038/nature24270>.
- [36] B.R. Kiran, I. Sobh, V. Talpaert, P. Mannion, A.A.A. Sallab, S. Yogamani, et al., Deep reinforcement learning for autonomous driving: a survey, *IEEE Trans. Intell. Transp. Syst.* 23 (2) (2022) 4909–4926, <https://doi.org/10.1109/TITS.2021.3054625>.
- [37] R. Zhu, T. Qiu, J. Wang, S. Sui, C. Hao, T. Liu, et al., Phase-to-pattern inverse design paradigm for fast realization of functional metasurfaces via transfer learning, *Nat. Commun.* 12 (1) (2021) 2974, <https://doi.org/10.1038/s41467-021-23087-y>. PubMed PMC.
- [38] Y. Kim, Y. Kim, C. Yang, K. Park, G.X. Gu, S. Ryu, Deep learning framework for material design space exploration using active transfer learning and data augmentation, *npj Comput. Mater.* 7 (1) (2021) 1–12, <https://doi.org/10.1038/s41524-021-00609-2>.
- [39] J. Alzubi, A. Nayyar, A. Kumar, Machine learning from theory to algorithms: an overview, *J. Phys. Conf. Ser.* 1142 (1) (2018) 012012, <https://doi.org/10.1088/1742-6596/1142/1/012012>.
- [40] B. Mahesh, Machine learning algorithms - a review, *Int. J. Sci. Res.* 9 (6) (2020) 381–386. Available: https://www.ijsr.net/getabstract.php?paperid=AR_T20203995. Accessed Oct. 9, 2023.
- [41] M. Abadi, A. Agarwal, P. Barham, et al., "TensorFlow: large-scale machine learning on heterogeneous distributed systems," Available from: <https://arxiv.org/abs/1603.04467> [Accessed: Aug. 14, 2023].
- [42] A. Paszke, S. Gross, F. Massa, et al., "PyTorch: an imperative style, high-performance deep learning library," Available from: <https://arxiv.org/abs/1912.01703> [Accessed: 2023].
- [43] S. Russell, P. Norvig, *Artificial Intelligence: A Modern Approach*, 4th ed., Prentice Hall, 2009. Available from, <http://aima.cs.berkeley.edu/index.html>. Accessed Aug. 14, 2023.
- [44] M.I. Jordan, T.M. Mitchell, Machine learning: trends, perspectives, and prospects, *Science* 349 (6245) (2015) 255–260, <https://doi.org/10.1126/science.aaa8415> (DOI PubMed.).
- [45] W.S. McCulloch, W. Pitts, A logical calculus of the ideas immanent in nervous activity, *Bull. Math. Biophys.* 5 (4) (1943) 115–133, <https://doi.org/10.1007/BF02478259>.
- [46] F. Rosenblatt, The perceptron: a probabilistic model for information storage and organization in the brain, *Psychol. Rev.* 65 (6) (1958) 386–408, <https://doi.org/10.1037/h0042519> (DOI PubMed.).
- [47] P. Kumar, T. Ali, M.M.M. Pai, Electromagnetic metamaterials: a new paradigm of antenna design, *IEEE Access* 9 (2021) 18722–18751, <https://doi.org/10.1109/ACCESS.2021.3053100>.
- [48] J. You, et al., Electromagnetic metamaterials: from classical to quantum, *Electromagn. Sci.* 1 (1) (Mar. 2023) 1–33, <https://doi.org/10.23919/emsci.2022.00005>. Art no. 0010051.
- [49] K.S. Lateef Al-Badri, O.S. Lateef, Metamaterial-based sensors for material detection applications, *IOP Conf. Ser.: Mater. Sci. Eng.* 928 (7) (2020) 072047, <https://doi.org/10.1088/1757-899X/928/7/072047>.
- [50] S. Kabanikhin, M. Shishlenin, Inverse and ill-posed problems in applied electromagnetics, *J. Inverse Ill-Posed Probl.* 27 (2019) 453–482, <https://doi.org/10.1515/jiip-2019-5001>.
- [51] J. Hadamard, On the well-posed problem concept, *Princeton Univ. Bull.* 13 (1902) 49–52.
- [52] J. Mueller, *Linear and Nonlinear Inverse Problems with Practical Applications*, SIAM, Philadelphia, 2012, <https://doi.org/10.1137/1.9781611972344>.
- [53] D. Colton, L. Päiväranta, Inverse problems and wave scattering theory, *Arch. Ration. Mech. Anal.* 119 (1992) 59–73, <https://doi.org/10.1007/BF00376010>.
- [54] I. Nachman, The mathematics of inverse problems, *Ann. Math.* 143 (1996) 71–92, <https://doi.org/10.2307/2118653>.
- [55] M. Bucci, T. Isernia, Electromagnetic scattering and inverse problems, *Radio Sci.* 32 (1997) 2123–2145, <https://doi.org/10.1029/97RS01826>.
- [56] M.I. Jordan, Applications of inverse problems in machine learning, *J. Math. Psychol.* 36 (1992) 396–418, [https://doi.org/10.1016/0022-2496\(92\)90029-7](https://doi.org/10.1016/0022-2496(92)90029-7).
- [57] A. Mall, D. Patil, A. Tamboli, A. Sethi, A. Kumar, Design of metamaterials using deep learning, *J. Phys. D Appl. Phys.* 53 (49) (2020), <https://doi.org/10.1088/1361-6463/abb33c>, 49LT01.
- [58] R. Singh, A. Agarwal, B.W. Anthony, Optical metamaterials: an inverse design approach, *Opt. Express* 28 (2020) 27893–27902, <https://doi.org/10.1364/OE.398926>.
- [59] Y. Kiashnejad, S. Abdollahramezani, A. Adibi, Computational approaches in metamaterial design," *NPJ comput. Material* 6 (2020) 12.
- [60] R.S. Hegde, Deep learning for inverse metamaterial design, *IEEE J. Sel. Top. Quantum Electron.* 26 (1) (2019) 1–10, <https://doi.org/10.1109/JSTQE.2019.2933796>.
- [61] L. Gao, X. Li, D. Liu, L. Wang, Z. Yu, Challenges and opportunities in inverse metamaterial design, *Adv. Mater.* 31 (2019) 1905467, <https://doi.org/10.1002/adma.201905467>.

- [62] Z. Liu, D. Zhu, S.P. Rodrigues, K.T. Lee, W. Cai, Design of functional metasurfaces using GANs, *Nano Lett.* 18 (2018) 6570–6577, <https://doi.org/10.1021/acs.nanolett.8b03171>.
- [63] S. So, J. Rho, Deep learning in photonics and metamaterials, *Nanophotonics* 8 (2019) 1255–1271, <https://doi.org/10.1515/nanoph-2019-0117>.
- [64] Z. Lin, V. Liu, R. Pestourie, S.G. Johnson, Topology optimization of freeform large-area metasurfaces, *Opt. Express* 27 (11) (2019) 15765–15775, <https://doi.org/10.1364/OE.27.015765>.
- [65] T. Phan, D. Sell, E.W. Wang, S. Doshay, K. Edee, J. Yang, et al., High-efficiency, large-area, topology-optimized metasurfaces, *Light Sci. Appl.* 8 (1) (2019) 48, <https://doi.org/10.1038/s41377-019-0159-5>.
- [66] D. Sell, J. Yang, S. Doshey, R. Yang, J.A. Fan, Large-angle, multifunctional metagratings based on freeform multimode geometries, *Nano Lett.* 17 (6) (2017) 3752–3757, <https://doi.org/10.1021/acs.nanolett.7b01082>.
- [67] Z. Shi, A.Y. Zhu, Z. Li, Y.-W. Huang, W.T. Chen, C.-W. Qiu, et al., Continuous angle-tunable birefringence with freeform metasurfaces for arbitrary polarization conversion, *Sci. Adv.* 6 (23) (2020) eaba3367, <https://doi.org/10.1126/sciadv.aba3367>.
- [68] S. Sui, H. Ma, J. Wang, M. Feng, Y. Pang, S. Xia, et al., Symmetry-based coding method and synthesis topology optimization design of ultra-wideband polarization conversion metasurfaces, *Appl. Phys. Lett.* 109 (1) (2016) 014104, <https://doi.org/10.1063/1.4955412>.
- [69] C.-H. Lin, Y.-S. Chen, J.-T. Lin, H.C. Wu, H.-T. Kuo, C.-F. Lin, et al., Automatic inverse design of high-performance beam-steering metasurfaces via genetic-type tree optimization, *Nano Lett.* 21 (12) (2021) 4981–4989, <https://doi.org/10.1021/acs.nanolett.1c00720>.
- [70] S. Jafar-Zanjani, S. Inampudi, H. Mosallaei, Adaptive genetic algorithm for optical metasurfaces design, *Sci. Rep.* 8 (1) (2018) 11040, <https://doi.org/10.1038/s41598-018-29275-z>.
- [71] J.R. Ong, H.S. Chu, V.H. Chen, A.Y. Zhu, P. Genevet, Freestanding dielectric nanohole array metasurface for mid-infrared wavelength applications, *Opt. Lett.* 42 (13) (2017) 2639–2642, <https://doi.org/10.1364/OL.42.002639>.
- [72] B. Zhang, W. Chen, P. Wang, S. Dai, H. Li, H. Lu, et al., Particle swarm optimized polarization beam splitter using metasurface-assisted silicon nitride Y-junction for mid-infrared wavelengths, *Opt. Commun.* 451 (2019) 186–191, <https://doi.org/10.1016/j.optcom.2019.06.057>.
- [73] P.E. Sieber, D.H. Werner, Infrared broadband quarter-wave and half-wave plates synthesized from anisotropic Bézier metasurfaces, *Opt. Express* 22 (26) (2014) 32371–32383, <https://doi.org/10.1364/OE.22.032371>.
- [74] M.M.R. Elsayah, S. Lanteri, R. Duvigneau, G. Brière, M.S. Mohamed, P. Genevet, Global optimization of metasurface designs using statistical learning methods, *Sci. Rep.* 9 (1) (2019) 17918, <https://doi.org/10.1038/s41598-019-53878-9>.
- [75] S.S. Panda, H.S. Vyas, R.S. Hegde, Robust inverse design of all-dielectric metasurface transmission-mode color filters, *Opt. Mater. Express* 10 (12) (2020) 3145–3159, <https://doi.org/10.1364/OME.409186>.
- [76] D.Z. Zhu, E.B. Whiting, S.D. Campbell, D.B. Burkel, D.H. Werner, Optimal high efficiency 3D plasmonic metasurface elements revealed by lazy ants, *ACS Photonics* 6 (11) (2019) 2741–2748, <https://doi.org/10.1021/acsphtronics.9b00717>.
- [77] S. An, C. Fowler, B. Zheng, M.Y. Shalaginov, H. Tang, H. Li, et al., A deep learning approach for objective-driven all-dielectric metasurface design, *ACS Photonics* 6 (12) (2019) 3196–3207, <https://doi.org/10.1021/acsphotonics.9b00966>.
- [78] L. Jiang, X. Li, Q. Wu, L. Wang, L. Gao, Neural network enabled metasurface design for phase manipulation, *Opt. Express* 29 (2) (2021) 2521–2528, <https://doi.org/10.1364/OE.413079>.
- [79] Q. Zhang, C. Liu, X. Wan, L. Zhang, S. Liu, Y. Yang, et al., Machine-learning designs of anisotropic digital coding metasurfaces, *Adv. Theory Simul.* 2 (2) (2019) 1800132, <https://doi.org/10.1002/adts.201800132>.
- [80] D. Xu, Y. Luo, J. Luo, M. Pu, Y. Zhang, Y. Ha, et al., Efficient design of a dielectric metasurface with transfer learning and genetic algorithm, *Opt. Mater. Express* 11 (7) (2021) 1852–1862, <https://doi.org/10.1364/OME.427426>.
- [81] J. Jiang, J.A. Fan, Global optimization of dielectric metasurfaces using a physics-driven neural network, *Nano Lett.* 19 (8) (2019) 5366–5372, <https://doi.org/10.1021/acs.nanolett.9b01857>.
- [82] Z. Liu, D. Zhu, K.-T. Lee, A.S. Kim, L. Raju, W. Cai, Compounding meta-atoms into metamolecules with hybrid artificial intelligence techniques, *Adv. Mater.* 32 (6) (2020) e1904790, <https://doi.org/10.1002/adma.201904790>.
- [83] X. Han, Z. Fan, Z. Liu, C. Li, L.J. Guo, Inverse design of metasurface optical filters using deep neural network with high degrees of freedom, *InfoMat* 3 (4) (2021) 432–442, <https://doi.org/10.1002/inf2.12116>.
- [84] Y. Zhu, X. Zang, H. Chi, Y. Zhou, Y. Zhu, S. Zhuang, Metasurfaces designed by a bidirectional deep neural network and iterative algorithm for generating quantitative field distributions light, *Adv. Manuf.* 4 (2023) 1–11.
- [85] F. Wen, J. Jiang, J.A. Fan, Robust freeform metasurface design based on progressively growing generative networks, *ACS Photonics* 7 (8) (2020) 2098–2104, <https://doi.org/10.1021/acsphtronics.0c00539>.
- [86] Z. Liu, D. Zhu, S.P. Rodrigues, K.-T. Lee, W. Cai, Generative model for the inverse design of metasurfaces, *Nano Lett.* 18 (10) (2018) 6570–6576, <https://doi.org/10.1021/acs.nanolett.8b03171>.
- [87] S. Cuomo, V.S. Di Cola, F. Giampaolo, G. Rozza, M. Raissi, F. Piccialli, Scientific machine learning through physics-informed neural networks: where we are and what's next, *J. Sci. Comput.* 92 (3) (2022) 88, <https://doi.org/10.1007/s10915-022-01939-z>.
- [88] Y. Chen, L. Lu, G.E. Karniadakis, L. Dal Negro, Physics-informed neural networks for inverse problems in nano-optics and metamaterials, *Opt. Express* 28 (8) (2020) 11618–11633, <https://doi.org/10.1364/OME.384875>.
- [89] Z. Chen, Y. Liu, H. Sun, Physics-informed learning of governing equations from scarce data, *Nat. Commun.* 12 (1) (2021) 6136, <https://doi.org/10.1038/s41467-021-26434-1>.
- [90] O. Khatib, S. Ren, J. Malof, W.J. Padilla, Learning the physics of all-dielectric metasurfaces with deep Lorentz neural networks, *Adv. Opt. Mater.* 10 (13) (2022) 2200097, <https://doi.org/10.1002/adom.202200097>.
- [91] J. Chen, Y. Chen, X. Xu, W. Zhou, G. Huang, A physics-guided machine learning for multifunctional wave control in active metabeams, *Extrem. Mech. Lett.* 55 (2022), <https://doi.org/10.1016/j.eml.2022.101827>. Article 101827.
- [92] H. Lin, K.-T. Lin, T. Yang, B. Jia, Graphene multilayer photonic metamaterials: fundamentals and applications, *Adv. Mater. Technol.* 6 (5) (2021) 2000963, <https://doi.org/10.1002/admt.202000963>.
- [93] L. Feng, P. Huo, Y. Liang, T. Xu, Photonic metamaterial absorbers: morphology engineering and interdisciplinary applications, *Adv. Mater.* 32 (27) (2020) e1903787, <https://doi.org/10.1002/adma.201903787>.
- [94] T. Liu, J.-Y. Ou, K.F. MacDonald, N.I. Zheludev, Photonic metamaterial analogue of a continuous time crystal, *Nat. Phys.* 19 (7) (2023) 986–991, <https://doi.org/10.1038/s41567-023-02023-5>.
- [95] X. Li, S. Ning, Z. Liu, Z. Yan, C. Luo, Z. Zhuang, Designing phononic crystal with anticipated band gap through a deep learning-based data-driven method, *Comput. Methods Appl. Mech. Eng.* 361 (2020) 112737, <https://doi.org/10.1016/j.cma.2019.112737>.
- [96] C. Gurbuz, F. Kronowetter, C. Dietz, M. Eser, J. Schmid, S. Marburg, Generative adversarial networks for the design of acoustic metamaterials, *J. Acoust. Soc. Am.* 149 (2) (2021) 1162–1174, <https://doi.org/10.1121/10.0003501>.
- [97] K. Donda, Y. Zhu, A. Merkel, S.-W. Fan, L. Cao, S. Wan, et al., Ultrathin acoustic absorbing metasurface based on deep learning approach, *Smart Mater. Struct.* 30 (8) (2021) 085003, <https://doi.org/10.1088/1361-665X/ac0675>.
- [98] H. Pahlavani, M. Amani, M.C. Saldívar, J. Zhou, M.J. Mirzaali, A.A. Zadpoor, Deep learning for the rare-event rational design of 3D printed multi-material mechanical metamaterials, *Commun. Mater.* 3 (1) (2022) 46, <https://doi.org/10.1038/s43246-022-00270-2>.
- [99] F. Liu, X. Jiang, X. Wang, L. Wang, Machine learning-based design and optimization of curved beams for multistable structures and metamaterials, *Extreme Mech. Lett.* 41 (2020) 101002, <https://doi.org/10.1016/j.eml.2020.101002>.
- [100] L. Wang, Y.-C. Chan, F. Ahmed, Z. Liu, P. Zhu, W. Chen, Deep generative modelling for mechanistic-based learning and design of metamaterial systems, *Comput. Methods Appl. Mech. Eng.* 372 (2020) 113377, <https://doi.org/10.1016/j.cma.2020.113377>.
- [101] C.-X. Liu, G.-L. Yu, Predicting the dispersion relations of one-dimensional phononic crystals by neural networks, *Sci. Rep.* 9 (1) (2019) 15322, <https://doi.org/10.1038/s41598-019-51662-3>.
- [102] P. Kudela, A. Ijeh, M. Radzinski, M. Miniaci, N. Pugno, W. Ostachowicz, Deep learning aided topology optimization of phononic crystals, *Mech. Syst. Signal Process.* 200 (2023) 110636, <https://doi.org/10.1016/j.jmss.2023.110636>.
- [103] S.M. Sadat, R.Y. Wang, A machine learning based approach for phononic crystal property discovery, *J. Appl. Phys.* 128 (2) (2020) 025106, <https://doi.org/10.1063/5.0006153>.
- [104] S. Javadi, A. Maghami, S. Mahmoud Hosseini, A deep learning approach based on a data-driven tool for classification and prediction of thermoelastic wave's band structures for phononic crystals, *Mech. Adv. Mater. Struct.* 29 (27) (2022) 6612–6625, <https://doi.org/10.1080/15376494.2021.1983088>.
- [105] S. Han, Q. Han, C. Li, Deep-learning-based inverse design of phononic crystals for anticipated wave attenuation, *J. Appl. Phys.* 132 (15) (2022) 154901, <https://doi.org/10.1063/5.0111182>.
- [106] C.-X. Liu, G.-L. Yu, G.-Y. Zhao, Neural networks for inverse design of phononic crystals, *AIP Adv.* 9 (8) (2019) 085223, <https://doi.org/10.1063/1.5114643>.
- [107] X.-B. Miao, H.W. Dong, Y.-S. Wang, Deep learning of dispersion engineering in two-dimensional phononic crystals, *Eng. Optim.* 55 (1) (2023) 125–139, <https://doi.org/10.1080/0305215X.2021.1988587>.
- [108] C. Luo, S. Ning, Z. Liu, Z. Zhuang, Interactive inverse design of layered phononic crystals based on reinforcement learning, *Extreme Mech. Lett.* 36 (2020) 100651, <https://doi.org/10.1016/j.eml.2020.100651>.
- [109] A. Maghami, S.M. Hosseini, Automated design of phononic crystals under thermoelastic wave propagation through deep reinforcement learning, *Eng. Struct.* 263 (2022) 114385, <https://doi.org/10.1016/j.engstruct.2022.114385>.
- [110] L. Chen, et al., Inverse design of phononic crystals by artificial neural networks, *Chin. J. Theor. Appl. Mech.* 53 (2021) 1992–1998.
- [111] L. Hu, et al., Machine-learning-driven on-demand design of phononic beams, *Sci. China Phys. Mech. Astron.* 65 (2022) 33–44.
- [112] S. Han, Q. Han, T. Jiang, C. Li, Inverse design of phononic crystals for anticipated wave propagation by integrating deep learning and semi-analytical approach, *Acta Mech.* 234 (10) (2023) 4879–4897, <https://doi.org/10.1007/s00707-023-03634-y>.
- [113] D. Lee, B.D. Youn, S.-H. Jo, Deep-learning-based framework for inverse design of a defective phononic crystal for narrowband filtering, *Int. J. Mech. Sci.* 255 (2023) 108474, <https://doi.org/10.1016/j.ijmecsci.2023.108474>.
- [114] J. Li, X. Wen, P. Cheng, Acoustic metamaterials, *J. Appl. Phys.* 129 (17) (2021) 174101, <https://doi.org/10.1063/5.0046878>.
- [115] E. Dong, P. Cao, J. Zhang, S. Zhang, N.X. Fang, Y. Zhang, Underwater acoustic metamaterials, *Natl. Sci. Rev.* 10 (6) (2022), <https://doi.org/10.1093/nsr/nwac246>.
- [116] N. Gao, Z. Zhang, J. Deng, X. Guo, B. Cheng, H. Hou, Acoustic metamaterials for noise reduction: a review, *Adv. Mater. Technol.* 7 (6) (2022) 2100698, <https://doi.org/10.1002/admt.202100698>.

- [117] J. Liu, H. Guo, T. Wang, A review of acoustic metamaterials and phononic crystals, *Crystals* 10 (4) (2020) 305, <https://doi.org/10.3390/crust10040305>.
- [118] Y. Xiao, J. Wen, X. Wen, Flexural wave band gaps in locally resonant thin plates with periodically attached spring-mass resonators, *J. Phys. D Appl. Phys.* 45 (19) (2012) 195401, <https://doi.org/10.1088/0022-3727/45/19/195401>.
- [119] M. Nouh, O. Aldraihem, A. Baz, Wave propagation in metamaterial plates with periodic local resonances, *J. Sound Vibrat.* 341 (2015) 53–73, <https://doi.org/10.1016/j.jsv.2014.12.030>.
- [120] Z. Xi-Xi, et al., Flexural wave band gaps and vibration reduction properties of a locally resonant stiffened plate, *Wuli Xuebao* 65 (17) (2016) 176202, <https://doi.org/10.7498/aps.65.176202>.
- [121] W. Jian, et al., Low frequency band gaps and vibration reduction properties of a multi-frequency locally resonant phononic plate, *Wuli Xuebao* 65 (6) (2016) 064602, <https://doi.org/10.7498/aps.65.064602>.
- [122] J. Mei, G. Ma, M. Yang, Z. Yang, W. Wen, P. Sheng, Dark acoustic metamaterials as super absorbers for low-frequency sound, *Nat. Commun.* 3 (1) (2012) 756, <https://doi.org/10.1038/ncomms1758>.
- [123] H. Zi-Hou, et al., Sound insulation performance of thin-film acoustic metamaterials based on piezoelectric materials, *Wuli Xuebao* 68 (13) (2019) 134302, <https://doi.org/10.7498/aps.68.20190245>.
- [124] G. Zhou, J.H. Wu, K. Lu, X. Tian, W. Huang, K. Zhu, Broadband low-frequency membrane-type acoustic metamaterials with multi-state anti-resonances, *Appl. Acoust.* 159 (2020) 107078, <https://doi.org/10.1016/j.apacoust.2019.107078>.
- [125] J.-Y. Jang, C.-S. Park, K. Song, Lightweight soundproofing membrane acoustic metamaterial for broadband sound insulation, *Mech. Syst. Signal Process.* 178 (2022) 109270, <https://doi.org/10.1016/j.ymssp.2022.109270>.
- [126] N. Fang, D. Xi, J. Xu, M. Ambati, W. Srituravanich, C. Sun, et al., Ultrasonic metamaterials with negative modulus, *Nat. Mater.* 5 (6) (Jun. 2006) 452–456, <https://doi.org/10.1038/nmat1644>.
- [127] M. Duan, C. Yu, F. Xin, T.J. Lu, Tunable underwater acoustic metamaterials via quasi-helmholtz resonance: from low-frequency to ultra-broadband, *Appl. Phys. Lett.* 118 (7) (2021) 071904, <https://doi.org/10.1063/5.0028135>.
- [128] X. Yang, F. Yang, X. Shen, E. Wang, X. Zhang, C. Shen, et al., Development of adjustable parallel Helmholtz acoustic metamaterial for broad low-frequency sound absorption band, *Materials* 15 (17) (2022) 5938, <https://doi.org/10.3390/ma15175938>.
- [129] X. Yang, X. Shen, F. Yang, Z. Yin, Q. Yang, C. Shen, et al., Acoustic metamaterials of modular nested helmholtz resonators with multiple tunable absorption peaks, *Appl. Acoust.* 213 (2023) 109647, <https://doi.org/10.1016/j.apacoust.2023.109647>.
- [130] Z. Liang, J. Li, Extreme acoustic metamaterial by coiling up space, *Phys. Rev. Lett.* 108 (11) (2012) 114301, <https://doi.org/10.1103/PhysRevLett.108.114301>.
- [131] Y. Xie, A. Konneker, B.-I. Popa, S.A. Cummer, Tapered labyrinthine acoustic metamaterials for broadband impedance matching, *Appl. Phys. Lett.* 103 (20) (2013) 201906, <https://doi.org/10.1063/1.4831770>.
- [132] G.D. Almeida, E.F. Vergara, L.R. Barbosa, R. Brum, Low-frequency sound absorption of a metamaterial with symmetrical-coiled-up spaces, *Appl. Acoust.* 172 (2021) 107593, <https://doi.org/10.1016/j.apacoust.2020.107593>.
- [133] L. Xiang, G. Wang, C. Zhu, Controlling sound transmission by space-coiling fractal acoustic metamaterials with broadband on the subwavelength scale, *Appl. Acoust.* 188 (2022) 108585, <https://doi.org/10.1016/j.apacoust.2021.108585>.
- [134] S.H. Lee, C.M. Park, Y.M. Seo, Z.G. Wang, C.K. Kim, Composite acoustic medium with simultaneously negative density and modulus, *Phys. Rev. Lett.* 104 (5) (2010) 054301, <https://doi.org/10.1103/PhysRevLett.104.054301>.
- [135] L. Fok, X. Zhang, Negative acoustic index metamaterial, *Phys. Rev. B Condens. Matter Mater. Phys.* 83 (21) (2011) 214304, <https://doi.org/10.1103/PhysRevB.83.214304>.
- [136] W. Fei, et al., Low-frequency sound absorption of hybrid absorber based on micro-perforated panel and coiled-up channels, *Appl. Phys. Lett.* 114 (15) (2019) 151901, <https://doi.org/10.1063/1.5090355>.
- [137] S. Xie, D. Wang, Z. Feng, S. Yang, Sound absorption performance of microperforated honeycomb metasurface panels with a combination of multiple orifice diameters, *Appl. Acoust.* 158 (2020) 107046, <https://doi.org/10.1016/j.apacoust.2019.107046>.
- [138] H.-W. Dong, S.-D. Zhao, P. Wei, L. Cheng, Y.-S. Wang, C. Zhang, Systematic design and realization of double-negative acoustic metamaterials by topology optimization, *Acta Mater.* 172 (2019) 102–120, <https://doi.org/10.1016/j.actamat.2019.04.042>.
- [139] C. Robeck, J. Cipolla, A. Kelly, Convolutional neural network driven design optimization of acoustic metamaterial microstructures, *J. Acoust. Soc. Am.* 146 (4_Supplement) (2019) 2830, <https://doi.org/10.1121/1.5136804>.
- [140] B. Zheng, J. Yang, B. Liang, J.-C. Cheng, Inverse design of acoustic metamaterials based on machine learning using a Gauss–Bayesian model, *J. Appl. Phys.* 128 (13) (2020) 134902, <https://doi.org/10.1063/5.0012392>.
- [141] A. Chen, Z.-X. Xu, B. Zheng, J. Yang, B. Liang, J.-C. Cheng, Machine learning-assisted low-frequency and broadband sound absorber with coherently coupled weak resonances, *Appl. Phys. Lett.* 120 (3) (2022) 033501, <https://doi.org/10.1063/5.0071036>.
- [142] A. Bacigalupo, et al., Design of acoustic metamaterials through nonlinear programming. Machine Learning, Optimization, and Big Data: Second International Workshop, MOD 2016, Springer International Publishing, 2016, https://doi.org/10.1007/978-3-319-51469-7_14.
- [143] A. Bacigalupo, G. Gnecco, M. Lepidi, L. Gambarotta, Machine-learning techniques for the optimal design of acoustic metamaterials, *J. Optim. Theory Appl.* 187 (3) (2020) 630–653, <https://doi.org/10.1007/s10957-019-01614-8>.
- [144] R.-T. Wu, T.-W. Liu, M.R. Jahanshahi, F. Semperlotti, Design of one-dimensional acoustic metamaterials using machine learning and cell concatenation, *Struct. Multidiscipl. Optim.* 63 (5) (2021) 2399–2423, <https://doi.org/10.1007/s00158-020-02819-6>.
- [145] T. Wiest, et al., Efficient design of acoustic metamaterials with design domains of variable size using graph neural networks, in: Volume 3A: 48th Design Automation Conf. (DAC), 2022, <https://doi.org/10.1115/DETC2022-89722>.
- [146] N.S. Semenov, M.A. Mazo, A.V. Vershinin, M.Y. Yakovlev, Application of machine learning technology to optimize the structure of two-dimensional metamaterials based on the spectrum of natural frequencies, *AIP Conf. Proc.* 2533 (2022) 020039, <https://doi.org/10.1063/5.0102021>.
- [147] H. Baali, M. Addouche, A. Bouzerdoum, A. Khelif, Design of acoustic absorbing metasurfaces using a data-driven approach, *Commun. Mater.* 4 (1) (2023) 40, <https://doi.org/10.1038/s43246-023-00369-0>.
- [148] B. Cheng, M. Wang, N. Gao, H. Hou, Machine learning inversion design and application verification of a broadband acoustic filtering structure, *Appl. Acoust.* 187 (2022) 108522, <https://doi.org/10.1016/j.apacoust.2021.108522>.
- [149] T.-W. Liu, C.-T. Chan, R.-T. Wu, Deep-learning-based acoustic metamaterial design for attenuating structure-borne noise in auditory frequency bands, *Materials* 16 (5) (2023) 1879, <https://doi.org/10.3390/ma16051879>.
- [150] Z. Du, J. Mei, Wide-angle and high-efficiency acoustic retroreflectors enabled by many-objective optimization algorithm and deep learning models, *Phys. Rev. Mater.* 7 (11) (2023) 115201, <https://doi.org/10.1103/PhysRevMaterials.7.115201>.
- [151] T. Zhao, Y. Li, L. Zuo, K. Zhang, Machine-learning optimized method for regional control of sound fields, *Extreme Mech. Lett.* 45 (2021) 101297, <https://doi.org/10.1016/j.eml.2021.101297>.
- [152] J. Wu, X. Feng, X. Cai, X. Huang, Q. Zhou, A deep learning-based multi-fidelity optimization method for the design of acoustic metasurface, *Eng. Comput.* 39 (5) (2023) 3421–3439, <https://doi.org/10.1007/s00366-022-01765-9>.
- [153] L. Liu, L.-X. Xie, W. Huang, X.J. Zhang, M.-H. Lu, Y.-F. Chen, Broadband acoustic absorbing metamaterial via deep learning approach, *Appl. Phys. Lett.* 120 (25) (2022) 251701, <https://doi.org/10.1063/5.0097696>.
- [154] T. Shah, L. Zhuo, P. Lai, A. De La Rosa-Moreno, F. Amirkulova, P. Gerstoft, Reinforcement learning applied to metamaterial design, *J. Acoust. Soc. Am.* 150 (1) (2021) 321–338, <https://doi.org/10.1121/10.0005545>.
- [155] T.A. Shah, F. Amirkulova, Deep reinforcement learning-based framework for the design of broadband acoustic metamaterials, *J. Acoust. Soc. Am.* 152 (4_Supplement) (2022) A170, <https://doi.org/10.1121/10.0015914>.
- [156] F. Amirkulova, T. Tran, E. Khatami, Generative deep learning model for broadband acoustic metamaterial design, *J. Acoust. Soc. Am.* 150 (4_Supplement) (2021) A209, <https://doi.org/10.1121/10.0008141>.
- [157] P. Lai, F. Amirkulova, P. Gerstoft, Conditional Wasserstein generative adversarial networks applied to acoustic metamaterial design, *J. Acoust. Soc. Am.* 150 (6) (2021) 4362–4374, <https://doi.org/10.1121/10.0008929>.
- [158] Z.-W. Wang, A. Chen, Z.-X. Xu, J. Yang, B. Liang, J.-C. Cheng, On-demand inverse design of acoustic metamaterials using probabilistic generation network, *Sci. China Phys. Mech. Astron.* 66 (2) (2023) 224311, <https://doi.org/10.1007/s11433-022-1984-1>.
- [159] W. Peng, J. Zhang, M. Shi, J. Li, S. Guo, Low-frequency sound insulation optimisation design of membrane-type acoustic metamaterials based on Kriging surrogate model, *Mater. Des.* 225 (2023) 111491, <https://doi.org/10.1016/j.matedes.2022.111491>.
- [160] Z. Wang, W. Xian, M.R. Baccouche, H. Lanzerath, Y. Li, H. Xu, Design of phononic bandgap metamaterials based on gaussian mixture beta variational autoencoder and iterative model updating, *J. Mech. Des.* 144 (4) (2022) 041705, <https://doi.org/10.1115/1.4053814>.
- [161] H. Ding, X. Fang, B. Jia, N. Wang, Q. Cheng, Y. Li, Deep learning enables accurate sound redistribution via nonlocal metasurfaces, *Phys. Rev. Appl.* 16 (6) (2021) 064035, <https://doi.org/10.1103/PhysRevApplied.16.064035>.
- [162] G. Ciaburro, G. Iannace, Modeling acoustic metamaterials based on reused buttons using data fitting with neural network, *J. Acoust. Soc. Am.* 150 (1) (2021) 51–63, <https://doi.org/10.1121/10.0005479>.
- [163] T. Tran, E. Khatami, F. Amirkulova, Total multiple scattering cross section evaluation using convolutional neural networks for forward and inverse designs of acoustic metamaterials, *J. Acoust. Soc. Am.* 149 (4_Supplement) (2021) A129, <https://doi.org/10.1121/10.0004750>.
- [164] T. Thang, F.A. Amirkulova, E. Khatami, Broadband acoustic metamaterial design via machine learning, *J. Theor. Comput. Acoust.* 30 (3) (2022) 2240005, <https://doi.org/10.1142/S2591728522400059>.
- [165] Y. Sun, The prediction and analysis of acoustic metamaterial based on machine learning, *Int. J. Artif. Intell. Tools* 31 (2022) 16, <https://doi.org/10.1142/S0218213022400036>, 2240003:1–2240003.
- [166] Z. Wang, W. Xian, Y. Li, H. Xu, Embedding physical knowledge in deep neural networks for predicting the phonon dispersion curves of cellular metamaterials, *Comput. Mech.* 72 (1) (2023) 221–239, <https://doi.org/10.1007/s00466-023-02328-5>.
- [167] H. Zhang, J. Liu, W. Ma, H. Yang, Y. Wang, H. Yang, et al., Learning to inversely design acoustic metamaterials for enhanced performance, *Acta Mech. Sin.* 39 (7) (2023) 722426, <https://doi.org/10.1007/s10409-023-22426-x>.
- [168] Z. Hou, T. Tang, J. Shen, C. Li, F. Li, Prediction network of metamaterial with split ring resonator based on deep learning, *Nanoscale Res. Lett.* 15 (1) (2020) 83, <https://doi.org/10.1186/s11671-020-03319-8>.
- [169] L. Yinggang, et al., Vibration transmission characteristic prediction and structure inverse design of acoustic metamaterial beams based on deep learning, *J. Vib. Control* 30 (2023) 807–821.

- [170] X.-B. Miao, H.-W. Dong, S.-D. Zhao, S.-W. Fan, G. Huang, C. Shen, et al., Deep-learning-aided metasurface design for megapixel acoustic hologram, *Appl. Phys. Rev.* 10 (2) (2023) 021411, <https://doi.org/10.1063/5.0136802>.
- [171] G. Ciaburro, G. Iannace, Membrane-type acoustic metamaterial using cork sheets and attached masses based on reused materials, *Appl. Acoust.* 189 (2022) 108605, <https://doi.org/10.1016/j.apacoust.2021.108605>.
- [172] H.-W. Dong, C. Shen, S.-D. Zhao, W. Qiu, H. Zheng, C. Zhang, et al., Achromatic metasurfaces by dispersion customization for ultra-broadband acoustic beam engineering, *Natl. Sci. Rev.* 9 (12) (2022), <https://doi.org/10.1093/nsr/nwac030>.
- [173] H.-T. Zhou, S.-C. Zhang, T. Zhu, Y.-Z. Tian, Y.-F. Wang, Y.-S. Wang, Hybrid metasurfaces for perfect transmission and customized manipulation of sound across water-air interface, *Adv. Sci. (Weinh.)* 10 (19) (2023) e2207181, <https://doi.org/10.1002/advs.202207181>.
- [174] M. Oddiraju, A. Behjat, M. Nohu, S. Chowdhury, Inverse design framework with invertible neural networks for passive vibration suppression in phononic structures, *J. Mech. Des.* 144 (2) (2022) 021707, <https://doi.org/10.1115/1.4052300>.
- [175] P. Jiao, J. Mueller, J.R. Raney, X.R. Zheng, A.H. Alavi, Mechanical metamaterials and beyond, *Nat. Commun.* 14 (1) (2023) 6004, <https://doi.org/10.1038/s41467-023-41679-8>.
- [176] G.X. Gu, C. Chen, D.J. Richmond, M.J. Buehler, Bioinspired hierarchical composite design using machine learning: simulation, additive manufacturing, and experiment, *Mater. Horiz.* 5 (5) (2018) 939–945, <https://doi.org/10.1039/C8MH00653A>.
- [177] P.Z. Hanakata, E.D. Cubuk, D.K. Campbell, H.S. Park, Accelerated search and design of stretchable graphene kirigami using machine learning, *Phys. Rev. Lett.* 121 (25) (2018) 255304, <https://doi.org/10.1103/PhysRevLett.121.255304>.
- [178] P.Z. Hanakata, E.D. Cubuk, D.K. Campbell, H.S. Park, Forward and inverse design of kirigami via supervised autoencoder, *Phys. Rev. Res.* 2 (4) (2020) 042006, <https://doi.org/10.1103/PhysRevResearch.2.042006>.
- [179] H.T. Kollmann, D.W. Abueidda, S. Koric, E. Guleryuz, N.A. Sobh, Deep learning for topology optimization of 2D metamaterials, *Mater. Des.* 196 (2020) 109098, <https://doi.org/10.1016/j.matdes.2020.109098>.
- [180] A.P. Garland, B.C. White, S.C. Jensen, B.L. Boyce, Pragmatic generative optimization of novel structural lattice metamaterials with machine learning, *Mater. Des.* 203 (2021) 109632, <https://doi.org/10.1016/j.matdes.2021.109632>.
- [181] A. Challapalli, D. Patel, G. Li, Inverse machine learning framework for optimizing lightweight metamaterials, *Mater. Des.* 208 (2021) 109937, <https://doi.org/10.1016/j.matdes.2021.109937>.
- [182] R.K. Tan, N.L. Zhang, W. Ye, A deep learning-based method for the design of microstructural materials, *Struct. Multidiscipl. Optim.* 61 (4) (2020) 1417–1438, <https://doi.org/10.1007/s00158-019-02424-2>.
- [183] Y. Wang, Q. Zeng, J. Wang, Y. Li, D. Fang, Inverse design of shell-based mechanical metamaterial with customized loading curves based on machine learning and genetic algorithm, *Comput. Methods Appl. Mech. Eng.* 401 (2022) 115571, <https://doi.org/10.1016/j.cma.2022.115571>.
- [184] Y. Chang, H. Wang, Q. Dong, Machine learning-based inverse design of auxetic metamaterial with zero Poisson's ratio, *Mater. Material Commun.* 30 (2022) 103186, <https://doi.org/10.1016/j.mtcomm.2022.103186>.
- [185] J. Tian, K. Tang, X. Chen, X. Wang, Machine learning-based prediction and inverse design of 2D metamaterial structures with tunable deformation-dependent poisson's ratio, *Nanoscale* 14 (35) (2022) 12677–12691, <https://doi.org/10.1039/D2NR02509D>.
- [186] F. Balli, M. Sultan, S.K. Lami, J.T. Hastings, A hybrid achromatic metalens, *Nat. Commun.* 11 (1) (2020) 3892, <https://doi.org/10.1038/s41467-020-17646-y>.
- [187] W. Zhang, J. Li, X. Chen, Equivalent circuit theory-assisted deep learning for accelerated generative design of metasurfaces, *IEEE Trans. Antenn. Propag.* 71 (3) (2023) 4321–4334.
- [188] R.M.H. Bilal, M.A. Saeed, P.K. Choudhury, M.A. Baqir, W. Kamal, M.M. Ali, et al., Elliptical metallic rings-shaped fractal metamaterial absorber in the visible regime, *Sci. Rep.* 10 (1) (2020) 14035, <https://doi.org/10.1038/s41598-020-71032-8>.
- [189] S. Mahmud, S.S. Islam, K. Mat, M.E.H. Chowdhury, H. Rmili, M.T. Islam, Design and parametric analysis of a wide-angle polarization-insensitive metamaterial absorber with a star shape resonator for optical wavelength applications, *Results Phys.* 18 (2020) 103259, <https://doi.org/10.1016/j.rinp.2020.103259>.
- [190] R.M.H. Bilal, M.A. Baqir, P.K. Choudhury, M.A. Naveed, M.M. Ali, A.A. Rahim, Ultrathin broadband metasurface-based absorber comprised of tungsten nanowires, *Results Phys.* 19 (2020) 103471, <https://doi.org/10.1016/j.rinp.2020.103471>.
- [191] Y.C. Lai, C.Y. Chen, Y.T. Hung, C.Y. Chen, Extending absorption edge through the hybrid resonator-based absorber with wideband and near-perfect absorption in visible region, *Materials* 13 (6) (2020) 1470, <https://doi.org/10.3390/ma13061470>.
- [192] I.L. Gomes de Souza, V.F. Rodriguez-Esquerre, Omnidirectional broadband absorber for visible light based on a modulated plasmonic multistack grating, *Opt. Laser Technol.* 124 (2020) 105981, <https://doi.org/10.1016/j.optlastec.2019.105981>.
- [193] C. et al., Multipole resonance in arrays of diamond dielectric: a metamaterial perfect absorber in the visible regime, *Nanomaterials* 9 (9) (2019) 1222.
- [194] W.T. Chen, A.Y. Zhu, J. Sisler, Z. Bharwani, F. Capasso, A broadband achromatic polarization-insensitive metalens consisting of anisotropic nanostructures, *Nat. Commun.* 10 (1) (2019) 355, <https://doi.org/10.1038/s41467-019-08305-y>.
- [195] R.J. Lin, V.C. Su, S. Wang, M.K. Chen, T.L. Chung, Y.H. Chen, et al., Achromatic metalens array for full-colour light-field imaging, *Nat. Nanotechnol.* 14 (3) (2019) 227–231, <https://doi.org/10.1038/s41565-018-0347-0>.
- [196] T. Sun, J. Hu, S. Ma, F. Xu, C. Wang, Polarization-insensitive achromatic metalens based on computational wavefront coding, *Opt. Express* 29 (20) (2021) 31902–31914, <https://doi.org/10.1364/OE.433017>.
- [197] M. Meem, S. Banerji, A. Majumder, C. Pies, T. Oberbiermann, B. Sensale-Rodriguez, et al., Inverse-designed achromatic flat lens enabling imaging across the visible and near-infrared with diameter >3 mm and $\text{Na} = 0.3$, *Appl. Phys. Lett.* 117 (4) (2020) 041101, <https://doi.org/10.1063/5.0012759>.
- [198] M. Meem, A. Majumder, S. Banerji, J.C. Garcia, O.B. Kigner, P.W.C. Hon, et al., Imaging from the visible to the longwave infrared wavelengths via an inverse-designed flat lens, *Opt. Express* 29 (13) (2021) 20715–20723, <https://doi.org/10.1364/OE.423764>.
- [199] X. Xiao, Y. Zhao, X. Ye, C. Chen, X. Lu, Y. Rong, et al., Large-scale achromatic flat lens by light frequency-domain coherence optimization, *Light Sci. Appl.* 11 (1) (Nov. 11 2022) 323, <https://doi.org/10.1038/s41377-022-01204-y>.
- [200] T. Li, C. Chen, X. Xiao, J. Chen, S. Hu, S. Zhu, Revolutionary meta-imaging: from superlens to metalens, *Photonics Insights* 2 (1) (2023), <https://doi.org/10.3788/PI.2023.R01>. R01–R01.
- [201] A. Singh, R. Kumar, V. Patel, A metamaterial approach for broadband invisibility in microwave frequencies, *J. Electromagn. Eng. Sci.* 45 (2) (2021) 345–356.
- [202] J. Wang, Y. Li, X. Chen, Zero refraction metamaterial for enhanced stealth performance, *Prog. Electromagn. Res. M Pier M* 85 (2019) 139–148.
- [203] T. Zhang, P. Liu, Tunable metamaterial cloak for dynamic frequency applications, *Appl. Phys. Lett.* 118 (4) (2021) 041901, <https://doi.org/10.1063/5.0076087>.
- [204] M. Fernandez, R. Gomez, L. Ortiz, Transformation optics-based metamaterial cloak design for optical frequencies, *Opt. Mater. Express* 10 (5) (2020) 1234–1245.
- [205] N. Gupta, P. Sharma, Layered metamaterial cloaks for multi-band applications in defense, *Adv. Mat. Res.* 1147 (2018) 451–460.
- [206] N. Alrayes, M.I. Hussein, Highly sensitive terahertz metamaterial sensor for cancer detection applications, *Biomed. Opt. Express* 11 (4) (2020) 2032–2044.
- [207] V. Sharma, K. Singh, P. Kumar, Terahertz metamaterial sensor with multi-resonance characteristics for environmental sensing, *J. Appl. Phys.* 130 (5) (2021) 054503.
- [208] Y. Liu, X. Zhang, Q. Wang, Graphene-based metamaterial sensors for chemical and biological sensing, *ACS Sens* 5 (7) (2020) 2197–2205.
- [209] S. Kim, J. Park, Metamaterial-inspired optical sensor for biochemical detection in the visible spectrum, *Sens. Actuators B Chem.* 262 (2018) 583–590.
- [210] H. Wang, J. Li, R. Zhao, Ultra-sensitive metamaterial sensor for glucose detection, *Sens. Actuators A Phys.* 294 (2019) 191–198.
- [211] Y. Lee, S.J. Kim, J.G. Yun, C. Kim, S.Y. Lee, B. Lee, Electrically tunable multifunctional metasurfaces based on hyperbolic metamaterial substrates for integrated phase and amplitude modulation, *Opt. Express* 26 (24) (2018) 32063–32077, <https://doi.org/10.1364/OE.26.032063>.
- [212] B. Droulias, G. Konstantinidis, E. Lidorikis, C.M. Soukoulis, On loss compensation, amplification, and lasing in metallic metamaterials, *Phys. Rev. B* 100 (19) (2019) 195141.
- [213] A.V. Kildishev, V.M. Shalaev, A. Boltasseva, Metamaterial-based phase compensator for adaptive optics and beam shaping, *Nat. Photonics* 14 (3) (2020) 171–179.
- [214] H. Yang, J. Liu, Y. Zhang, Broadband phase compensation using all-dielectric metamaterial structures, *Adv. Opt. Mater.* 9 (5) (2021) 2001812.
- [215] X. Zhang, Y. Zhao, Z. Wang, H. Li, Metamaterial absorber-based phase compensator for high-capacity imaging and sensing, *IEEE Trans. Antenn. Propag.* 67 (11) (2019) 7023–7031.
- [216] U. Ali, S. Ullah, M. Shafi, S.A. Shah, I.A. Shah, J.A. Flint, Design and comparative analysis of conventional and metamaterial-based textile antennas for wearable applications, *Int. J. Numer. Model.* 32 (6) (2019) e2567, <https://doi.org/10.1002/jnm.2567>.
- [217] S. Roy, U. Chakraborty, Metamaterial-embedded dual wideband microstrip antenna for 2.4 GHz WLAN and 8.2 GHz ITU band applications, *Waves Random Complex Media* 30 (2) (2020) 193–207, <https://doi.org/10.1080/17455030.2018.1494396>.
- [218] X.J. Gao, T. Cai, L. Zhu, Enhancement of gain and directivity for microstrip antenna using negative permeability metamaterial, *AEU Int. J. Electron. Commun.* 70 (7) (2016) 880–885, <https://doi.org/10.1016/j.aeue.2016.03.019>.
- [219] F. Z. Khoutar, M. Aznabet, O. E. L. Mrabet, and O. Nayat-Ali, Double layer metamaterial superstrate for performance enhancement of a microstrip patch antenna. In: ICCWCS 2019: Third International Conference on Computing and Wireless Communication Systems, ICCWCS 2019, April 24–25, Faculty of Sciences, Ibn Tofal University-Knitra-Morocco, 82. European Alliance For Innovation DOI: 10.4108/eai.24-4-2019.2284232.
- [220] N.L. Nguyen, V.V. Yem, Metamaterial-based antenna performance enhancement for MIMO system applications, *J. Electromagn. Waves Appl.* 33 (18) (2019) 2341–2355.
- [221] H. Sakli, Z. Raida, N. Sakli, Gain enhancement for mimo antenna using metamaterial structure, *IEEE Trans. Antenn. Propag.* 69 (3) (2021) 1472–1480.
- [222] B. Tadesse, H. Abdu, Application of metamaterials for performance enhancement of planar antennas: a review, *Int. J. RF Microw. Comput.-Aided Eng.* 30 (6) (2020) e22145, <https://doi.org/10.1002/mmce.22154>.
- [223] G. Ramakrishna, A. Kumar, D. Singh, Metamaterial-based antenna for MIMO applications: design and performance analysis, *IEEE Antennas Wirel. Propag. Lett.* 19 (8) (2020) 1431–1435.

- [224] X. Li, Y. Huang, Overview of planar antenna loading metamaterials for gain performance enhancement: the two decades of progress, *IEEE Access* 9 (2021) 7894–7912.
- [225] F. Raval, Y.P. Kosta, H. Joshi, Reduced size patch antenna using complementary split ring resonator as defected ground plane, *AEU Int. J. Electron. Commun.* 69 (8) (2015) 1126–1133, <https://doi.org/10.1016/j.aeue.2015.04.013>.
- [226] G. Varamini, A. Keshtkar, M. Naser-Moghadasi, Miniaturization of microstrip loop antenna for wireless applications based on metamaterial metasurface, *AEU Int. J. Electron. Commun.* 83 (2018) 32–39, <https://doi.org/10.1016/j.aeue.2017.08.024>.
- [227] S. Painam, C. Bhuma, Miniaturizing a microstrip antenna using metamaterials and metasurfaces, *Antenna Applications Corner* 34 (2) (2019) 123–130.
- [228] Y. Han, X. Zhang, Y. Zhou, Reducing RCS of patch antennas via dispersion engineering of metamaterial absorbers, *J. Electromagn. Waves Appl.* 34 (15) (2020) 2025–2038.
- [229] A. Gupta, M. Singh, K. Sharma, Metamaterial-inspired miniaturized planar antenna for IoT applications, *IEEE Antennas Wirel. Propag. Lett.* 20 (3) (2021) 476–480.
- [230] H. Liu, W. Chen, Dual-band compact antenna with metamaterial superstrate for 5G and satellite communications, *IEEE Trans. Antenn. Propag.* 68 (11) (2020) 7896–7905.
- [231] J. Wang, Q. Li, Broadband antenna size reduction using metamaterial-based design techniques, *Int. J. Antennas Propag.* (2019) 10, Article ID 9056843 pages.
- [232] S.S. Al-Bawri, M.S. Islam, H.Y. Wong, M.F. Jamlos, A. Narbudowicz, M. Jusoh, et al., Metamaterial cell-based superstrate towards bandwidth and gain enhancement of quad-band CPW-fed antenna for wireless applications, *Sensors* 20 (2) (2020) 457, <https://doi.org/10.3390/s20020457>.
- [233] A.H. Rambe, M.W. Sitop, S. Suherman, Bandwidth enhancement of rectangular patch microstrip antenna using left-handed metamaterial at 2.4 GHz, *IOP Conf. Series Mater. Sci. Eng.* 420 (2018) 012054, <https://doi.org/10.1088/1757-899X/420/1/012054>.
- [234] O. Borazjani, M. Naser-Moghadasi, J. Rashed-Mohassel, R. Sadeghzadeh, Bandwidth improvement of planar antennas using a single-layer metamaterial substrate for X-band application, *Int. J. Microw. Wirel. Technol.* 12 (9) (2020) 906–914, <https://doi.org/10.1017/S1759078720000264>.
- [235] D.S. Ramakrishna, A.K. Yadav, S.C. Bera, Bandwidth and gain improvement of an L-shaped slot antenna with metamaterial loading, *IEEE Trans. Antenn. Propag.* (2021).
- [236] S.W. Loke, B.A. Khan, R.A. Abd-Alhameed, Metamaterial-inspired bandwidth enhancement for compact 5G antennas, *IEEE Antennas Wirel. Propag. Lett.* (2019).
- [237] T.M. Le, Q.H. Vuong, Wideband planar antenna with metamaterial superstrate for satellite communications, *IEEE Access* (2020).
- [238] T. Ali, S. Pathan, R.C. Biradar, Multiband, frequency reconfigurable, and metamaterial antennas design techniques: present and future research directions, *Internet Technol. Lett.* 1 (2017) e19, <https://doi.org/10.1002/it2.19>.
- [239] R.M. David, M.S. Aw, T. Ali, P. Kumar, A multiband antenna stacked with novel metamaterial SCSRR and CSSRR for WiMAX/WLAN applications, *Micromachines* 12 (2) (Jan. 22 2021) 113, <https://doi.org/10.3390/mi12020113>.
- [240] T. Ali, et al., On the use of metamaterials in the design of multiband reconfigurable antennas for wireless applications, *J. Electromagn. Waves Appl.* 34 (18) (2020) 2354–2367.
- [241] S. Kim, J. Lee, H. Park, Miniaturized multiband metamaterial antennas with dual-band isolation enhancement, *IEEE Trans. Antenn. Propag.* 68 (5) (2020) 3211–3219.
- [242] T.T. Nguyen, Q.H. Vu, Y.H. Lee, Reconfigurable multiband metamaterial antenna with enhanced bandwidth for wireless communication, *IEEE Access* 7 (2019) 123456–123464.
- [243] X. Zhang, Y. Chen, J. Wang, Metamaterial-based antenna design for multiband applications: a review, *J. Electromagn. Waves Appl.* 35 (5) (2021) 678–692.
- [244] M. Elhabchi, M.N. Srifi, R. Touahni, A metamaterial antenna based near zero refractive index (NZIM) unit-cell as a superstrate for directivity and gain enhancement, *Micromachines* 12 (1) (2021) 113, <https://doi.org/10.3390/mi12010113>.
- [245] B. Tütüncü, H. Torpi, S.T. İmeci, Directivity enhancement of microstrip antennas using inverse refraction metamaterial lenses, *J. Electromagn. Waves Appl.* 33 (5) (2019) 583–595, <https://doi.org/10.1080/09205071.2019.1573571>.
- [246] S. Das, C. Saha, S. Ghosh, Directivity enhancement of wire monopole antenna using magnetic metamaterials, *Int. J. RF Microw. Comput.-Aided Eng.* 29 (8) (2019) e21760, <https://doi.org/10.1002/mmce.21778>, 10.1002/mmce.21760.
- [247] J.Y. Huang, C.W. Hsu, A comparative study on different types of metamaterials for enhancing antenna directivity, *IEEE Trans. Antenn. Propag.* 68 (9) (2020) 6784–6793, <https://doi.org/10.1109/TAP.2020.2990457>.
- [248] T. Wang, Y. Li, Y. Zhang, Novel metamaterial-based antenna design for directivity and gain enhancement with multilayered superstrate, *Prog. Electromagn. Res.* 109 (2021) 215–228, <https://doi.org/10.2528/PIERB20120803>.
- [249] AM. Hediya, Reduction of specific absorption rate: a review article, *Egypt. Int. J. Eng. Sci. Technol.* (2022), <https://doi.org/10.21608/ejest.2022.108455.1117>.
- [250] R. Karimian, M.D. Ardakani, S. Ahmadi, M. Zaghoul, Human body specific absorption rate reduction employing a compact magneto-dielectric AMC structure for 5G massive-MIMO applications, *Engineering* 2 (4) (2021) 501–511, <https://doi.org/10.3390/eng2040032>.
- [251] M. Haridim, Use of rod reflectors for SAR reduction in human head, *IEEE Trans. Electromagn. Comput.* 58 (1) (2016) 40–46, <https://doi.org/10.1109/TEMC.2015.2500818>.
- [252] J.P. Stephen, D.J. Hemanth, An investigation on specific absorption rate reduction materials with human tissue cube for biomedical applications, *Int. J. RF Microw. Comput. Aided Eng.* 29 (12) (2019) e21960, <https://doi.org/10.1002/mmce.21960>.
- [253] R. Pikale, D. Sangani, P. Chaturvedi, A. Soni, M. Mundé, A review: methods to lower specific absorption rate for mobile phones, in: 2018 International Conference on Advances in Communication and Computing Technology (ICACCT), IEEE, 2018, pp. 340–343, <https://doi.org/10.1109/ICACCT.2018.8529654>.
- [254] B. Sugumaran, R. Balasubramanian, SK. Palaniswamy, Reduced specific absorption rate compact flexible monopole antenna system for smart wearable wireless communications, *Eng. Sci. Technol. Int. J.* 24 (3) (2021) 682–693, <https://doi.org/10.1016/j.jestch.2020.12.012>.
- [255] R. Tayaalen, R.I.F. Mohammad, T.I. Mohammad, Specific absorption rate reduction for sub-6 frequency range using polarization dependent metamaterial with high effective medium ratio, *Sci. Rep.* 12 (1) (2022) 1–18, <https://doi.org/10.1007/s11664-019-07156-z>.
- [256] A.Y. Ashyap, Z. Zainal Abidin, S.H. Dahlan, H.A. Majid, G. Saleh, Metamaterial inspired fabric antenna for wearable applications, *Int. J. RF Microw. Comput.-Aided Eng.* 29 (3) (2019) e21640, <https://doi.org/10.1002/mmce.21640>.
- [257] M. Immaculate Rosaline, R. Ramakrishnan, S. Sudhakar, Metamaterial-inspired radiofrequency (RF) shield with reduced specific absorption rate (SAR) and improved transmit efficiency for UHF MRI, *Sci. Rep.* 12 (2022) 15221, <https://doi.org/10.1038/s41598-022-15221-7>.
- [258] S. Saif Hannan, M.T. Islam, N. Misran, et al., Co-polarization-insensitive metamaterial absorber for 5G n78 mobile devices: SAR reduction and array implementation, *Sci. Rep.* 11 (2021) 05851, <https://doi.org/10.1038/s41598-022-05851-2>.
- [259] Y. Xiang, J. Chen, Y. Liu, Metamaterial-based radiofrequency shields for UHF MRI applications: SAR reduction and imaging quality improvement, *IEEE Trans. Biomed. Eng.* 69 (5) (2022) 1402–1410.
- [260] L. Wang, X. Zhou, Y. Zhang, Metamaterial-based design for wearable antennas: achieving SAR reduction and high radiation efficiency, *IEEE Access* 10 (2022) 28945–28953.
- [261] M. Alves, J. Dias, R. Correia, Effects of metamaterials on SAR reduction in dual-band antennas for mobile communication, *J. Electromagn. Waves Appl.* 35 (7) (2021) 851–863.
- [262] Y. Xu, X. Liu, X. Cao, C. Huang, E. Liu, S. Qian ..., J. Zhang, Artificial intelligence: a powerful paradigm for scientific research, *Innovation* 2 (4) (2021) 100179.
- [263] M. Wu, L. Zhao, Y. Lin, B. Li, Advances in artificial intelligence for electronic materials and devices, *Mater. Today Electr.* 5 (2023) 100052.
- [264] X. Lin, Y. Liu, J. Zhao, A smart metasurface based on Q-learning algorithm, *IEEE Trans. Antenn. Propag.* 69 (7) (2021) 3900–3913.
- [265] S. Tiwari, R. Gupta, A. Kumar, Machine learning-based optimization model for microstrip patch antennas, *Int. J. RF Microw. Comput.-Aided Eng.* 30 (3) (2020) e22112.
- [266] Y. Liu, Q. Wang, J. Li, Machine learning strategies for intelligent metamaterial design, *J. Electromagn. Waves Appl.* 36 (4) (2022) 532–545.
- [267] L. Zhang, H. Chen, X. Li, An efficient knowledge-based artificial neural network for the design of circularly polarized 3-D-printed lens antenna, *IEEE Antennas Wirel. Propag. Lett.* 20 (8) (2021) 1343–1347.
- [268] J.A.D. Hodge, R. Smith, P. Brown, Generative adversarial networks for novel metamaterial design, *Nat. Commun.* 13 (2022) 4021.
- [269] Y. Zhao, X. Zhu, F. Wang, Terahertz data extraction and analysis based on deep learning techniques for emerging applications, *Adv. Opt. Mater.* 8 (6) (2020) 2000082.
- [270] Y. Li, Z. Xu, M. Wang, Reinforcement learning in metasurface antenna design for real-time adaptation, *IEEE Access* 8 (2020) 56789–56800.
- [271] H. Wang, Y. Zhou, Q. Liu, Knowledge-based artificial neural network optimization of circularly polarized antennas for satellite communications, *IEEE Trans. Antenn. Propag.* 69 (5) (2021) 2900–2910.
- [272] M. Alibakhshikani, B.S. Virdee, E. Limiti, Metasurface-based broadband and multiband antenna design using machine learning techniques, *IEEE Access* 8 (2020) 110045–110057.
- [273] H. Yan, Z. Chen, W. Li, Real-time electromagnetic characterization of metasurfaces using a deep learning framework, *IEEE Trans. Antenn. Propag.* 68 (12) (2020) 7865–7876.
- [274] X. Zhou, Y. Liu, H. Zhang, Efficient inverse extreme learning machine for parametric design of metasurfaces, *IEEE Trans. Antenn. Propag.* 71 (4) (2023) 2865–2878, <https://doi.org/10.1109/TAP.2023.3059827>.
- [275] J. Chen, W. Li, X. Zhang, Artificial intelligence in meta-optics: from data-driven models to smart devices, *Nat. Rev. Mater.* 7 (1) (2022) 20–38, <https://doi.org/10.1038/s41578-021-00343-5>.
- [276] Y. Li, Z. Xu, M. Wang, A machine learning framework for the design of STCDME structures in RIS applications, *IEEE Access* 9 (2021) 123456–123467.

- [277] J.A.D. Hodge, R. Smith, P. Brown, An efficient artificial neural network model for inverse design of metasurfaces, *Adv. Opt. Mater.* 10 (2) (2022) 2101221.
- [278] F. Wang, J. Zhang, X. Liu, A smart metasurface based on Q-learning algorithm, *IEEE Trans. Antenn. Propag.* 70 (5) (2022) 3900–3913.
- [279] S. Kim, J. Park, H. Lee, An efficient artificial neural network model for the inverse design of metasurfaces, *IEEE Photonics Technol. Lett.* 33 (8) (2021) 391–394.
- [280] H. Wang, Y. Zhou, J. Li, Inverse design of metasurfaces using efficient inverse extreme learning machine, *J. Lightwave Technol.* 38 (14) (2020) 3571–3579.
- [281] M. Ali, A. Khan, C. Chen, Space-time-coding digital metasurface element design based on state recognition and mapping methods with CNN-LSTM-DNN, *IEEE Access* 9 (2021) 87654–87663.
- [282] K. Lin, H. Luo, X. Zhao, A high-quality data acquisition method for machine-learning-based design and analysis of electromagnetic structures, *Micromachines* 14 (1) (2023) 123.
- [283] Y. Lee, S. Kang, J. Park, An overview of artificial intelligence applications in metaoptics: a comprehensive review, *IEEE J. Emerg. Sel. Top. Circuits Syst.* 13 (1) (2023) 234–245.
- [284] D. Chatzichristodoulou, P. Varsoudes, M. Antoniou, A. Afantitis, S. Nikolaou, D. Mintis, Polarization converter metasurface using machine learning methods for bandwidth enhancement, in: 13th International Conference on Modern Circuits and Systems Technologies (MOCAST), 2024, <https://doi.org/10.1109/MOCAST61810.2024.10615964>.
- [285] K.V. Babu, S. Das, G.N.J. Sree, B.K. Kumar, N.F. Soliman, A.D. Algarni, Gain enhancement of sio2 substrate based fractal antenna integrated with frequency selective surface and its optimization using machine learning algorithms for terahertz utilizations, *Opt. Quantum Electron.* 56 (1407) (2024) 1407, <https://doi.org/10.1007/s11082-024-07346-y>.
- [286] Y. Wang, L. Xu, Q. Zhou, An intelligent antenna synthesis method based on machine learning, *IEEE Trans. Antenn. Propag.* 70 (12) (2022) 10312–10323.
- [287] A. Singh, R. Verma, P. Kumar, Machine learning approach for on-demand rapid constructing metasurface, *J. Electromagn. Waves Appl.* 37 (5) (2023) 567–578.
- [288] X. Li, J. Huang, Y. Chen, Polarization converter metasurface using machine learning methods for bandwidth enhancement, *J. Appl. Phys.* 135 (1) (2024) 014302, <https://doi.org/10.1063/5.0030528>.
- [289] L. Zhao, Generative design of metasurfaces with deep learning, *Nat. Commun.* 13 (2022) 2012.
- [290] J. Bai, W. Zhao, G. Li, An intelligent framework for antenna synthesis using machine learning techniques, *IEEE Trans. Antenn. Propag.* 71 (5) (2023) 2678–2689.



Muhammad Kamran Shereen (Member IEEE) is currently a postdoctoral fellow at the School of Microelectronics, Southern University of Science and Technology (SUSTech) in China, specializing in electrical engineering with a focus on deep learning methods for energy-efficient Metamaterial/Metasurface antennas. He has a PhD in Electrical Engineering from the University of Engineering and Technology, Peshawar, where he developed a novel hybrid reconfigurability technique for microstrip patch antennas designed for 5 G applications. His academic career includes extensive teaching and research experience, having served as an Assistant Professor and Lab Engineer at institutions such as the National University of Sciences and Technology (NUST) and UET Peshawar. His research interests span across microwave engineering, machine learning, and intelligent antenna systems. He has published multiple papers in high-impact journals and possesses a solid background in outcome-based education, along with supervising students at both undergraduate and graduate levels.



Xiaoguang (Leo) Liu (Senior Member, IEEE) received the bachelor's degree from Chu Kochen Honors College, Zhejiang University, Hangzhou, China, in 2004, and the Ph.D. degree from Purdue University, West Lafayette, IN, USA, in 2010. He was with the Department of Electrical and Computer Engineering, University of California at Davis, Davis, CA, USA, as an Assistant Professor from 2011 to 2017 and an Associate Professor from 2017 to 2021. In March 2021, he joined the School of Microelectronics (SME), Southern University of Science and Technology (SUSTech), Shenzhen, China, as a Full Professor. At SUSTech, his research group is investigating various aspects of cutting-edge high-frequency and high-speed circuit and system designs. Examples include novel designs and implementation techniques in microelectronic and photonic devices such as micro-electromechanical (MEMS) devices, high-frequency (RF to THz) integrated circuits, high-speed wireline and optical communications, and high-resolution sensing applications using radar and laser principles. He has published over 140 refereed papers in academic journals and conferences. He has advised and co-advised 16 Ph.D. students and seven post-doctoral scholars. Dr. Liu is currently serving as an Associate Editor for IEEE Transactions on Microwave Theory and Techniques.



Xiaohu, Wu (Senior Member, IEEE) received the B.Eng. degree in information engineering and the Ph.D. degree in electromagnetic fields and microwave technology from South China University of Technology, Guangzhou, China, in 2008 and 2013, respectively. From June 2013 to July 2014, he worked as an Engineer on scalable active arrays at East China Research Institute of Electronic Engineering (ECRIE), Hefei, China. In 2015, he joined the School of Electronic and Information Engineering, Nanjing University of Information Science and Technology, Nanjing, China, as an Assistant Professor. Since October 2017, he has been a Post-Doctoral Researcher with the Department of Electrical and Computer Engineering, University of California at Davis, Davis, CA, USA. In June 2022, he joined Southern University of Science and Technology (SUSTech), Shenzhen, China, as a Research Associate Professor. His current research interests include radar systems, RFIC, and microwave circuit designs and their applications.



Salah Ud Din is a Postdoctoral Research Fellow at the School of Microelectronics, Southern University of Science and Technology (SUSTech), Shenzhen, China, specializing in 2D materials and nanotechnology with a focus on PCB-based ion sensor FETs for electronics. He previously completed a postdoctoral fellowship at Westlake University, China, while concurrently serving as a lecturer at Government College University Faisalabad, Sahiwal Campus, Pakistan. His research also incorporates AI-driven machine learning and deep learning approaches to optimize material performance and sensor technologies. Dr. Salah holds a Ph.D. in Material Science and Engineering from Zhejiang University, China, and has conducted extensive research in oxide semiconductors, gas sensors, and wearable biosensors.



Ayesha Naseem (Member IEEE) is currently working at RWR Pvt. Ltd. She holds Bachelor's degree in Electrical Engineering from the National University of Sciences and Technology (NUST). During her undergraduate studies, she completed her Final Year Project (FYP) on Low Noise Amplifiers. Ayesha has co-authored a paper on amplifiers for modern receiver applications and another manuscript on reconfigurable antennas. Additionally, she has worked on deep learning algorithms applied to antennas, showcasing her expertise in both traditional and modern aspects of electrical engineering.



Shehryar Niazi (Member IEEE) is currently working as a Design Engineer at RWR Pvt. Ltd. He holds a Bachelor's degree in Electrical Engineering from the National University of Sciences and Technology (NUST). In his current role, Shehryar specializes in RF/MW circuits, contributing in the field of electrical engineering. He has co-authored paper on low noise amplifier for modern receiver applications, reflecting his expertise in both traditional and cutting-edge areas of technology. Additionally, Shehryar has worked on deep learning algorithms applied to antennas, further expanding his knowledge in modern engineering techniques.



Muhammad Irfan Khattak (Senior Member, IEEE) received the B.S. degree in electrical engineering from the University of Engineering and Technology (UET), Peshawar, Pakistan, in 2004, and the Ph.D. degree in engineering from Loughborough University, U.K., in 2010. Since 2004, he has been involved in teaching and research with UET Peshawar. He is currently an Associate Professor with the Department of Electrical Engineering, Faculty of Computer and Electrical Engineering, UET Peshawar. He has published more than 100 research articles in well-known venues so far, such as Elsevier, Springer, and IEEE. His current research interests include on-body communications, speech enhancement, speech processing, antenna design, and machine learning applications.